Acoustically Excited Heated Jets

I—Internal Excitation

J. Lepicovsky, K. K. Ahuja, W. H. Brown,
M. Salikuddin, and P. J. Morris

NASA

NF01835

NASA Contractor Report 4129
Part I

Acoustically Excited Heated Jets

I—Internal Excitation

J. Lepicovsky, K. K. Ahuja,
W. H. Brown, and M. Salikuddin
Lockheed Aeronautical Systems Company–Georgia
Marietta, Georgia

P. J. Morris
Pennsylvania State University
University Park, Pennsylvania

N/\S/\

National Aeronautics
and Space Administration

Scientific and Technical
Information Division

1988

FOREWORD

This report was prepared by Lockheed Aeronautical Systems Company - Georgia Division, Marietta, Georgia for NASA-Lewis Research Center, Cleveland, Ohio under contract NAS3-23708, entitled "Experimental Investigation of the Effects of Acoustic Excitation on Hot Jet Mixing." The work was performed under a two phase effort.

The program was conducted over a period of five years. During this period, however, the originally proposed goals for this study were substantially modified by the NASA project manager and emphasis was put on the investigation of excitability of high speed, highly heated jets. Because of this, the final report presents a chronological rather than a thematic development of the subject.

Mr. James R. Stone was the Project Manager for NASA-Lewis Center for the Phase I effort. Lockheed's Program Manager was Dr. H. K. Tanna. Dr. Ed Rice was the Project Manager for NASA Lewis Center for the Phase II effort. Lockheed's Program Manager was Dr. K. K. Ahuja.

Technical help from Messrs. R. H. Burrin, C. R. Huie, and J. F. Songer is particularly acknowledged.

The authors are particularly grateful to Mr. Uwe von Glahn of NASA Lewis for his continuous support, various lively discussions and useful suggestions during the course of this work.

This Page Intentionally Left Blank

CONTENTS

SUMMARY

The major goal of this investigation was to obtain detailed experimental
data on the effects of acoustic excitation on the mixing of heated jets
with the surrounding air. To determine the extent of the available
information on experiments and theories dealing with the effects of
acoustic excitation on hot jet mixing, an extensive literature survey was
conducted at the outset of this program. Based on the information gathered
in the literature survey, a technical approach was developed to carry out a
systematic set of flowfield measurements and flow visualization for a broad
range of jet operating and flow excitation conditions. The highest flow
total temperature used was 800 K and the highest Mach number 1.16. The
maximum achievable sound levels, as measured at the nozzle exit, were 150
dB. The exit diameter of the test nozzle was 50.8 mm.

Before acquiring the mean flow data, it was found necessary to first
determine the effects of jet operating conditions on the nature of the
boundary layer at the nozzle exit. Detailed optimization experiments were
then carried out to determine the excitation Strouhal number that produced
the strongest effects in the centerline mean velocity. Radial profiles
and centerline distributions of the mean velocity and jet temperature were
acquired for a range of jet-operating and acoustic excitation conditions.
Phase-locked flow visualization experiments were also performed at some of
the test conditions.

A theoretical analysis of excited jets, which includes the region
downstream of the potential core, was also developed in this study. The
results of theoretical predictions were compared with experimentally
acquired data.

The main conclusions drawn from Part 1 of this study are as follows:

1. The sensitivity of heated jets to upstream acoustic excitation
   strongly varies with the jet operating conditions.

2. The threshold excitation level increases with increasing jet
   temperature.

3. Preferential excitation Strouhal number does not change significantly
   with a change of the jet operating conditions.

4. The effects of the nozzle exit boundary layer thickness are similar
   for both heated and unheated jets at low Mach number.

5. A coherent periodic structure in a form of ring vortices is formed in the near flowfield of an acoustically exited free jet. The structure is very stable with well defined ring vortices at low Mach numbers. Certain distortion of this structure was observed for high Mach number, unheated jets.

6. Vortex pairing has been observed on schlieren pictures at some of the excitation conditions at low Mach numbers. At high Mach numbers no mutual vortex interaction was traceable.

7. The mean flow measurements are qualitatively supported by the results of the flow visualizations.

8. The predictions from the upgraded theory, compare extremely well with the measurements at moderate jet Mach numbers and total temperatures. These comparisons are, however, made only for the mean flow data. Therefore, further work is needed by way of comparing the measured and the predicted unsteady flow quantities.

It was found that unlike the unheated jets, the high-speed, highly heated jets did not respond to internal upstream acoustic excitation. To improve our understanding of the excitability of highly heated high speed jets, the experiments using external acoustic excitation were also performed. Results for the external acoustic excitation are presented separately in Part 2 of this report.

Finally, the plotted results of detailed measurements of Mach number and temperature in the jet flowfield, including tabulated experimental data, are presented in Part 3.

1.0 INTRODUCTION

The main objective of the program described here was to obtain detailed experimental data on the effects of relatively strong upstream acoustic excitation on the mixing of heated jets with the surrounding air. The emphasis was on the assessment of the possibility of obtaining beneficial effects from acoustic excitation of heated jets and on the development of a better fundamental understanding of the phenomena involved.

This report describes the results of Part 1 of a two phase study. An extensive literature survey was conducted at the outset of this program, and is described in Section 2.0 along with a detailed list of relevant papers on the subject of jet excitation presented in the section, References. The main purpose of this literature survey, was to determine the extent of the available information on experiments and theories dealing with the effects of acoustic excitation on hot jet mixing. The information gathered from this literature survey was then used to plan a technical approach to accomplish the study objectives. The technical approach is presented in Section 3.0, followed by a description of the facility and test procedures used for the experiments. The test facility, and data acquisition and reduction procedures are described in Section 4.0.

For reasons given later, it was decided that an effective approach to obtain meaningful results would be to first determine the effects of jet operating conditions on the nature of the nozzle exit boundary layer. These results are described in Section 5.0. This is followed by a description of the detailed optimization experiments in Section 6.0. These optimization experiments served to determine the Strouhal number that produces the strongest effects in the centerline mean velocity. Results of phase-locked flow visualization of heated and unheated, excited and unexcited jets operated at the conditions determined by the optimization experiments are presented in Section 7.0. The theoretical analysis of excited jets, which includes the region downstream of the jet potential core, is presented in Section 8.0. A comparison of the calculated velocities with the experimental data is also presented in this section. Finally, the general discussion and conclusions are presented in Section 9.0.

Detailed quantitative results for the mean Mach number and temperature measurements, consisting of radial profiles and centerline distributions measured at selected jet operating conditions, are presented in Part 3 of this report, which also contains temperature probe calibration curves.

2.0 LITERATURE SURVEY

2.1 INTRODUCTORY REMARKS

The main objective of this literature survey was to determine the extent of the available information on experiments and theories dealing with the effects of acoustic excitation on hot jet mixing. After an extensive and detailed literature search, it was concluded that the available literature dealing with experiments on acoustically excited heated jets is limited to a few papers only.

After having completed the review of the literature on heated excited jets, attention was focused on surveying unheated jets, which were excited in either acoustical or nonacoustical ways. It was expected that lessons learned from the unheated excited jets may have considerable direct bearing on the global performance of the heated jets.

Because of the important role of the organized coherent structures in jet mixing, papers on this subject were also reviewed. Since there is a myriad of papers dealing with the large-scale or organized turbulent structures, most of which were published during the last 10 years, only the papers that may have a direct bearing on the subject of excited hot jet mixing were encompassed in the present literature survey.

Attention was paid also to the acoustic/flow interaction in flames and combustion. It should be borne in mind that it was the change in the flame shape due to the sound effect, observed by Leconte [A.9] in the middle of the last century, that led to the discovery of the jet sensitivity to sound excitation.

In summary, altogether approximately 300 papers were reviewed, from which about 50 percent have been incorporated in the literature survey described below, because of their relevance to the subject of acoustically excited hot jet mixing.

2.2 THEMATIC CATEGORIZATION

In order to make the reading of the reviewed literature easier and keep things in their proper perspective, the papers reviewed in the literature survey have been divided into the following six groups.

    Group A: Acoustic/flow interaction in flames and combustion
    Group B: Coherent structures and jet mixing

Group C: Nonacoustic excitation of jets
Group D: Acoustic excitation of unheated jets
Group E: Acoustic excitation of heated jets
Group F: Theoretical models for excited jets

Reviewed papers, listed in the section, References, are arranged in an alphabetical order within each group. Some of the papers may cover more than one category and may, thus, appear in more than one group.

In the course of the literature search, the results of previous literature surveys on the subject of acoustically excited jets made by Brown [A.2] in 1932, Chanaud and Powell [A.3] in 1962, and Chambers and Goldschmidt [D.10] in 1977 were also used. Previous results presented in a tabular form by Chambers and Goldschmidt [D.10] have been included in Tables 2.1 and 2.2 to summarize the important parameters of the previous experiments on excited jets (Groups D and E).

A short description of the work done under each group of papers is now presented. The emphasis is, of course, placed on the last three groups.

2.2.1 Acoustic/Flow Interaction in Flames and Combustion

The influence of sound upon jets has been observed since at least 1858, when Leconte [A.9] noticed gas lamp flames pulsating in synchronization to music. In 1867 Tyndall [A.18] found that the flame was unnecessary, the fluid of the jet itself was sensitive to sound (Figure 2.1 [A.3]). Tyndall explained the effect as early transition of the jet to turbulence, Lord Rayleigh [A.15] followed Tyndall's studies with his own studies of flames, smoke jets, and liquid jets disturbed by acoustic standing waves. Brown [A.2], in 1932, reviewed the early research on the phenomenon, and continued the study of acoustically produced transition in flames and smoke jets. Hahnemann and Ehret [A.8], in 1943, were first to use the upstream internal excitation by a vibrating diaphragm. Similarly, the internal excitation was used by Loshaek et al [A.11] in 1949. Since then, many more papers have been published on this subject. In the early stages of the research, the flame served merely to visualize the changes in the jet. The later works [A.1, A.4 – A.7, A.10, A.12 – A.14, A. 16, A.17, A.19, A.20], however, pay considerable attention to the improvement of the mixing and consequently the combustion efficiency and heat transfer by the acoustic excitation of flows.

Thus, what started out as purely a curiosity for Leconte has become a subject of many modern studies primarily motivated by practical considerations.

AUTHOR [REFERENCE]. YEAR	NOZZLE SIZE	EXIT MACH NUMBER	REYNOLDS NUMBER	STROUHAL NUMBER	REMARKS
Ahuja et al [D.3] 1982	Round 51 mm	0.34 - 0.96	360,000 - 970,000	0.1 - 1.0	Flowfield and acoustic measurements
Bechert and Pfizenmaier [D.5] 1975	Round 40 mm	0.6	500,000	0.48	Acoustic measurements
Berman [D.7] 1981	Round Coaxial 88 mm (125 mm)	0.36	660,000	0.8	Bypass jet excitation
Chanaud and Powell [D.12]	Plane 1 x 75 mm	0.003	68	0.45	Experimental study of laminar jets
Crow and Champagne [D.13] 1970	Round 50 mm	0.07 - 0.12	77,500 - 130,000	0.15 0.6	Flowfield measurements
Heavens [D.17] 1979	Plane 4 x 30 mm	0.6	146,000	1.25	Flow visualization

Table 2.1 Important test parameters of reviewed experiments on acoustic excitation of unheated jets.

AUTHOR [REFERENCE] YEAR	NOZZLE SIZE	EXIT MACH NUMBER	REYNOLDS NUMBER	STROUHAL NUMBER	REMARKS
Hussain and Thompson [D.22] 1980	Plane 31 x 1400 mm	0.004 - 0.015	8,000 - 31,000	0.15 - 0.6	Experimenal study in the jet initial region
Jubelin [E.3] 1980	Round 80 mm	0.47	785,000	0.3 - 0.8	Acoustic measurements
Kibens [D.24] 1979	Round 25 mm	0.1 - 0.2	50,000 104,000	3.7 - 5.50	Acoustic measurements
Lu [D.27] 1981	Round coaxial 62 mm (151 mm)	1	1,295,000	0.2 - 5.0	Acoustic measurements
Moore [D.29] 1976	Round 39 mm	0.3 - 0.49	275,000 - 400,000	0.3 - 1.27	Shear layer instability measurements
Morris and Baltas [F.7] 1981	Round 76 mm	0.24	375,000	0.3	Comparison between theory and experiment

Table 2.1 (continued) Important test parameters of reviewed experiments
on acoustic excitation of unheated jets.

AUTHOR [REFERENCE] YEAR	NOZZLE SIZE	EXIT MACH NUMBER	REYNOLDS NUMBER	STROUHAL NUMBER	REMARKS
Morrison and McLaughlin [B.43] 1980	Round 7 mm 10 mm	1.4 – 2.5	3,700 – 8,700	0.14 – 0.18	Low Reynolds number supersonic jet
Sarohia and Massier [D.37] 1977	Round 42 mm	0.1 – 0.9	100,000 – 860,000	0.14	Flow visualization
Schmidt [D.39] 1978	Round 85 mm	0.4 – 0.6	710,000 – 1,065,000	0.53 – 0.62	Flowfield measurements
Vlasov and Ginevskii [D.44] 1967	Round 10 mm 30 mm	0.04 – 0.35	30,000 – 260,000	0.26 – 3.89	Flowfield measurement
Zaman and Hussain [D.48] 1980	Round 25 mm 53 mm 76 mm	0.08 – 0.15	12,000 – 120,000	0.3 – 1.6	Vortex pairing experiment
Zhangwei [D.50] 1982	Round 12.5 m	0.15	35,000	1.0	Acoustic and flowfield measurements

Table 2.1 (concluded) Important test parameters of reviewed experiments on acoustic excitation of unheated jets.

Author [Reference] Year	Nozzle Size	Exit Mach Number	Total Temperature	Reynolds Number	Strouhal Number	Remarks
Ahuja et al [E.1] 1982	Round 51 mm	0.78	800 K	285,000	0.5	Converging nozzle flow and acoustic measurements
Ivanov [E.2] 1969	Round 12 mm	0.25	400 K	52,000	0.031 – 0.054	Diverging diffuser flow and acoustic measurements
Jubelin [E.3] 1980	Round 80 mm	0.47	600 K – 900 K	250,000 – 390,000	0.3 – 0.8	Acoustic measurements
Lu [E.4] 1981	Round Coaxial 62 mm (152 mm)	1	810 K	500,000	0.2 – 5.0	Acoustic measurements

Table 2.2 Important test parameters of reviewed experiments on acoustic excitation of heated jets.

In conclusion, the important results derived from the survey of papers in the first group can be summarized as follows:

o   jet excitation may improve the combustion process and consequently the combustion efficiency

o   acoustic excitation may be used to control the temperature distribution at the combustion-chamber exit.

2.2.2   Coherent Structures and Jet Mixing

One of the most important discoveries in the field of fluid dynamics in the last 15 years is the fact that turbulence is characterized by a remarkable degree of order [B.15]. However, the progress in incorporating this structure into practical engineering methods has been very slow, mainly because the prediction of the large scale turbulent structure behavior, under given conditions, is still very uncertain. A simplified view of a free jet developing from a thin laminar nozzle boundary layer, showing the growth of the coherent structure, is shown in Figure 2.2 [B.58].

The intense current interest in large-scale coherent structures stems from the expectation that these structures play a key role in the transports of heat, mass, and momentum and noise production in turbulent shear flows [B.25]. The large-scale processes and the resulting mean flow seem to be little affected by viscosity [B.48]. The effects of viscosity appear indirectly through the initial shear layer conditions and not through direct action of viscosity on the developing turbulent structure. The evolution of the mixing layer depends significantly on the initial state: laminar or turbulent [B.24]. Under certain conditions, the mixing layer would spread first, stop spreading for a short distance, and then begin spreading again [B.12]. There is little doubt that by choosing the proper parameters and conditions, it will be possible to affect the process of jet mixing in a desired way.

The available literature about coherent structures and jet mixing is rather vast. It was not our intention to make a complete literature survey on this subject. Extensive literature surveys on this subject have been published by others from time to time, notably by Laufer [B.38] in 1975, Roshko [B.48] in 1976, Yule [B.58] in 1978, Hussain [B.25] in 1980, and Cantwell [B.12] in 1981. Our literature survey of the papers on coherent structures [B.1 - B.58] is restricted to the papers that are most relevant to the present program.

The most important results of this part of the literature search relevant to the present program are:
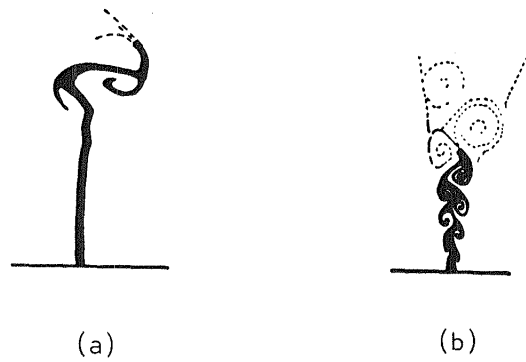
10

Figure 2.1 (a) Unexcited smoke jet and
            (b) excited smoke jet [A.3].
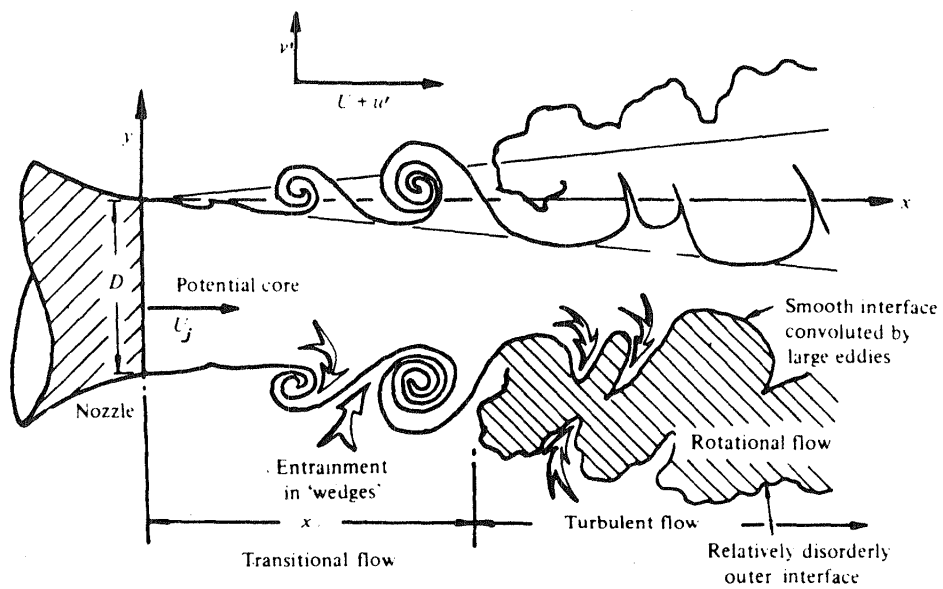

Figure 2.2 Turbulent coherent structure development in a
            free jet [B.58].

o   jet mixing is controlled by the large-scale structure in the flow

o   more efficient mixing can be achieved by a more rapid growth of
     the large-scale structure in the jet shear layer

o   the evolution of the large-scale structure depends significantly
     on the type of the nozzle exit boundary layer (i.e., whether it is
     laminar or turbulent)

The key role, which the type of the nozzle exit boundary layer may play in
the coherent structure growth, requires that any experimental investigation
of the coherent structure behavior must pay proper attention to possible
changes of the nozzle exit boundary layer as a function of the experimental
conditions.

2.2.3 Nonacoustic Excitation of Jets

Many efforts have recently been directed towards improving the mixing based
on the recognized role of the developed large-scale structures in the
mixing process. The growth of the large-scale structure can be stimulated
when the jet is excited by rotating flow [C.4 – C.7, C.9, C.18], by forced
pulsation [C.1, C.3 , C.10, C.13, C.15 – C.19], by oscillating vanes or
plates [C.2, C.11, C.12, C.14, C.18], and, of course, by acoustic
excitation, which is described in the next subsection.

The regimes of a planar jet mechanically excited by an oscillating plate
are shown in Figure 2.3 [C.11].

Upper Zone Regime.   For excitation frequencies higher than the order of
three to four times the natural breakdown frequency, the jet was
essentially unaffected by the excitation.

Preservation Regime. The core flow of the jet tended to be preserved if
the excitation frequency fell within the region designated in Figure 2.3.

Matched Excitation Regime.   When the excitation frequency was matched with
the natural breakdown frequency, the effect was to hasten the process of
vortex formation and growth relative to the natural breakdown state.

Forced Fusion Regime.   At applied frequencies on the order of one-third the
natural breakdown frequency of the jet, the natural breakdown vortices were
forced   to undergo early fusion (or coalescence), which results in
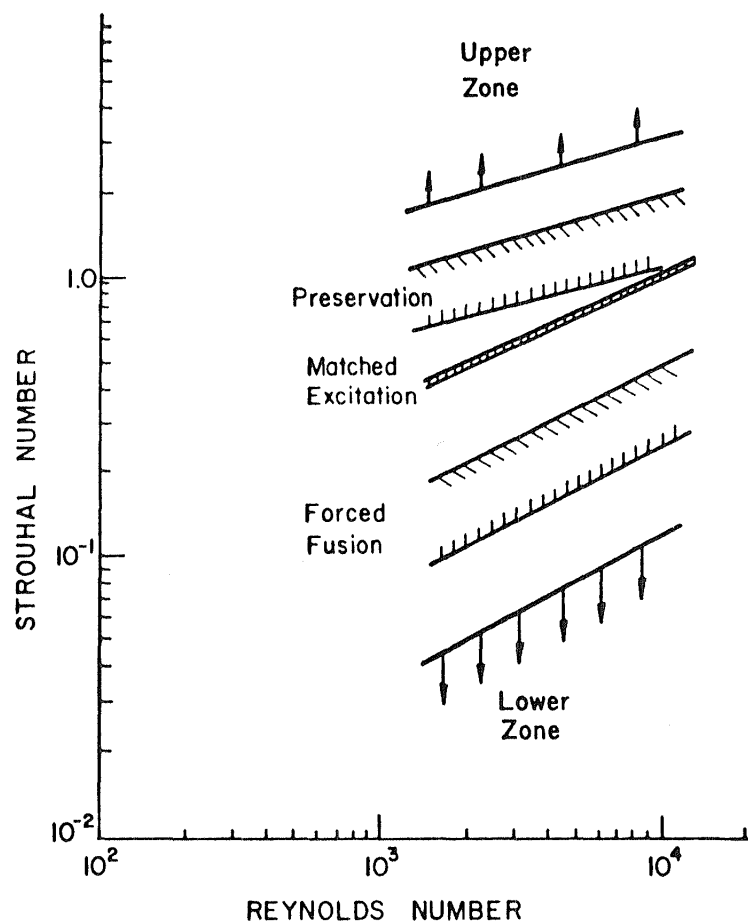formation of large major vortices.

Figure 2.3 Dimensionless plot of Strouhal number versus Reynolds
number indicating regimes of excited jets [C.11].

Lower Zone Regime. At excitation frequencies approximately one tenth (or lower) of the natural breakdown frequency of the jet, vortex growth was unaffected in the formation region.

In summary, it was found that:

o   the reaction of a jet to an applied disturbance can be grouped into several regimes

o   an evolution of the large scale structure in the jet shear layer is more rapid if the frequency of an applied disturbance is close to the jet natural break down frequency (which is a function of the jet Reynolds number).

2.2.4   Acoustic Excitation of Unheated Jets

Brown's study [D.9] in 1935 may be considered as the first modern study of the phenomenon of acoustic excitation of jets. In recent years, many studies [D.1 – D.50] have been initiated to examine the sensitivity of the planar and circular jets to acoustic excitation. In most cases, upstream or internal acoustic excitation has been used, but some experiments have also been conducted by using external acoustic excitation.

Previous literature surveys on the subject of jet acoustic excitation have been made or cited by Chanaud and Powell [D.12] in 1962, Hussain and Zaman [D.20] in 1975, Chambers and Goldschmidt [D.10] in 1977, Vlasov and Ginevskii [D.45] in 1979, and Ahuja, et al [D.3] in 1982.

The effects of acoustic excitation on jet behavior are summarized in Figures 2.4 [D.3], 2.5 [D.45], and 2.6 [D.45]. The effect of a low-frequency acoustic signal excitation (St_j = 0.2 – 0.6) on a turbulent jet results in the enhancement of turbulent mixing, the shear layer broadens, the length of the potential core decreases, and turbulence intensity level increases significantly in the nozzle near region as seen in Figure 2.4 by Ahuja et al [D.3] and in Figure 2.5 taken from Reference D.45. Similar results were obtained in 1971 by Crow and Champagne [D.13] and later confirmed by Sarohia and Massier [D.37], Schmidt [D.39], Vlasov and Ginevskii [D.44, D.45], Hussain [D.21], and Zaman [D.49], amongst others.

The enhancement of turbulent mixing can be produced by exciting the shear layer with a fluctuating pressure at the nozzle of only 0.08% of the jet dynamic head but with the correct Strouhal number, as found by Moore [D.29]. This was also observed and confirmed by others [D.3, D.45].

On the other hand, the effect of a high-frequency acoustic signal (St_j = 2 – 5) on a turbulent jet results in the attenuation of the turbulent mixing,
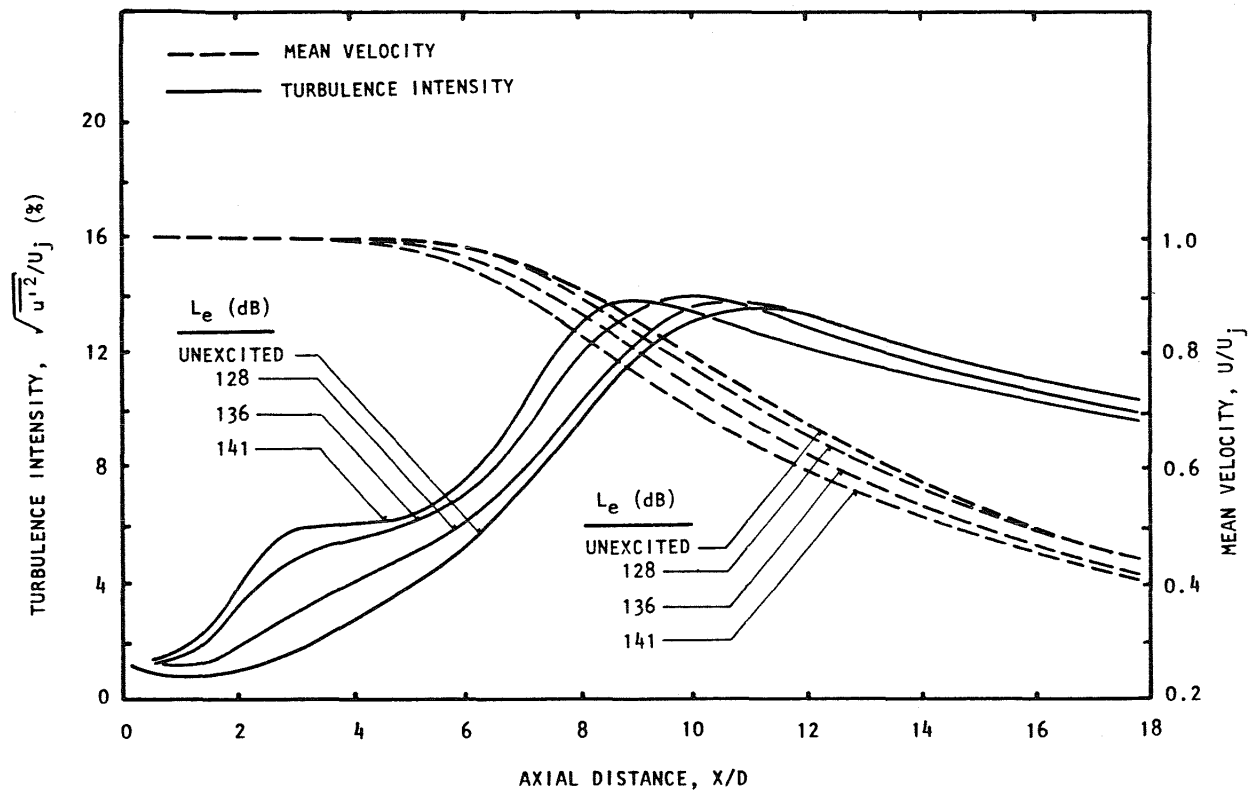
14

Figure 2.4   Excitation-level effects on centerline distributions.
$M_j = 0.78$, $U_j = 255$ m/s, Unheated, Static, $St_j = 0.5$, (0,0) Mode [D.3].
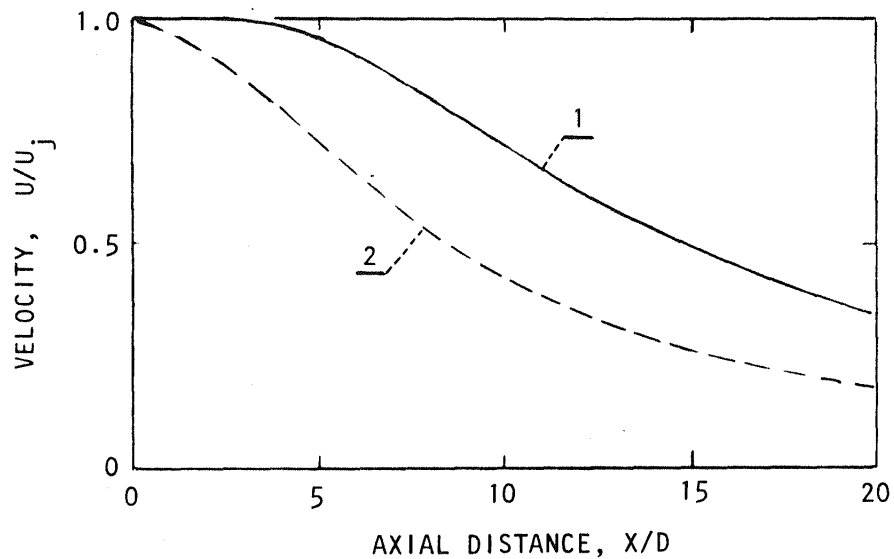
Figure 2.5 Effect of acoustic excitation on centerline distribution
of mean velocity of a transonic jet.
M_j = 0.93, Re_j = 1,260,000
1) unexcited jet
2) tone excited jet, St_j = 0.25, L_e = 170 dB [D.45]

Figure 2.6 See next page
Centerline distribution of turbulence intensity and
mean velocity at various excitation Strouhal numbers.
M_j ~ 0.2, Re_j ~ 15,000
a) axial turbulence intensity
b) radial turbulence intensity
c) axial mean velocity
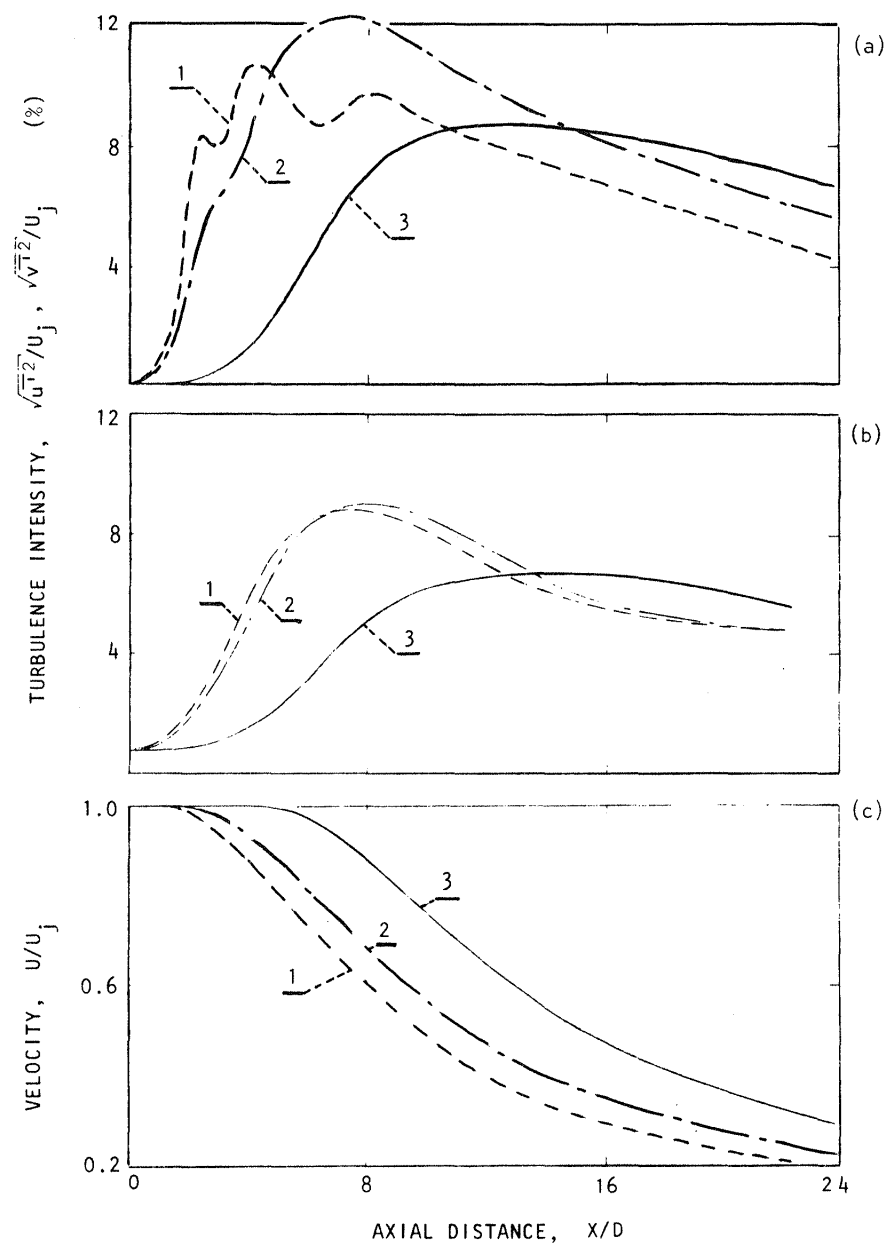1) St_j = 0.25, 2) St_j = 0.3, 3) St_j = 2.75 [D.45]

16

Figure 2.6 For caption see previous page.

the periodic vortices break up into smaller elements, the shear layer becomes thinner, and the length of the potential core increases. A comparison of the low and high frequency acoustic excitation effects upon jet behavior is shown in Figure 2.6 [D.45]. Similar results were obtained also by Zaman and Hussain [D.48, D.49], who found that a noticeable suppression occurs over the Strouhal number range $0.008 \leq St_\theta \leq 0.024$, and the minimum point falls roughly in the St_θ range of $0.016 - 0.019$. The Strouhal number (St_θ) in this case was based on the initial shear layer momentum thickness rather than on the jet diameter.

The important parameters of reviewed experimental investigations are summarized in Table 2.1.

It seems reasonable to expect that the jet sensitivity to the acoustic upstream excitation is affected by the nozzle exit boundary layer conditions. The strong dependance of the large-scale structure growth on the jet initial condition (i.e., laminar or turbulent nozzle exit boundary layer [B.24]) has already been discussed. Zaman and Hussain found [D.48] that, for laminar exit boundary layer, the vortex pairing in the jet shear layer occurs regularly in space and time, for $Re_j < 5 \times 10^4$, but becomes intermittent with increasing Re_j or fluctuation intensity in the initial boundary layer.

Finally, some of the listed references deal with the state-of-the-art experimental techniques suitable for visualization and measurements in unheated and heated jets under acoustic excitation. Stroboscopic visualization techniques are presented in References D.17 and D.47, and a laser velocimeter capable of conditionally sampled measurements is described in References D.6 and D.26.

The lessons learned from these studies can be summarized as follows:

o   acoustic excitation of unheated jets can cause either enhancement or suppression of the turbulence intensity levels in the nozzle near field

o   the jet mixing rate, and consequently the jet spreading rate, can also be increased or decreased by the upstream acoustic excitation

o   the jet mixing enhancement or suppression, in the case of unheated jets, depends on the excitation Strouhal number and on the flow Reynolds number

o   the jet mixing enhancement or suppression depends strongly on the type of the nozzle exit boundary layer (laminar or turbulent) and on the nozzle exit boundary layer thickness

18

These results are consistent with the findings of Subsection 2.2.2, where the effects of large-scale structures on jet mixing were discussed.

The results emphasize the role of the initial condition of the jet shear layer (i.e., the type of the nozzle exit boundary layer), and the role of the excitation Strouhal number on jet mixing of a tone excited jet.

2.2.5 Acoustic Excitation of Heated Jets

As already pointed out, there is a shockingly short list of studies on the behavior of tone excited heated jets in comparison with a preponderance of papers on the behavior of excited unheated jets. In all, we found only 6 papers [E.1 - E.6] dealing with tone excited heated jets. To some extent, it would be possible to consider the early experiments on tone sensitive flames as the experiments on heated jets, too. But for all these cases, the Reynolds numbers were very small, because of very low operating flow velocities to keep the flame stable, and are thus out of the range of flow conditions of practical interest to the present program. The important parameters of reviewed experimental investigations are summarized in Table 2.2.

Jubelin [E.3] investigated the tone excited heated jets of Mach number equal to 0.47 at two temperatures equal to 300 K and 600 K and for Strouhal number range of 0.4 to 0.7. His investigation was made only from a noise generation point of view, and no flow measurements were obtained. He found that the noise response of hot jets to acoustic excitation is appreciably different from that of unheated jets. By examining the resulting changes in the far field jet noise levels, Jubelin concluded that the maximum jet sensitivity to excitation decreases slightly when the jet temperature increases. On the other hand, by examining the acoustic results in a different way, it was also concluded by Jubelin that "hot jets appear to be more easily 'excitable' than unheated jets."

A jet of Mach number 0.98 heated up to 800 K was acoustically excited in one configuration of Lu's experiments [E.4] on the effects of upstream acoustic excitation on coaxial jets. Similar to Jubelin, Lu obtained only the acoustic measurements, and no flow measurements were obtained.

Mickelsen and Baldwin [E.5] investigated the aerodynamic mixing by a standing sound wave downstream from a continuous line source of heat. The temperature of the flow behind the heat source was very mild, approximately 10 K higher than the temperature of the surroundings. They found that the velocity fluctuations in a periodic sound field contribute to increased aerodynamic mixing.

Ivanov [E.2] measured mean velocity and turbulence intensity behind a

conical diffuser, which was attached to a convergent nozzle. The length of the diffuser was 6.25 nozzle exit diameters. Mach number of the flow at the diffuser exit was equal to 0.25 and total temperature was equal to 400 K. The Strouhal number based on the diffuser exit diameter ranged from 0.031 to 0.054. He found that the effect of low-frequency acoustic excitation was to increase the rate of velocity decay slightly, and simultaneously to decrease the turbulence intensity level substantially up to 9 diffuser exit diameters.

All of Ivanov's measurements were made practically beyond the end of the jet potential core emanating from the nozzle (the attached diffuser was longer than the corresponding length of the jet potential core). Ivanov's hot jet results indicate trends similar to those seen in Ahuja et al's unheated jet results for axial distances beyond $X/D = 9$ shown in Figure 2.4 [D.2].

For the heated jet, however, Ahuja et al's experiments [E.1] showed an opposite trend. As is seen in Figure 2.7, acoustic excitation of the heated jet ($M_j = 0.78$, $T_t = 800$ K, and $St_j = 0.5$) increased the length of the potential core a little, and decreased the turbulence intensity level up to $X/D = 8$. At larger distances increased turbulence intensity levels were measured.

The above mentioned discrepancy complemented by a severe lack of experimental data show that further work is definitely needed to assess the effects of upstream acoustic excitation on heated jets. No firm conclusion can, therefore, be drawn from the results discussed above.

Despite the lack of sufficient knowledge about excited heated jets, an important practical application of this phenomenon was shown by Vermeulen et al [E.6]. Acoustic control of mixing process in a small combustor was successfully tested. The desired exit plane temperature distribution was achieved, while the pressure loss of the combustor and its combustion efficiency were insignificantly affected by the acoustic excitation. The acoustic modulation can be used to control the exit plane temperature distribution. As seen in Figure 2.8 [E.6], it is possible to trim the temperature profiles. The temperature profile behavior indicates that improved mixing may be due to vortex action.

The important results learned from this part of the literature survey can be summarized as follows:

o   there is a serious lack of experimental data on the subject of the effects of acoustic excitation on hot jet mixing
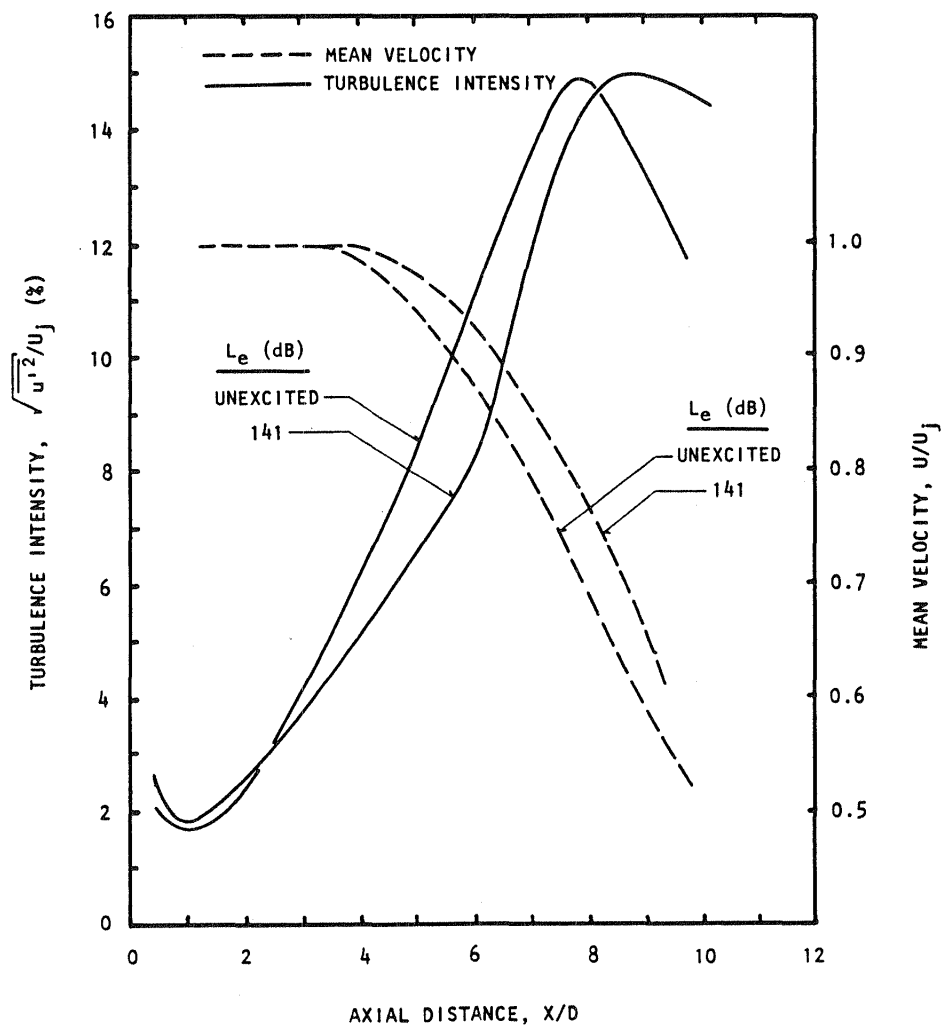
20

Figure 2.7   Effects of upstream excitation on the
centerline distributions of the heated jet.
M_j = 0.78, U_j = 428 m/s, T_t = 800 K, Static,
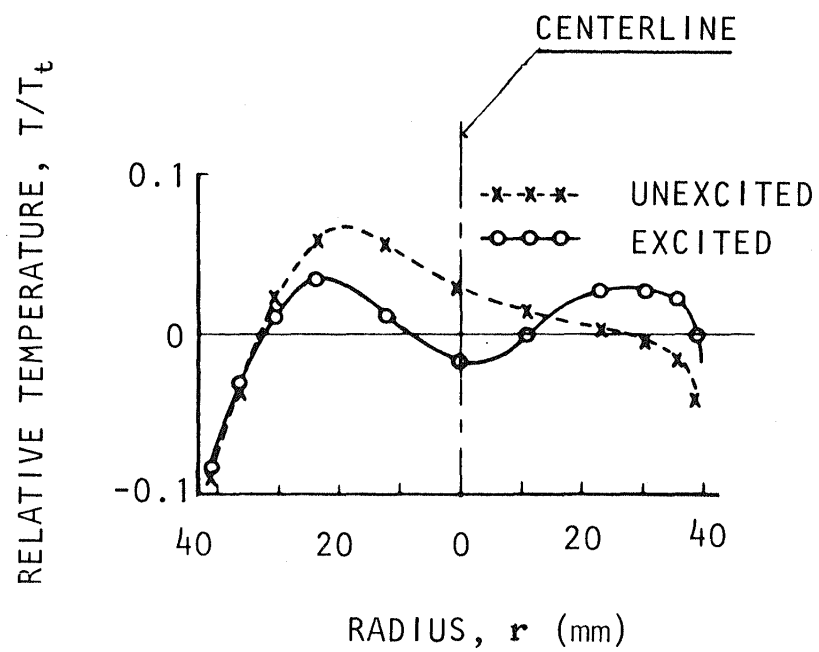St_j = 0.5, (0,0) Mode [E.1].

Figure 2.8   Exit plane dimensionless radial temperature
             profiles [E.6].

o   no firm conclusions, as far as the trends in hot jet mixing due to acoustic jet excitation are concerned, can be drawn but a strong dependence on the excitation Strouhal number, flow Reynolds and Mach numbers, and jet temperature may be expected as indicated by the discrepancy between known experimental results .

2.2.6 Theoretical Models for Excited Jets

The first theoretical model of the stability of tone excited jets was given by Rayleigh [F.10] in 1878. Rayleigh's analysis, based on inviscid models, did not agree fully with the experiment.

Savic [F.11] developed a theory by applying Tollmien's general criterion of instability; he assumed an inflection in the velocity boundary of the jet near the nozzle exit [D.14]. Savic's theoretical results appeared to explain the results obtained by Brown [D.9].

Michelsen and Baldwin [F.4] based their theory on a kinetic analysis of the motion of the molecular-diffusion wake and derived equations for the time variation of temperature and the time mean temperature at points throughout the mixing region. This analysis showed that standing sound waves displace the diffusion wake in a manner similar to the displacements of a flag waving to a harmonic mode. The wake deformation is greater for higher sound intensities.

McCormack and Cochran [F.3] divided the jet in two separate regions: (a) the near field, which contains the potential core; (b) the far field, beyond the potential core, which is all mixing region. The near field region is considered as a case of the mixing of two uniform streams, one of which is at rest. Mathematically, the problem that is dealt with here is that of the effect of a periodic source of vorticity on an incompressible submerged laminar gas jet. A sort of pressure gradient is set up near the jet axis, which results in more rapid transport of momentum in the radial direction. Thus, the rate of mixing is accelerated and the potential core length shortened.

Maestrello and Bayliss [F.2] simulated numerically the interaction of an acoustic pulse with the experimentally determined mean flowfield of a spreading jet. The simulation was obtained by solving the Euler equations linearized about the spreading jet. It was shown that some of the observed differences in the acoustic spectra of heated and unheated jets can be attributed to differences in the stability characteristics of the jets. The heating of the jet reduces the amplification of sound due to the flow and causes a shift of the farfield spectra toward lower frequencies.

To date, the most advanced theory of a tone excited jet appears to be that of Morris and Tam [F.1, F.5 - F.9, F.12 - F.16]. The theory predicts the change in turbulent structure of a round jet in the presence of an acoustic excitation. The excitation is assumed to trigger instability waves of a known initial amplitude at the jet exit. As these waves propagate downstream, they extract energy from the mean flow and transfer it to the random turbulence. This results in an increase in the levels of the turbulence and a resulting increase in the radiated broadband noise. The numerical procedure allows for radial as well as axial variations in the averaged properties of the jet. The theory agrees very well with an experiment for unheated tone excited jets [F.1, F.6]. A comparison between the measured and the predicted rates of spread of unheated unexcited and unheated tone excited jets is shown in Figure 2.9. However, a discrepancy was found for the case of heated tone excited jet [F.1].

In summary, it was found that:

o   only a few attempts have been made at developing theoretical models of acoustically excited jets, but the most complete model was found to be that of Morris and Tam

o   Morris-Tam model compared well with measurements for unheated jets

o   the same model, however, failed to predict the trends for the corresponding measurements (to date) for heated jets

2.3   CONCLUDING REMARKS

After having reviewed the literature in each of the six groups, it becomes quite clear that there exists a shockingly short list of investigations on the behavior of acoustically excited heated high speed jets. In fact, in addition to the Lockheed work [E.1], only one other experimental study [E.2] directly dealing with the subject of the effects of acoustic excitation on mixing of high speed hot jets was found in the open literature. Furthermore, the findings of these two experiments contradict each other.

What is clear, however, is that, for the unheated jets, the acoustic excitation can produce either enhancement or suppression of the turbulence intensity level in the nozzle near field, and consequently, the jet mixing. The severity of this effect depends on the excitation Strouhal number, excitation level, and on the flow Reynolds number. The literature survey also revealed that, for the unheated jets, the type of the nozzle exit boundary layer (laminar or turbulent) may play a key role in the nature of
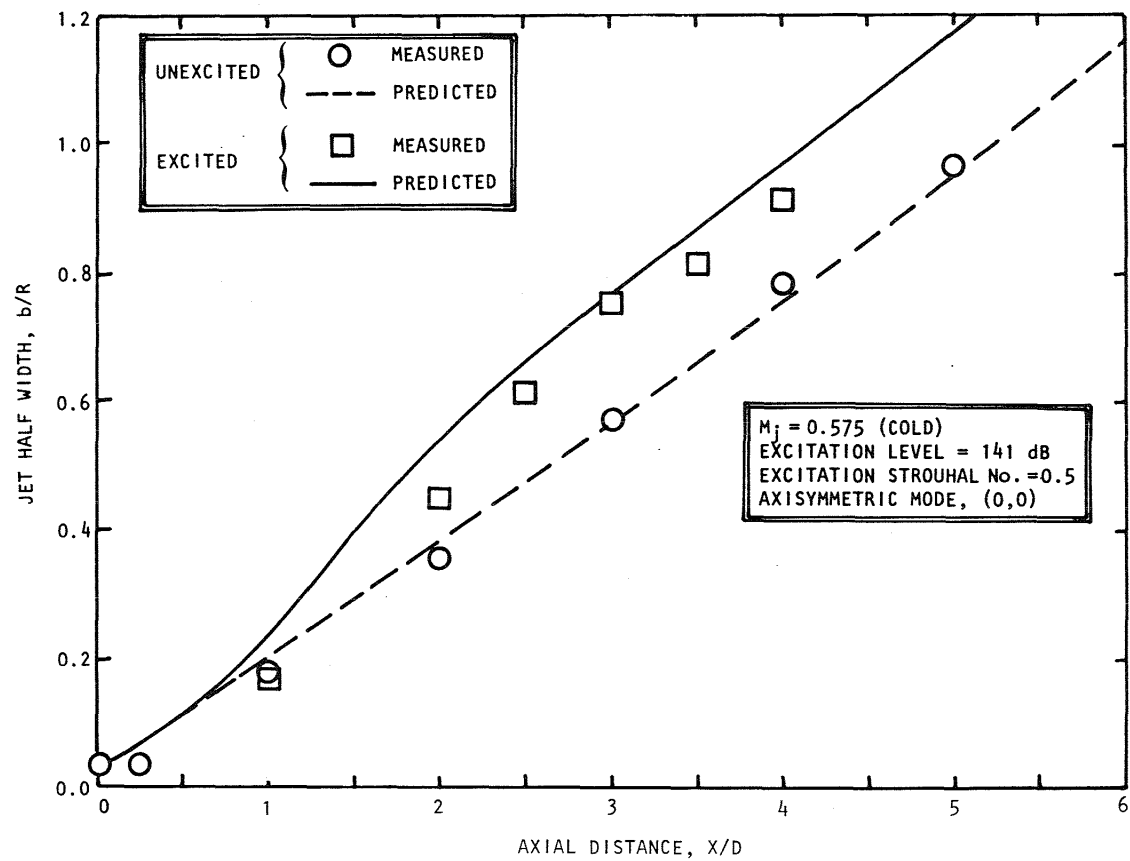
24

Figure 2.9   Comparison between measured and predicted rate of spread
             of jet [F.1].

the jet response to the upstream acoustic excitation.

As regards the theoretical models of acoustically excited jets, the model developed at Lockheed [F.1] under a previous NASA-Lewis contract (NAS3-21987) by Morris and Tam still stands out as the most complete model. It takes into account the various aspects of flow/acoustic interaction, and fully incorporates the role of large-scale turbulent structures on jet mixing. This theory has been, to a large extent, verified for the unheated jets, but a large discrepancy obtained on comparing it with the results for the heated jets [E.1], still remain to be resolved.

The moral to be derived from this literature survey is that acoustic excitation as a means of increasing mixing of heated jets holds great potential, but a carefully planned and well-controlled experimental study is desperately needed.

3.0 TECHNICAL APPROACH

The objective of this program was to obtain detailed experimental data on the effects of relatively strong upstream acoustic excitation on the mixing of heated jets with the surrounding air. The major effort was devoted to the experimental data acquisition. Some of the experimental results were compared with available theory in terms of the relationship between the excitation characteristics and changes in the mean velocity distribution of the jet for a given jet operating condition. The theory used for this comparison was an extension of the theory presented in Reference F.1.

The major objectives of this work were accomplished by conducting work under the following three tasks:

Task 1: Optimization Study

Task 2: Flowfield Experiments

Task 3: Theoretical analysis

The emphasis was on Task 2 so as to acquire a sufficient amount of reliable experimental data for a future detailed analysis.

3.1 RELEVANT TEST PARAMETERS

In an experimental program of the present nature, a large number of parameters needs to be considered to determine the effects of acoustic excitation on the hot jet mixing. The success of such a program depends heavily upon whether the correct excitation parameters and flow conditions that show strongest flow changes in response to acoustic excitation can be identified. Based upon the literature survey presented in Section 2.0 and our experience gained from our earlier work on similar studies, the following parameters appear to be the most important for the present program.

<u>Jet operating conditions:</u>

Nozzle pressure ratio ζ

Fully expanded jet Mach number M_j

Jet total temperature T_t

27

Upstream acoustic excitation conditions:

Frequency f_e

Strouhal number St_j

Level L_e

3.2 TEST PLAN

In order to determine the effects of the individual parameters on hot jet mixing, one significant parameter was varied at a time. The salient details of the jet operating and the acoustic excitation conditions at which the majority of the experiments were conducted are given below.

3.2.1 Jet Operating Conditions

The test plan, as far as jet operating conditions are concerned, is summarized in Figure 3.1 and Table 3.1.

Since the main purpose of this program was to study the mixing in heated jets, the test matrix had to cover a suitable range of jet temperatures. Also, since the Reynolds number of a fixed Mach number gas jet is reduced considerably by heating, the question of Reynolds number dependence was also addressed. Keeping this in mind, the test matrix, shown in Figure 3.1, was carefully selected to provide information for:

(1) varying total temperature at fixed jet Mach number (line A),

(2) varying jet pressure ratio at fixed jet temperature ratio (lines B and C),

(3) varying jet pressure and temperature ratios at fixed Reynolds number (curves D, E, and F),

(4) varying jet pressure and temperature ratios at fixed jet velocity ratio, U_j/a_o (curves G and H).

The solid dots (labeled 1 - 8), shown in Figure 3.1, represent the basic jet operating conditions. Additional jet operating conditions were set up, to clarify in greater detail the effects of any of the jet parameters on hot jet mixing. These additional jet operating conditions are marked by empty circles in Figure 3.1.
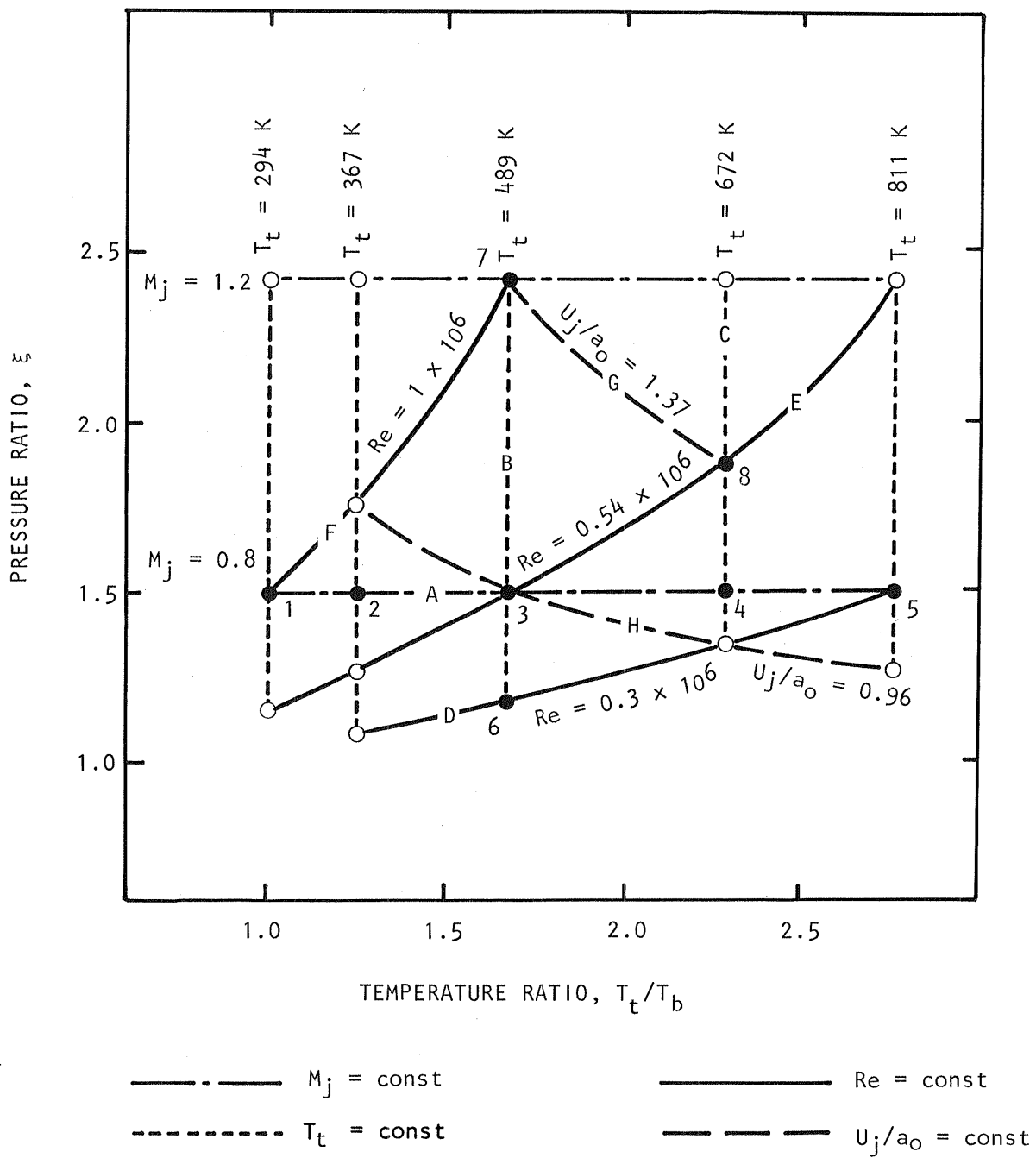
28

Figure 3.1 Jet operating conditions.

TEST POINT	TOTAL TEMPERATURE T_t K (°F)	PRESSURE RATIO ξ	JET MACH NUMBER M_j	REYNOLDS NUMBER Re_j (MILLION)	VELOCITY RATIO U_j/a_o
1	294 (70)	1.50	0.78	1.0	0.74
2	367 (200)	1.50	0.78	0.8	0.83
3	489 (420)	1.50	0.78	0.5	0.95
4	672 (750)	1.50	0.78	0.4	1.12
5	811 (1000)	1.50	0.78	0.3	1.23
6	489 (420)	1.17	0.48	0.3	0.60
7	489 (420)	2.43	1.20	1.0	1.36
8	672 (750)	1.88	0.99	0.5	1.38

Table 3.1 Test matrix of jet operating conditions.

3.2.2 Acoustic Excitation Conditions

Acoustic excitation conditions were restricted to a relatively narrow range because of the low response of most commercially available acoustic drivers at high frequencies. Thus, the maximum achievable excitation frequency, at reasonably high excitation level, was f_e = 4500 Hz, which limited the excitation Strouhal number to the range of St_j < 0.6 at the extreme jet operating conditions. The maximum achievable excitation levels (L_e), measured at the nozzle exit, were L_e = 150 $\pm$ 1 dB.

3.3 PILOT STUDY

Prior to acquiring comprehensive data, a pilot study was carried out in two parts. In part 1, the experiments were carried out to clarify the effects of jet Mach number and jet total temperature on the nozzle exit boundary layer displacement thickness distribution, and to study the dependence on jet Reynolds number. Simultaneously, the type of boundary layer at the nozzle exit at various experimental conditions was determined, because it was expected that the nature of the boundary layer may play an important role in determining the behaviour of acoustically excited jets. These experiments are described in Section 5.0.

In the second part of the pilot study, optimization experiments were carried out to determine the excitation Strouhal number that produces the strongest effects in terms of the changes in the mean velocities and temperatures. As described in Section 6.0, the Strouhal number optimization was based on changes of local Mach number on the jet centerline at nine nozzle exit diameters downstream of the nozzle exit. For each test condition, the Strouhal number that produced the maximum change in the local Mach number on the jet centerline at X/D = 9 was selected as the peak Strouhal number for the following flowfield experiments . The effects of excitation level on jet behaviour at different jet total temperatures were also investigated under the pilot study.

3.4 FLOWFIELD EXPERIMENTS

The objective of the experiments under this task was to obtain a general mean flow survey of the acoustically excited heated jets. These experiments were carried out only for those jet operating conditions, where the effects of upstream acoustic excitation on jet behaviour were determined by the pilot study. The flowfield experiments were performed under two tasks consisting of (1) mean flow survey and (2) flow visualization.

The mean flow survey consisted of one centerline distribution and five radial profile measurements of Mach number and jet temperature for each of the jet operating conditions. The results of flowfield measurements are given in Part 3.

The second task consisted of flow visualization using a unique laser schlieren system, developed recently at Lockheed. Phase-locked flow pictures were taken for those flow conditions that showed significant modification due to upstream tone excitation. The results of flow visualization experiments are discussed in detail in Section 7.0.

3.5 THEORETICAL ANALYSIS

The formulation of the theoretical analysis, described in Reference F.1 was capable of predicting flow behaviour only up to the end of the jet potential core . As a part of this program, this analysis of excited jets has now been extended to consider the region downstream of the potential core. This enables the decay of the centerline velocity to be predicted as a function of jet operating and excitation conditions. The analysis in this region is more complicated than in the potential core region. This is due mainly to the dependence of the mean density on the local centerline velocity, which is a dependent variable in the analysis. Two computer programs have been written. The first evaluates the coupling between the acoustic excitation and the instability wave in the potential core region as well as the local growth rates of the instability waves. This calculation is performed for given jet operating conditions and a specified Strouhal number and azimuthal mode number for the excitation. The second program calculates the axial development of the jet and the instability wave for specified excitation levels.

4.0 FACILITIES AND DATA ACQUISITION

All experiments described in this report were conducted in Lockheed's Jet-Flow Facility. This facility was also used for all measurements presented in Reference D.3. Further details of the test facility and test procedures are given below.

4.1 TEST FACILITY

4.1.1 Jet-Flow Facility

The jet-flow facility used in this program is designed to produce parallel, low-turbulence, coaxial flows, or single-stream flow with provision for simulating flight effects with a large secondary nozzle. Only the primary or inner flow was used for the present experiments. A general view of the Jet-Flow Facility is shown in Figure 4.1. A cross-sectional view of the facility is shown in Figure 4.2. The primary flow enters through a 256-mm-dia plenum, followed by an initial contraction to the 102-mm-dia source-section duct. The 50.8-mm-dia test nozzle is attached to the source-section duct. The plenum to nozzle area contraction ratio is 25.

Two precisely-machined stainless steel nozzles were used in the present program. One of the nozzles is convergent, while the other one is convergent-divergent with fully-expanded design Mach number of 1.2. The exit diameter of each nozzle is 50.8 mm.

The jet flow in this facility can be heated to temperature reaching 1000 K at pressure ratio exceeding 4. The flow is heated by a through-flow propane burner. Both pressure and temperature conditions can be controlled either by a computer or manually.

4.1.2 Upstream Acoustic Excitation Source

The source section used in this series of experiments is the same source section that was used in Lockheed's earlier studies on acoustically excited jets [D.2,D.3], but this time it was provided with four additional drivers. The source section is depicted in Figure 4.2. It is centered around a 102-mm-dia air sup ply duct, which is connected to a test nozzle. It utilizes eighth 100-W ALTEC model 290E acoustic driver units. Each driver is enclosed in a pressure vessel to equalize the pressure across the driver
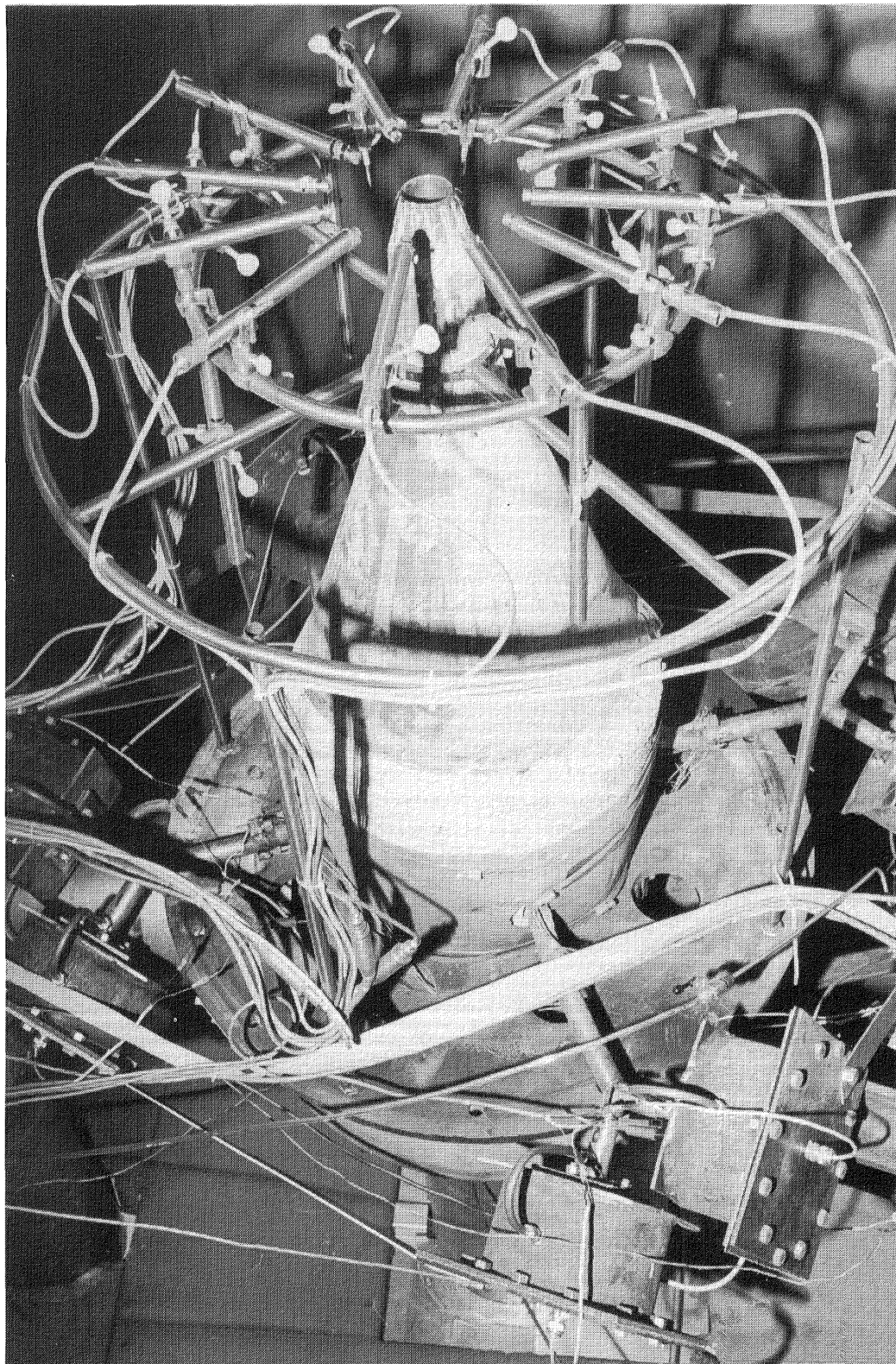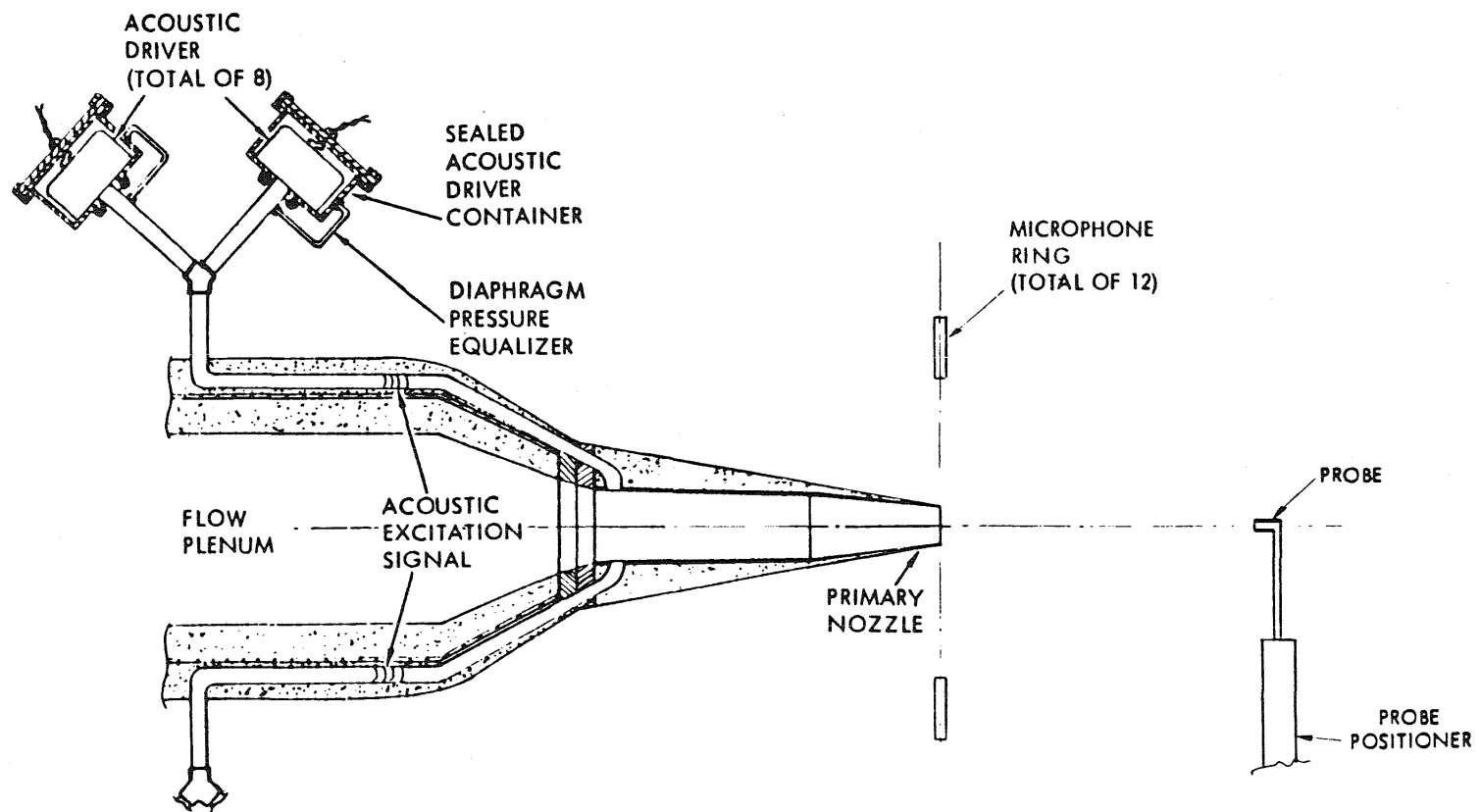
Figure 4.1 Jet flow facility.

Figure 4.2   Jet flow facility and source section.

diaphragm. The tubes connecting the drivers to the 102-mm-dia air supply duct have provision for cooling air for the high-temperature tests, in order to protect the diaphragms.

The sound is funneled to the 102-mm-dia duct through four 25.4-mm-dia tubes, each tube connected to a pair of acoustic drivers through a "Y" connector, as seen in Figure 4.3.

Since it is important that the 25.4-mm-dia tubes connecting the driver section to the air supply duct do not produce significant flow disturbances other than the excitation signal itself, the source-duct-nozzle system has been thoroughly calibrated in the past and found to be aerodynamically acceptable.

To ensure that the plane wave (0,0) mode of acoustic excitation was generated, both phases and amplitudes of sound at the nozzle exit plane were measured by 12 microphones as shown in Figures 4.1 and 4.5. The scheme used in this study for excitation mode detection is described in detail in Reference D.3.

4.1.3 Flow Visualization Setup

The jet-flow facility is equipped with a single-converging-mirror schlieren system shown in Figure 4.4. In this system, the light makes a double-pass through the test section. The system uses a wedge mirror instead of a splitter plate to separate the source and return beams.

The schlieren system was used for a photographic ensemble averaging of periodic structures in a tone excited jet. The method of photographic ensemble averaging consists of repeated synchronized triggering of a light source and superposition of all the schlieren images on a single photographic film to reinforce the image of the coherent periodic structure in the flow. The frequency of repeated photographic shots is usually limited to low frequencies by shutter mechanical restrictions or light-source recharging limitations. The schlieren system used here is unique in that it enables photographic ensemble averaging of periodic flow structures with frequencies up to the order of 100 kHz.

The system uses monochromatic laser light. The light source consists of a continuously operating 18-W Ar-Ion laser, Bragg cell modulator, and a spatial filter. In operation, the excited Bragg cell acts as a shutter deflecting the laser beam off the spatial filter and thus effectively blocking the laser beam from a photographic plate. Because the Bragg cell is excited by an electronic signal of a frequency in a MHz range, the shutter is no longer limited to low frequencies. A simple electronic device controlling the Bragg cell excitation enables the selection of both
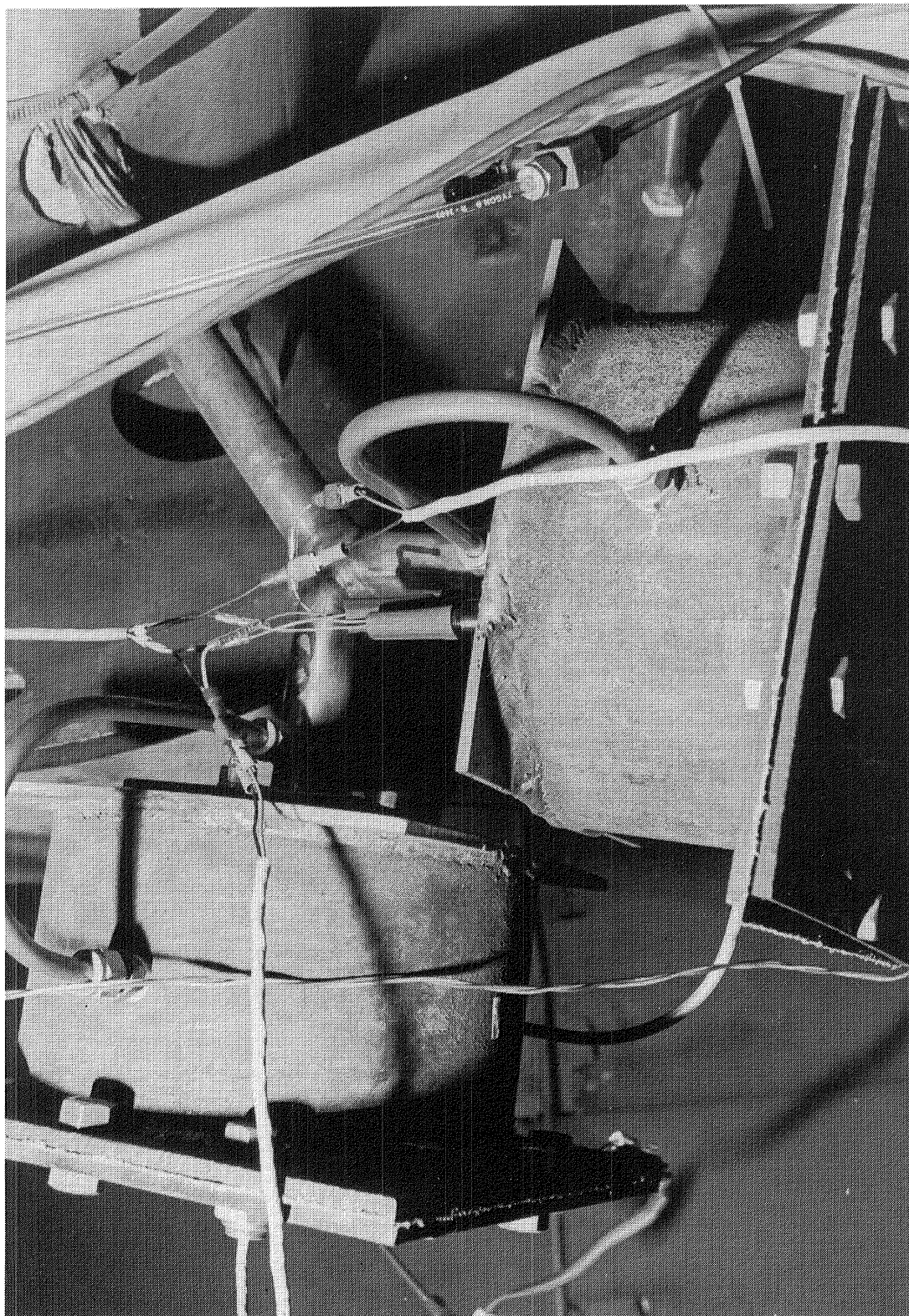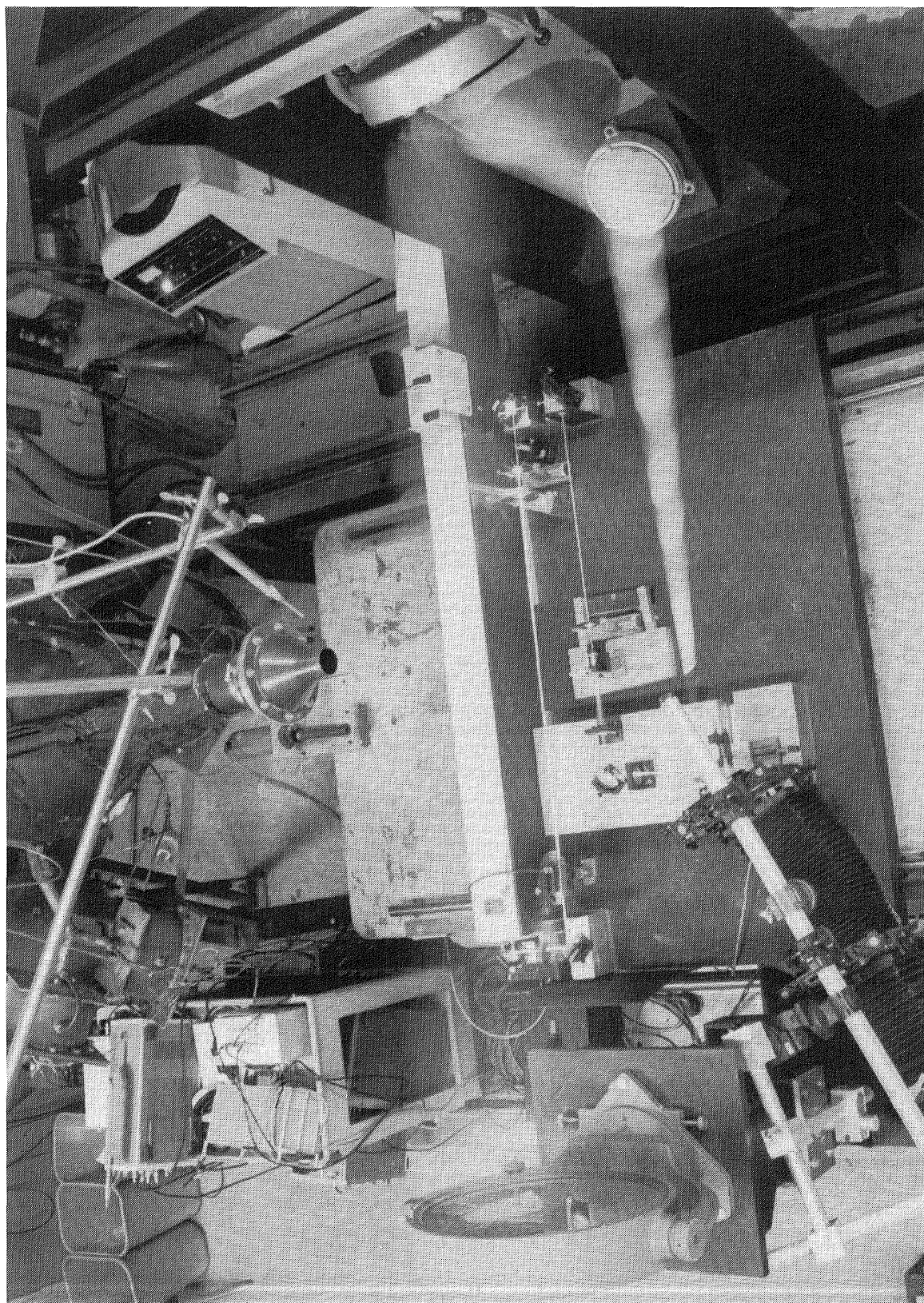
Figure 4.3 Pair of acoustic drivers.

Figure 4.4 Flow visualization setup.

the frequency of photographic shot repetition and the time exposure of each
of the shots.

4.2   DATA ACQUISITION AND INSTRUMENTATION

4.2.1   Excitation Level Measurement

The excitation levels at the nozzle exit plane, were measured directly only
for the unheated jets using a 6.4-mm-dia Bruel & Kjaer microphone, fitted
with a nose cone.   For heated jets, however, the excitation level was
measured indirectly by a microphone ring placed outside the nozzle but in
the plane of the jet exit.   The radial distance between microphone ports
and the jet axis was 100 mm.   The ring consisting of 12 Bruel & Kjaer
microphones is shown in Figure 4.5.   The 12.7-mm-dia Bruel & Kjaer
microphones were used for this ring. Since the sound pressure levels
measured by these microphones are not necessarily equal to those present at
the nozzle exit, the necessary corrections were obtained in advance by
making simultaneous measurements of the sound levels present at the nozzle
exit, using a 6.4-mm-dia Bruel & Kjaer microphone, fitted with a nose cone
and the levels at this microphone ring, for all test conditions and
excitation frequencies.   These calibrations were made for unheated
conditions, and it was assumed that the corrections from exit plane to the
ring position were the same for the heated jets.

4.2.2   Flow Data Acquisition and Reduction

In view of the large number of data points acquired in this program, it was
almost imperative that the data acquisition and reduction scheme be as
automated as possible.   A block diagram for acquisition, processing, and
evaluation of the data is shown in Figure 4.6. The measured pressures are
converted to analog   signals   by pressure transducers.   These signals,
together with the signals from temperature probes, are sampled by a Digi-
Link data acquisition unit.   The Digi-Link converts these signals into
digital values of pressures and temperatures using the probe-static-
calibration curves. The converted values, expressed in engineering units,
are then supplied to the VAX computer.   The flow parameters such as Mach
and Reynolds numbers, flow velocity and temperature are then computed. All
the flow characteristics at a given probe location in the jet are
immediately displayed in a graphical form on the computer terminal. These
plots are automatically updated with every newly acquired experimental
point from the jet flowfield.   Also a graphical comparison with the data
already acquired at   other experimental conditions can be made during a
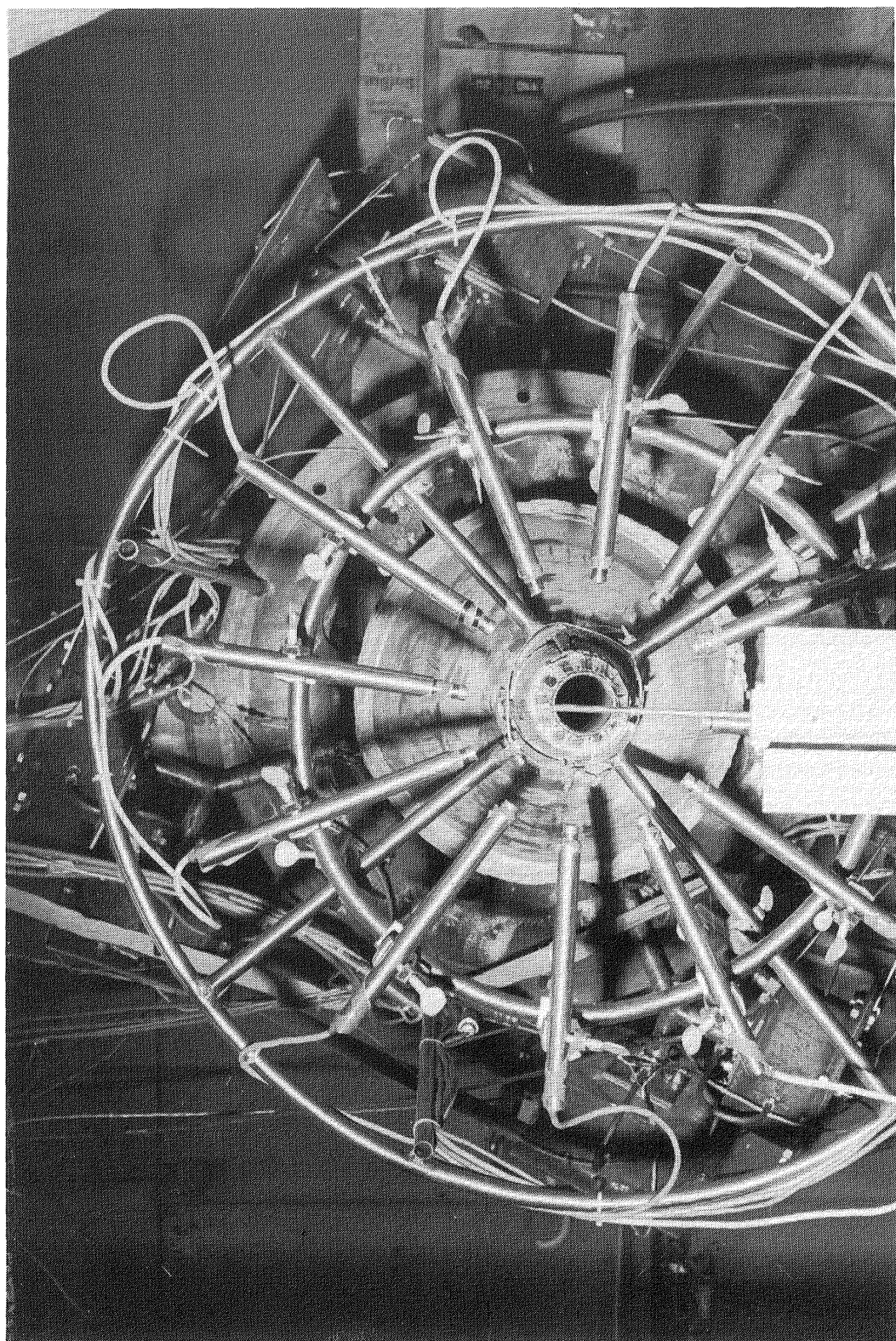particular test run.   The information from the probe positioner is also

Figure 4.5 Microphone ring. Front view.

Figure 4.6   Data acquisition and reduction scheme.

stored in the computer memory for subsequent data processing. The data for the given experimental condition are kept in the temporary data storage until the entire flowfield is mapped. Finally, when the measurement is finished the data are transferred in the permanent data storage.

4.2.3 Instrumentation

United Sensor probes were used for flow measurements as well as for measurements in the nozzle exit boundary layer. The flow survey was made with the combined pressure and temperature probe DAT-187-12-CD-C/A-36, shown in Figure 4.7. The dynamic temperature calibration of this probe is discussed in detail in Part 3. The boundary layer probe BR-.020-12-C-11-.120 was used for boundary layer experiments. The probe is shown in Figure 4.8. Pressure transducers Validyne P 305D, rated for pressure ranges of 86 kPa and 350 kPa, were used in connection with the above mentioned probes.
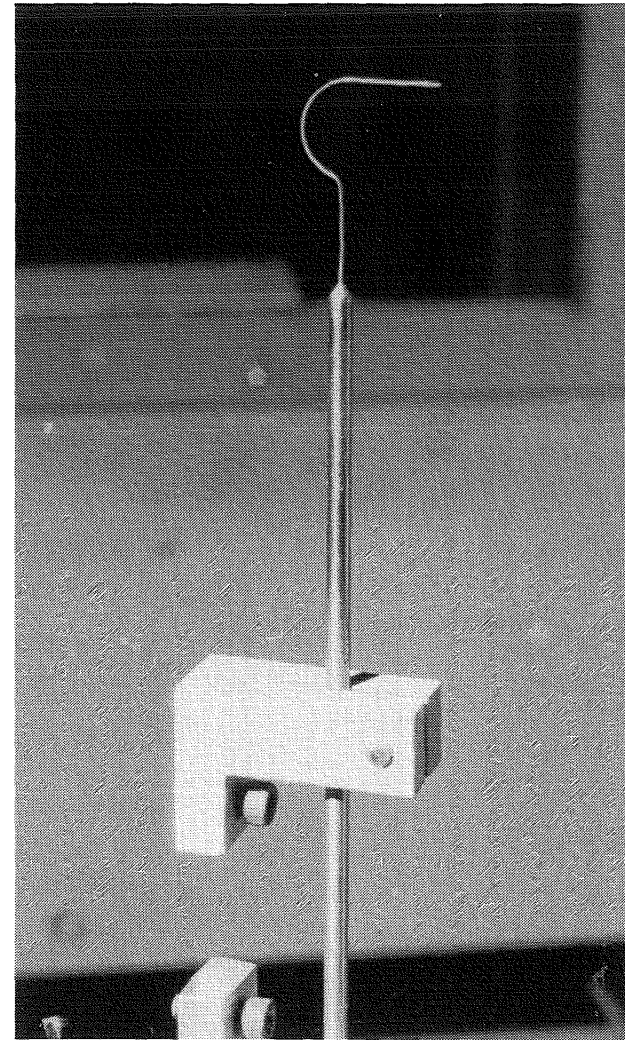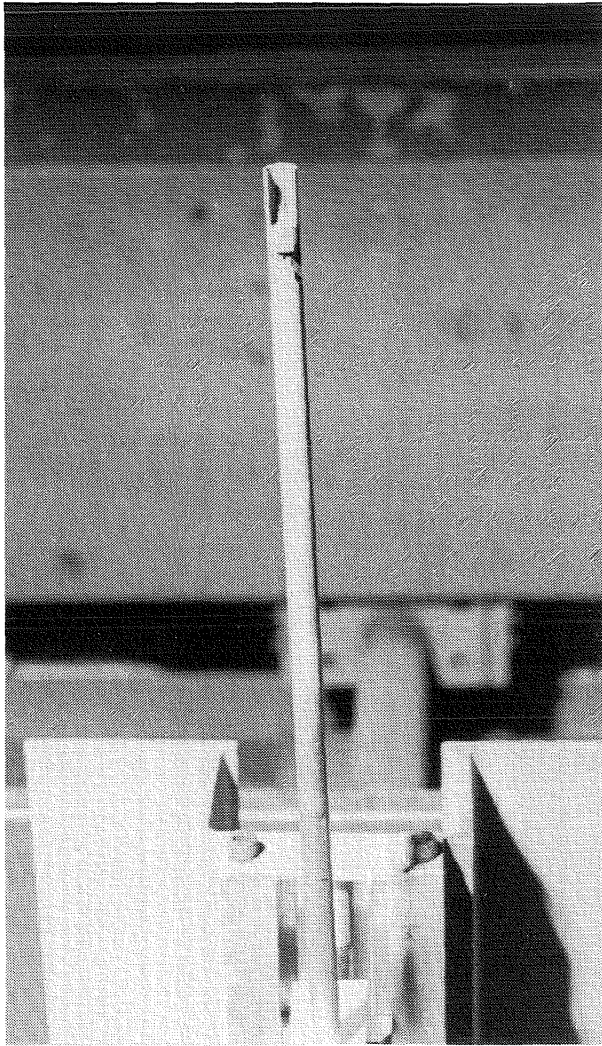
Figure 4.7 Combined pressure and temperature probe.

Figure 4.8 Boundary layer probe.

5.0 NOZZLE EXIT BOUNDARY LAYER EXPERIMENTS

As pointed out in Section 2.0, considerable discrepancy exists between various experimental results on excited hot jets. It was also mentioned that one of the possible explanations for this may be attributed to differences in the type of the nozzle exit boundary layer that might have prevailed in different experiments. Therefore, before proceeding with detailed optimization experiments, described in the next section, the nature of the nozzle exit boundary layer was investigated. The effects of jet Mach number and jet total temperature were investigated for both the untripped and tripped nozzle exit boundary layers. The details of these experiments and the results therefrom are given below.

The characteristic thicknesses and shape factors of the boundary layer used in the following subsections are defined by the following formulae:

Displacement Thickness, δ :

$$\delta = \int_0^\zeta \left(1 - \frac{U}{U_j} \right) dz$$

Momentum thickness, Θ :

$$\theta = \int_0^\zeta \left(1 - \frac{U}{U_j} \right) \left(\frac{U}{U_j} \right) dz$$

Energy thickness, ε :

$$\varepsilon = \int_0^\zeta \left[1 - \left(\frac{U}{U_j} \right)^2 \right] \left(\frac{U}{U_j} \right) dz$$

Shape factor, $H_{\delta\Theta}$:

$$H_{\delta\theta} = \delta/\theta$$

44

<u>Shape factor, $H_{\varepsilon\Theta}$</u> :

$$H_{\varepsilon\theta} = \varepsilon/\theta$$

5.1 UNTRIPPED BOUNDARY LAYER

5.1.1 Mach Number Effects

The effects of Mach number on the nozzle exit boundary-layer behaviour were studied by measuring the boundary layer velocity profiles for various jet exit Mach numbers in the range M_j = 0.16 through 0.9 (see Figure 5.1). Most of these initial measurements were for the unheated jet only. Figures 5.2 and 5.3 show nozzle exit boundary layer profiles normalized by boundary layer momentum thickness as measured for low and high jet exit Mach numbers. It was found that for the nozzle arrangement used, the nozzle exit boundary layer gradually changed from laminar at low Mach numbers to turbulent at high Mach numbers. This becomes clearer on examining the variation of the nozzle exit boundary layer displacement thickness, with Reynolds number, based on the nozzle exit diameter, as shown in Figure 5.4. Variations of the laminar and turbulent boundary layers of the "equivalent flat plate" are also shown in this figure.

The process of boundary layer transition, from laminar to turbulent boundary layer profile, involves a large decrease in the shape factor $H_{\delta\Theta}$ = δ/Θ. In the case of a flat plate, the shape factor decreases from $H_{\delta\Theta}$ = 2.6 in the laminar regime to $H_{\delta\Theta}$ = 1.4 in the turbulent regime. In the case of the present nozzle-exit boundary layer this change in the shape factor was not so significant, as seen in Figure 5.5. The transition of the laminar boundary layer to a turbulent one occurs at a jet Reynolds number Re_j = 350,000.

5.1.2 Total Temperature Effects

The effects of the jet total temperature on nozzle exit boundary layer behaviour were studied at a jet exit Mach number of M_j = 0.8. A family of nozzle exit boundary layer profiles for different jet total temperatures
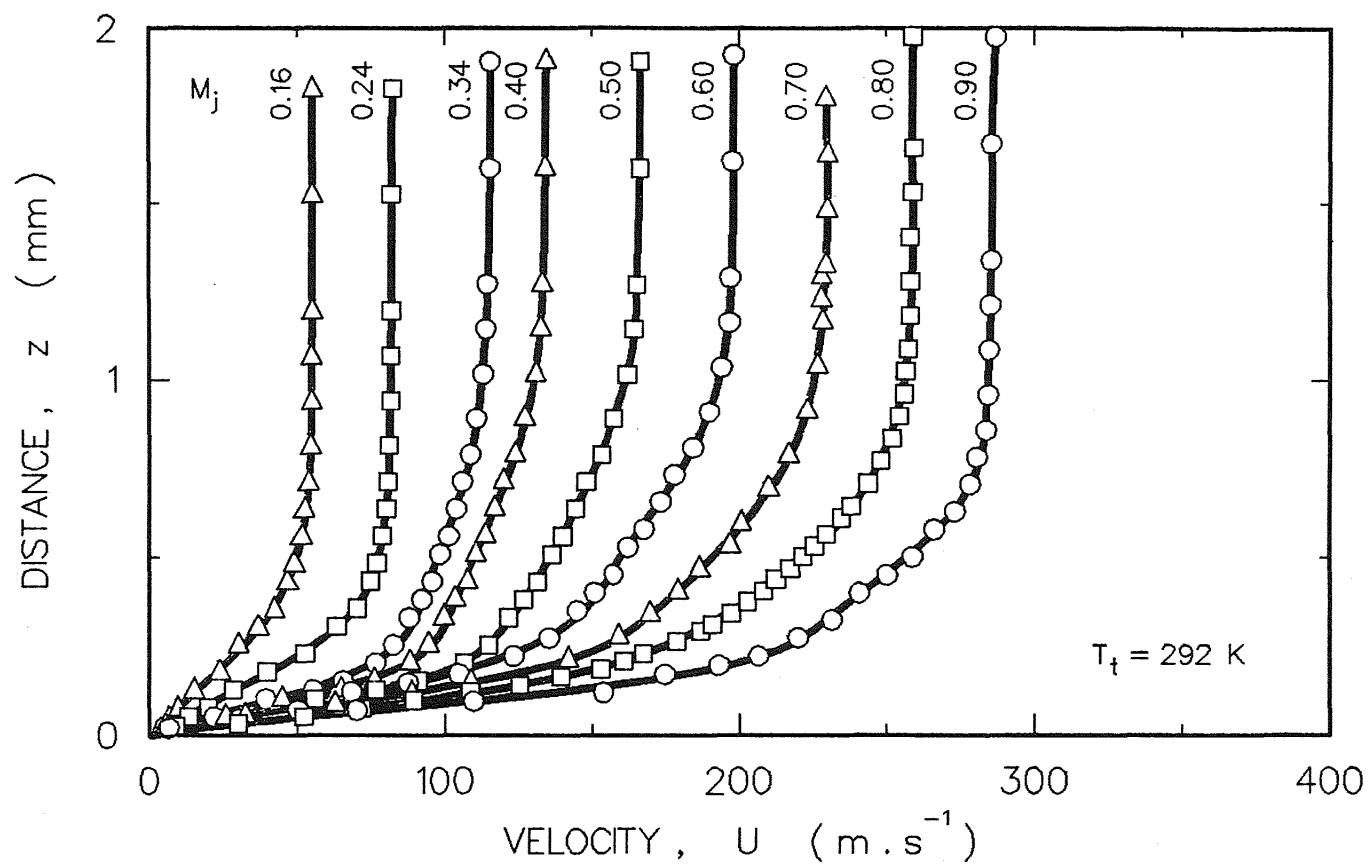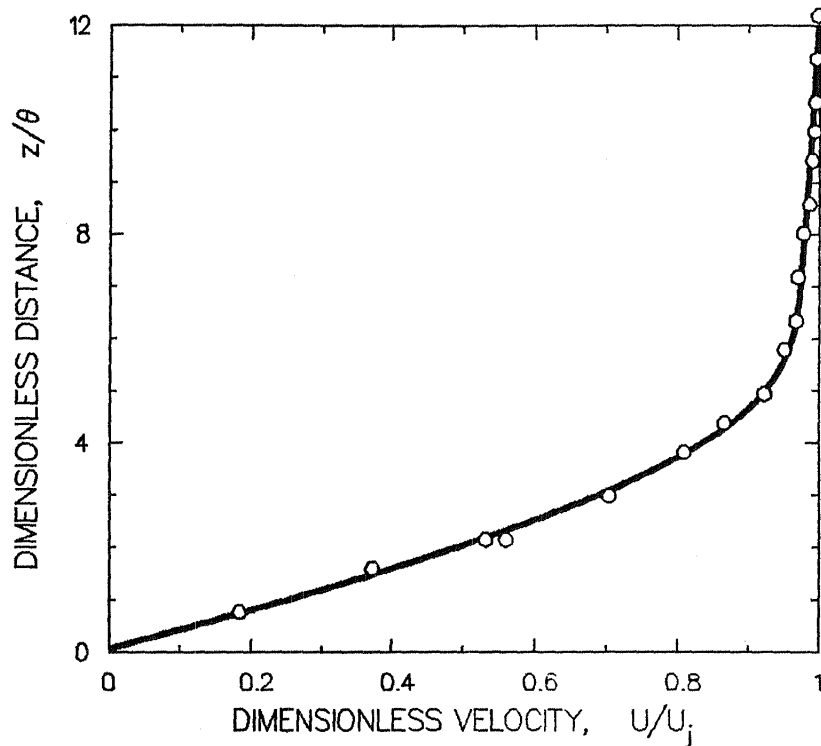
Figure 5.1 Jet Mach number effects on nozzle exit boundary layer profiles.

NOZZLE EXIT BOUNDARY LAYER
VELOCITY PROFILE

FLOW CONDITIONS:
$M_j = 0.201$ $U_j = 69.1$ m/s

$T_t = 296.6$ K $Re_j = 226482$ $Re_\theta = 406$

UNEXCITED FLOW:
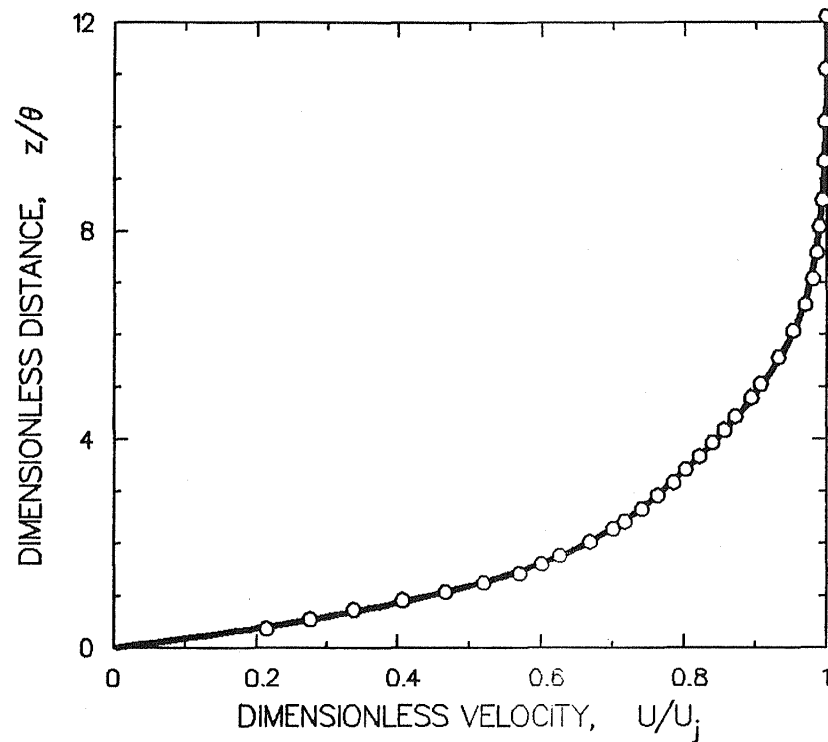$f_e = 0$ Hz $L_e = 0$ dB

$St_j = 0.00$ $St_\theta = 0.0000$

BOUNDARY LAYER PARAMETERS:

$\delta = 0.219$ mm $\theta = 0.091$ mm $\varepsilon = 0.146$ mm

$H_{\delta\theta} = 2.407$ $H_{\varepsilon\theta} = 1.604$

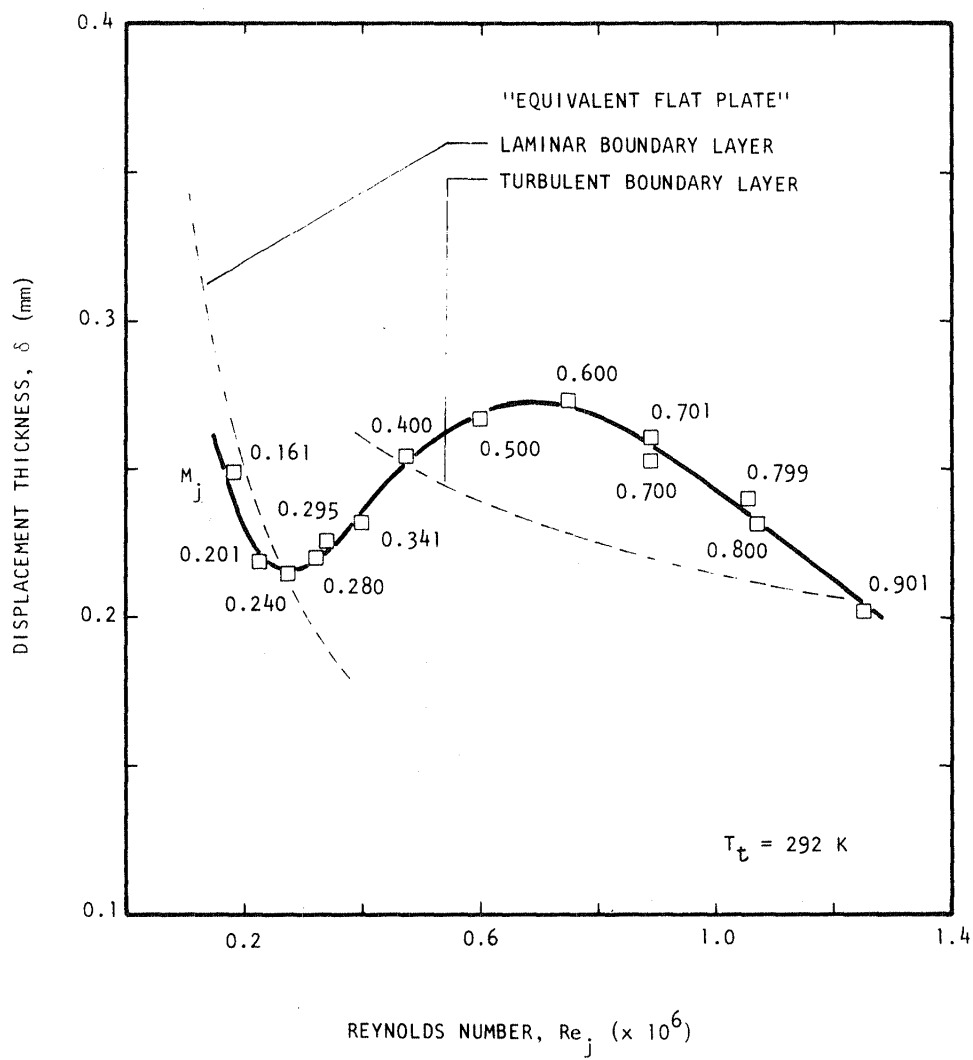Figure 5.2   Low Mach number nozzle exit boundary layer profile.

NOZZLE EXIT BOUNDARY LAYER VELOCITY PROFILE

FLOW CONDITIONS: M_j = 0.799 U_j = 258.3 m/s

T_t = 292.7 K Re_j = 1055916 Re_θ = 2619

UNEXCITED FLOW: f_e = 0 Hz L_e = 0 dB

St_j = 0.00 St_θ = 0.0000

BOUNDARY LAYER PARAMETERS:

δ = 0.240 mm θ = 0.126 mm ε = 0.210 mm

$H_{\delta\theta}$ = 1.905 $H_{\varepsilon\theta}$ = 1.667

Figure 5.3   High Mach number nozzle exit boundary layer profile.

Figure 5.4 Jet Mach number effects on variation of nozzle exit boundary layer displacement thickness.
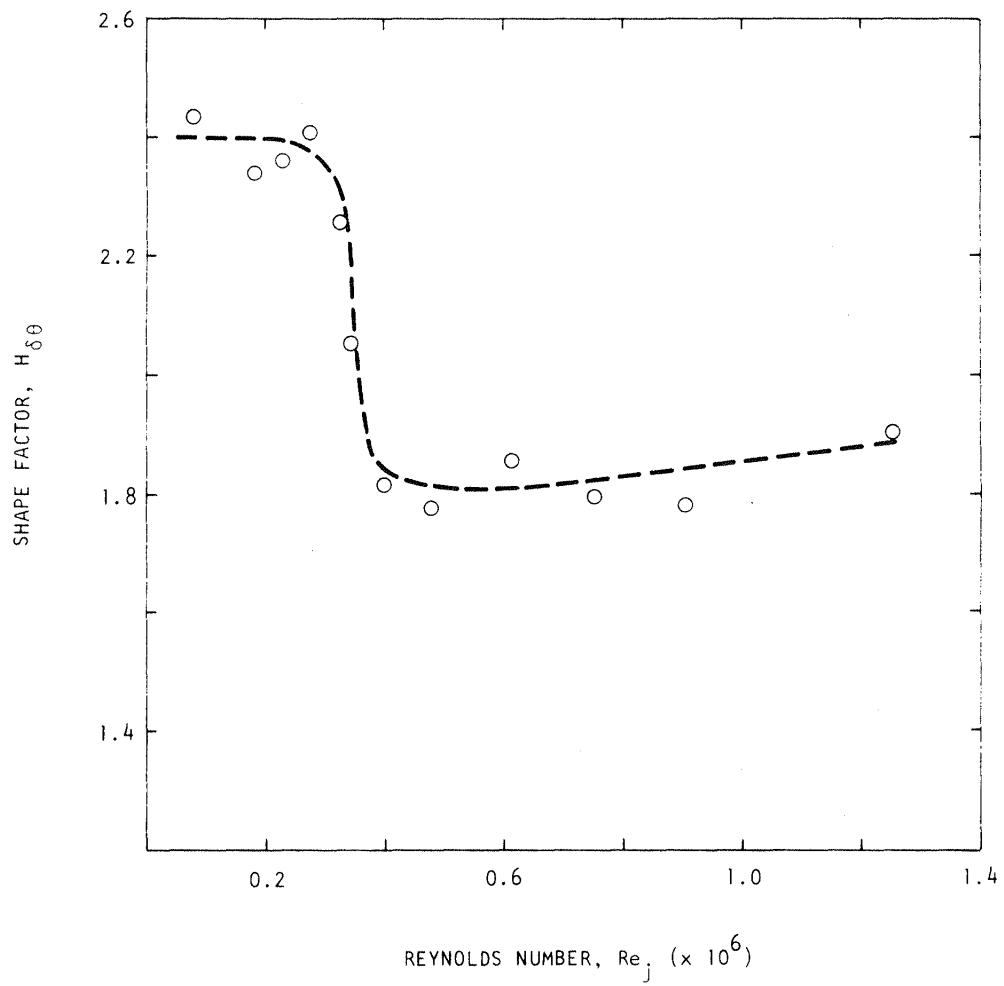
Figure 5.5 Effects of jet Reynolds number on boundary layer shape factor.

and constant jet Mach number of M_j = 0.8 is shown in Figure 5.6. In order to make the profile changes more visible, the curves are plotted in physical coordinates. The same figure shows also two additional nozzle exit boundary layer profiles for jet exit Mach number of 0.3. As shown in the previous subsection, at a jet exit Mach number of 0.8 and unelevated flow temperature, the exit boundary layer was found to be turbulent (Figures 5.3 and 5.5). A nozzle exit boundary layer profile for Mach number 0.8 and heated jet (T_t = 809 K) is shown in Figure 5.7.

At Mach number 0.8, on raising the plenum total temperature gradually from T_t = 290 K (unheated case) to T_t = 809 K, the nozzle exit boundary layer changed from turbulent to laminar, as seen in Figure 5.8 depicting the effects of jet Reynolds number on the boundary layer shape factor. It should be noticed that in this process, Reynolds number decreased from Re_j = 1.06 x 10^6 to Re_j = 0.31 x 10^6, as the kinematic viscosity increases with increasing temperature. The effect of temperature on the nozzle exit boundary layer can best be summarized by plotting the variation of the nozzle exit boundary layer displacement thickness, with jet total temperature as shown in Figure 5.9. On comparing similar data for the unheated jet shown earlier in Figure 5.4, the difference seems to indicate that the effects of jet Mach number and jet total temperature do not scale universally as a function of nozzle-diameter based Reynolds number.

5.2 TRIPPED BOUNDARY LAYER

5.2.1 Tripping Devices

As a result of the earlier described experiments, it becomes obvious, that significant changes take place in the nozzle exit boundary layer as the jet total temperature increases. To avoid changes of the nozzle-exit boundary layer characteristics due to heating of the flow, a tripping device was employed. Two types of tripping devices were used and are designated as type A and type B (Figure 5.10). Type A device utilized a 1.6-mm-dia wire ring, mounted in the nozzle with a 0.1-mm-gap between the ring and the nozzle inner wall. Type B device, on the other hand, utilized a 0.4-mm-dia wire ring attached firmly to the nozzle inner wall. Both devices consisted of a wire ring fitted inside the nozzle and located 6.4 mm upstream of the nozzle exit plane. The reasons for this location close to the nozzle exit plane were dictated by the nozzle design and by the requirement of simple and fast device installation.
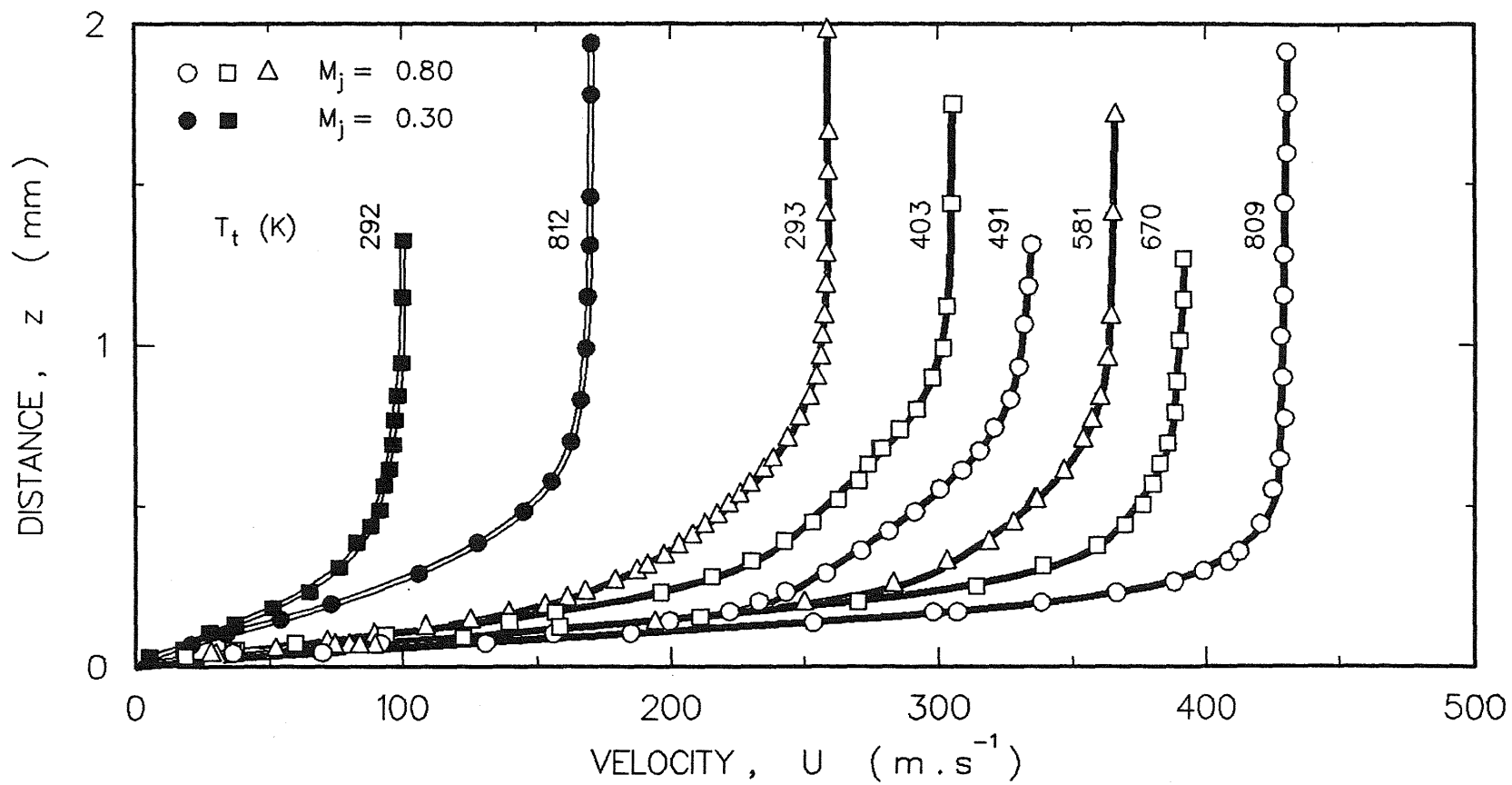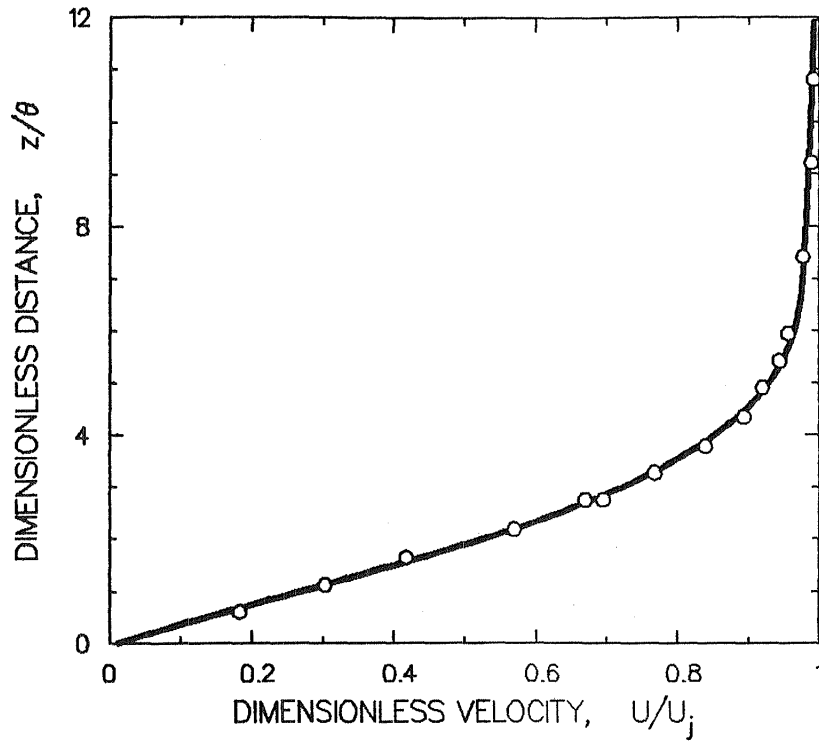
Figure 5.6 Jet total temperature effects on nozzle exit boundary layer profiles.

NOZZLE EXIT BOUNDARY LAYER
VELOCITY PROFILE

FLOW CONDITIONS: $M_j = 0.809$ $U_j = 430.5$ m/s

$T_{t} = 809.4$ K $Re_j = 305278$ $Re_\theta = 355$

UNEXCITED FLOW: $f_e = 0$ Hz $L_e = 0$ dB

$St_j = 0.00$ $St_\theta = 0.0000$

BOUNDARY LAYER PARAMETERS:

$\delta = 0.136$ mm $\theta = 0.059$ mm $\varepsilon = 0.096$ mm

$H_{\delta\theta} = 2.305$ $H_{\varepsilon\theta} = 1.627$

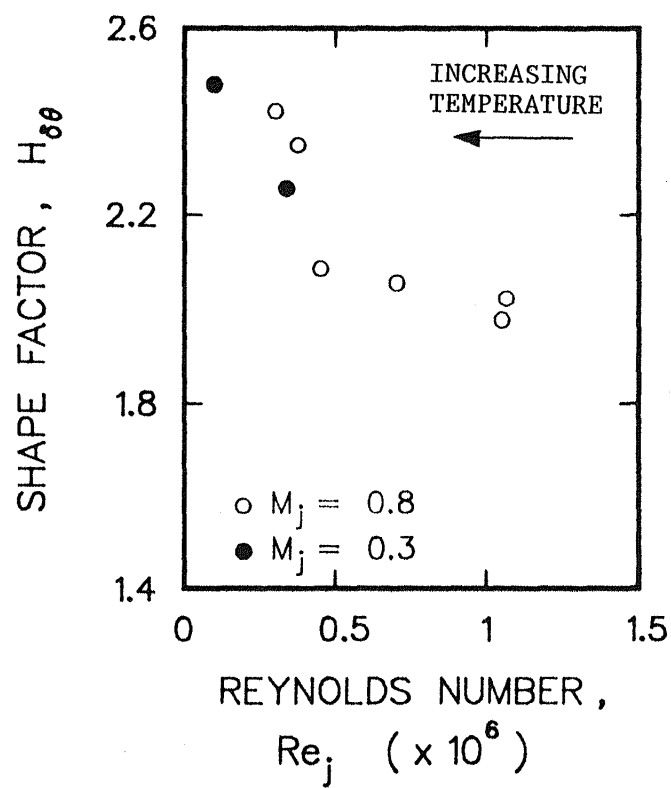Figure 5.7 Heated jet nozzle exit boundary layer profile.

Figure 5.8   Jet total temperature effects on nozzle exit boundary-
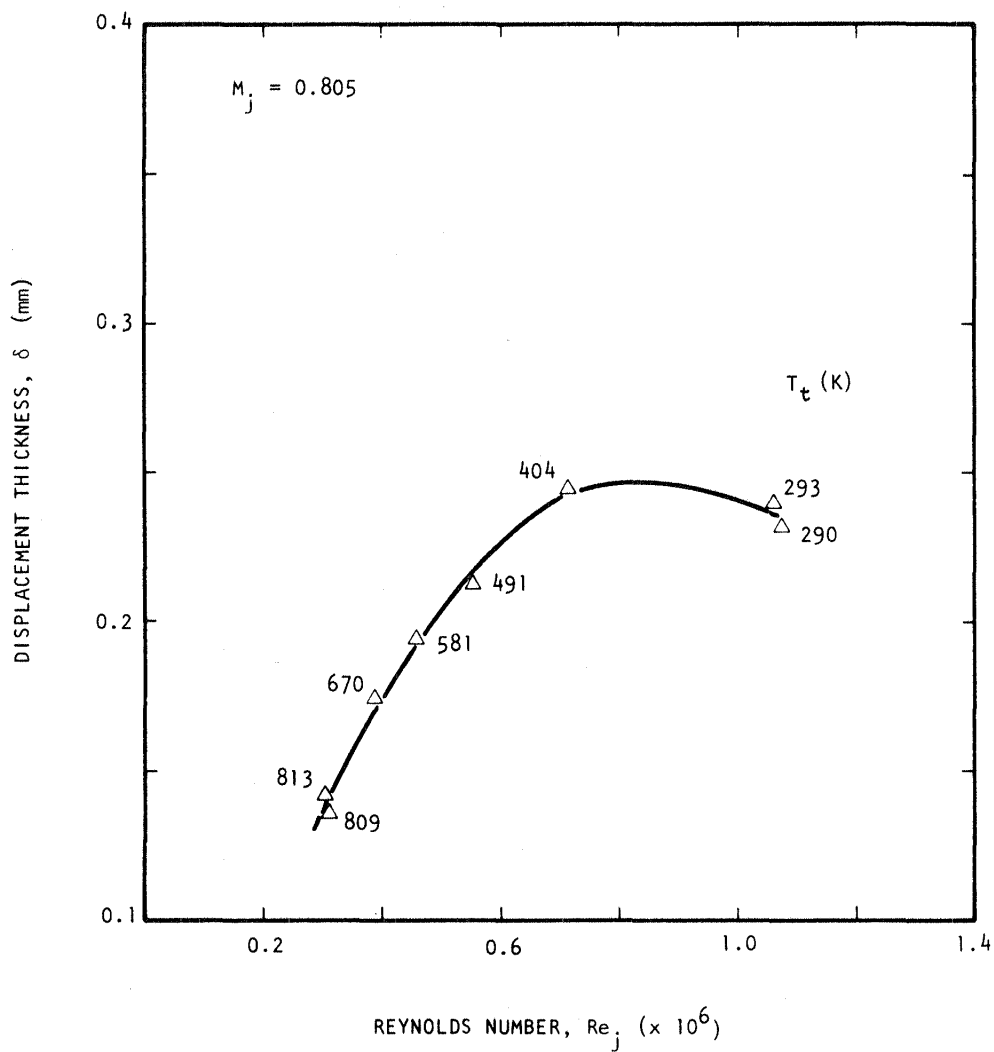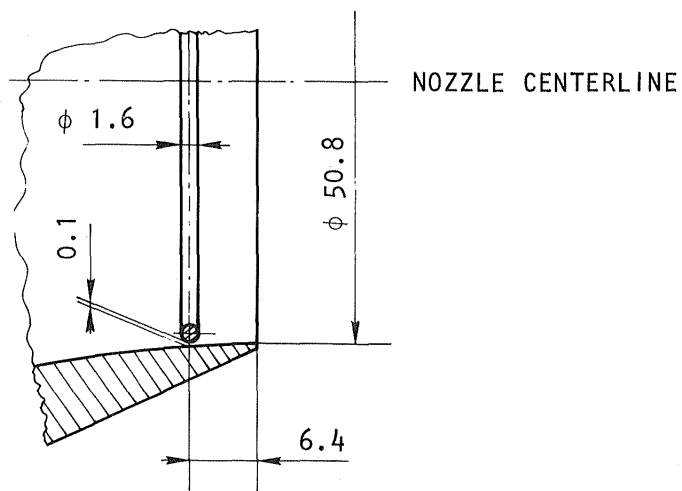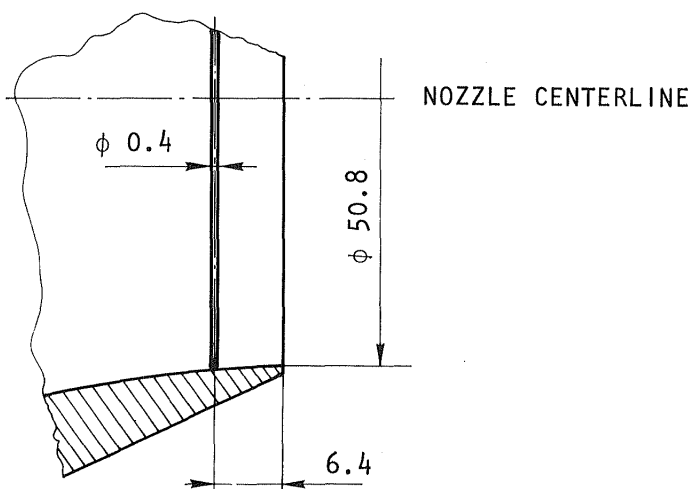layer shape factor.

Figure 5.9 Jet total temperature effects on variation of nozzle exit boundary-layer displacement thickness.

NOZZLE CENTERLINE

φ 1.6

0.1

φ 50.8

6.4

TRIPPING DEVICE A

NOZZLE CENTERLINE

φ 0.4

φ 50.8

6.4

TRIPPING DEVICE B

Figure 5.10   Boundary layer tripping devices.
All dimensions are in mm.

5.2.2 Velocity Profiles

The exit boundary layer velocity profile of the tripped, unheated jet at constant Mach number of M_j = 0.8, for the A-type tripping device is plotted in Figure 5.11 together with the shear layer velocity profile measured at axial station X/D = 0.098. As seen from this figure, the A-type tripping device did not generate a smooth nozzle exit velocity profile. The additional humps near the nozzle wall in the Mach number profiles appear to be the result of a "jet" through the gap, and a "wake" produced by the rather large diameter of the tripping wire. Thus even though the velocity profile recovered and smoothed out relatively rapidly, the excessive width of the shear layer very close to the nozzle exit was not considered adequate to meet the objective of this program.

The B-type tripping device generated more favorable velocity profiles as seen in Figures 5.12 and 5.13. The velocity profiles of tripped, unheated and heated jets at constant jet Mach number of M_j = 0.8 were measured at axial stations X/D = 0.0, 0.125, and 0.25. Momentum/displacement nozzle-exit boundary-layer shape factors were calculated for profiles measured at X/D = 0. The shape factor for the unheated tripped jet was 2.89 and for the heated tripped jet it was 2.84. The similarity of the shape factors for both tripped jets indicate that the velocity profiles are unaffected by heating of the jet, although the tripped nozzle exit boundary layer of the unheated jet is thicker than the untripped one at the same jet operating conditions.

The proximity of the tripping device to the nozzle exit plane strongly effects the shape of the nozzle exit boundary layer. Thus no conclusion, as far as boundary layer character (laminar/turbulent) is concerned, was reached from the given set of experimental data. For this reason, the test facility was later modified to accommodate a tripping device located farther upstream of the nozzle-exit plane. The experiments were rerun with this updated tripping device under the Phase II effort and are described in Part II of this report.
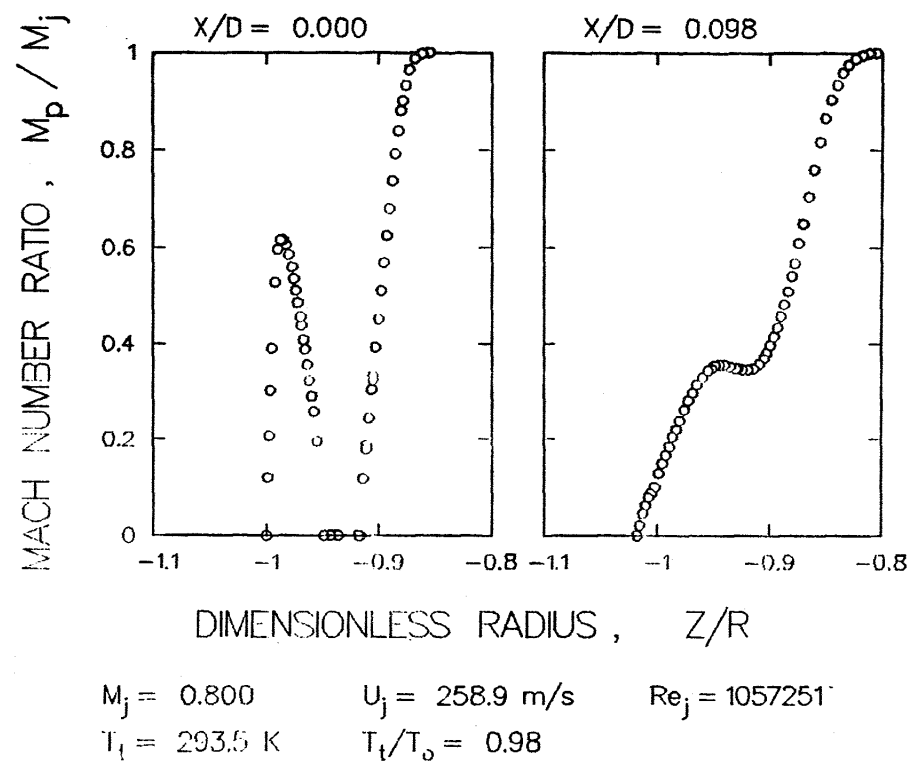
57

VELOCITY RADIAL PROFILES

$M_j = 0.800$ $U_j = 258.9$ m/s $Re_j = 1057251$

$T_t = 293.5$ K $T_t/T_o = 0.98$

Figure 5.11   Velocity radial profiles of unheated, tripped jet.   Tripping device A.

VELOCITY RADIAL PROFILES

X/D = 0.000 X/D = 0.125 X/D = 0.250

MACH NUMBER RATIO, M_p / M_j

DIMENSIONLESS RADIUS, Z/R

$M_j = 0.795$ $U_j = 256.3$ m/s $Re_j = 1055722$

$T_t = 290.5$ K $T_t/T_o = 0.99$
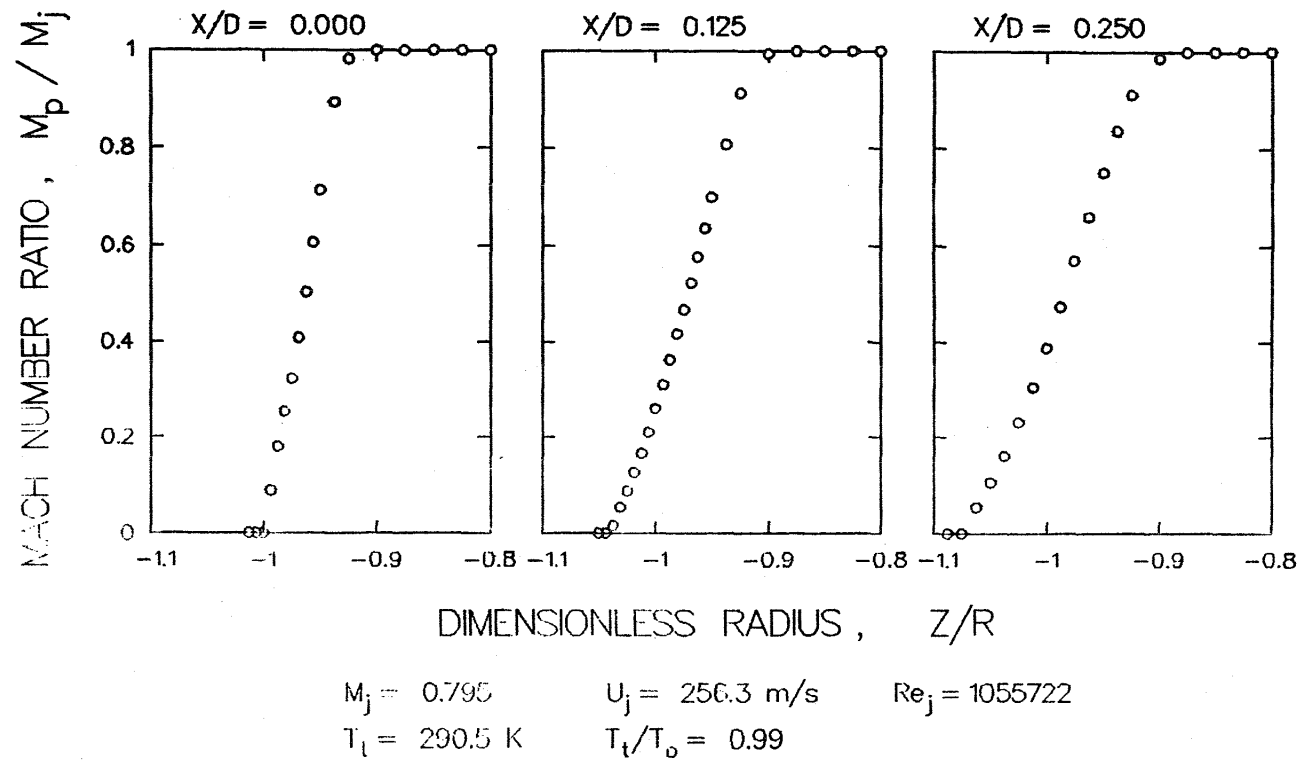
Figure 5.12 Velocity radial profiles of unheated, tripped jet. Tripping device B.

VELOCITY RADIAL PROFILES

MACH NUMBER RATIO, M_p / M_j

X/D = 0.000   X/D = 0.125   X/D = 0.250

DIMENSIONLESS RADIUS, Z/R

M_j = 0.799 U_j = 389.0 m/s Re_j = 373517

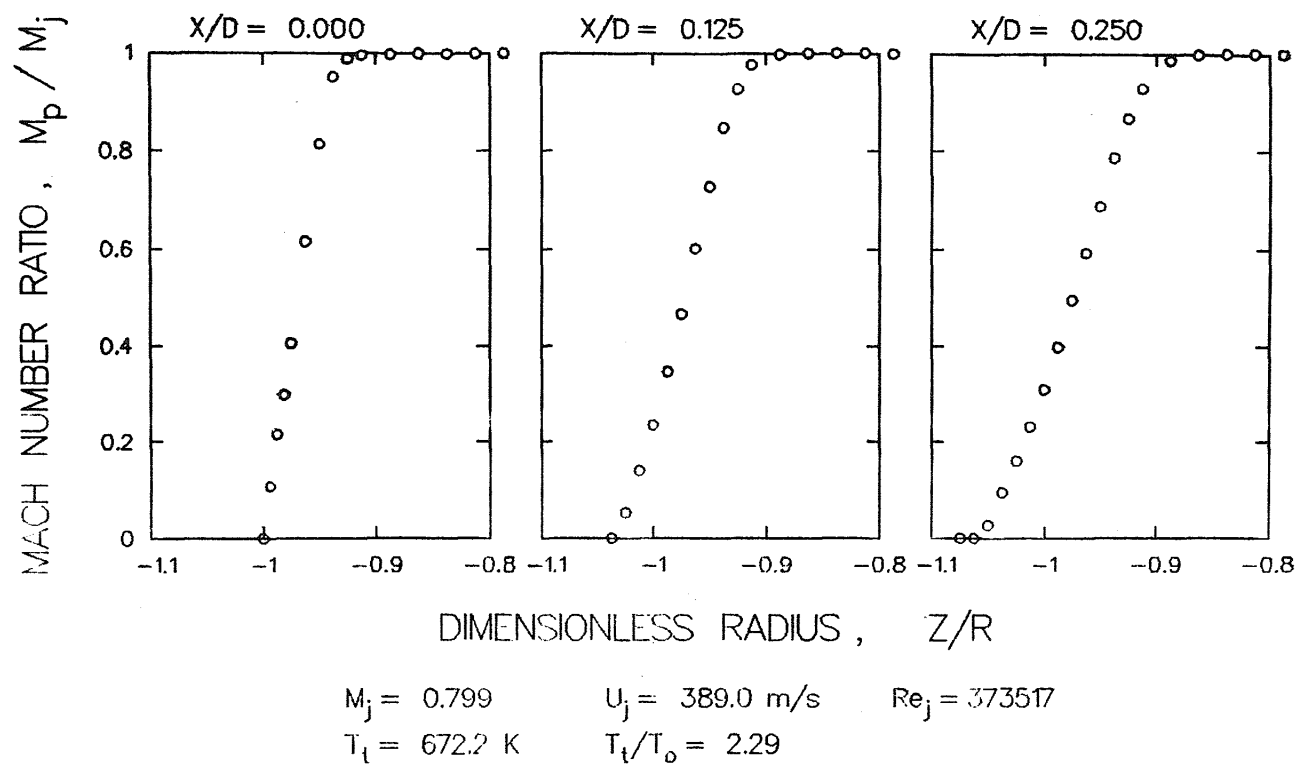T_t = 672.2 K T_t/T_o = 2.29

Figure 5.13 Velocity radial profiles of heated, tripped jet. Tripping device B.

6.0 EXCITATION PARAMETER OPTIMIZATION EXPERIMENTS

The experiments described here were designed to determine the excitation parameters that affect the heated jets most strongly. Both, the excitation Strouhal numbers and the excitation levels were considered in this optimization. In order to truly assess the effects of sound on heated jets, complementary measurements for the unheated jets were also made.

To improve the time efficiency of the entire study, the optimization experiments were based on single point flowfield measurements rather than on the more time-consuming comparisons of radial profiles and centerline distributions. The detailed measurements of the entire flowfield were conducted for only those conditions which indicated a significant effect of acoustic excitation.

6.1 EXCITATION STROUHAL NUMBER EFFECTS

The Strouhal number optimization was based on changes of local Mach number on the jet centerline at nine nozzle exit diameters downstream of the nozzle exit plane. The local Mach number at this point was compared with the Mach number at the same point but in the absence of upstream acoustic excitation. The excitation sound pressure levels were the maximum levels of excitation achievable at the particular Strouhal number.

The optimization exercise for the Strouhal number effects was carried out in three parts: (1) unheated subsonic jets, (2) heated subsonic jets, and (3) supersonic jets. The results for each of these jets are described separately below.

6.1.1 Unheated Subsonic Jets

Typical distributions of relative Mach number as a function of excitation Strouhal number for a low and a high Mach number are plotted in Figures 6.1 and 6.2 . On the same figures are plotted the excitation levels existent at the nozzle exit. As seen in these figures, the most effective Strouhal numbers are St_j = 0.5 and 0.4 for jet Mach numbers M_j = 0.3 and 0.8, respectively.

The above described results of Figures 6.1 and 6.2 were for an untripped nozzle exit boundary layer. Similar experiments were carried out also for
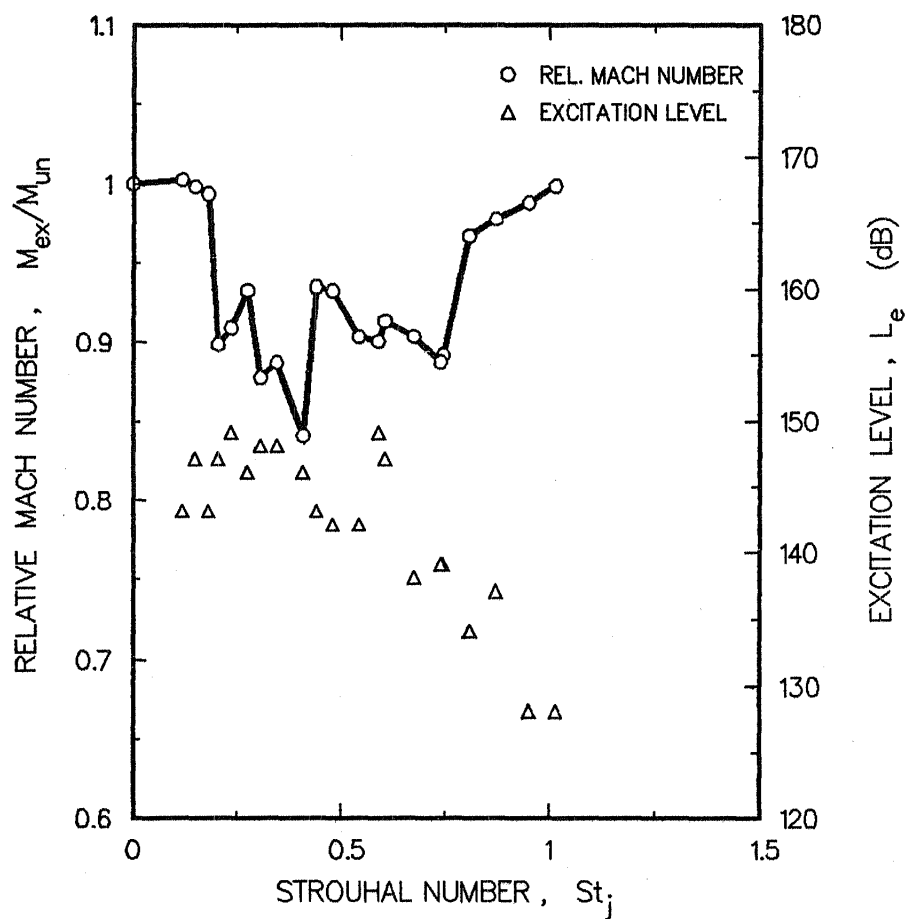
EXCITATION STROUHAL NUMBER EFFECTS ON RELATIVE MACH NUMBER ON JET AXIS AT $X/D_j = 9$
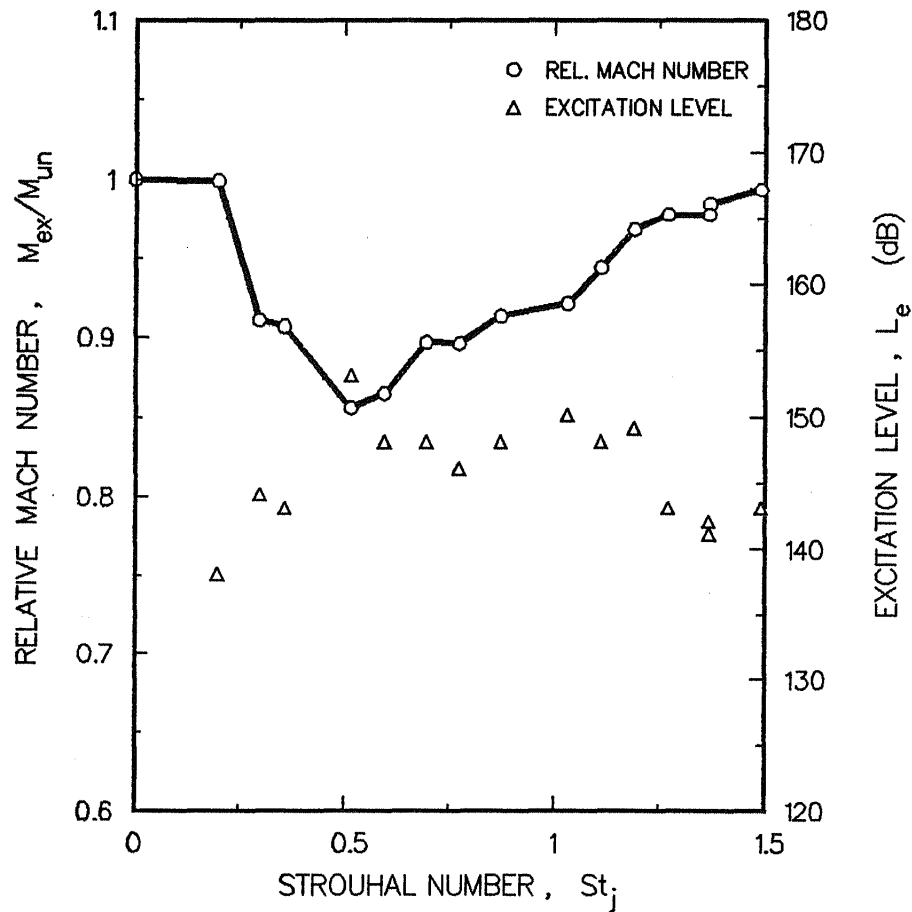
FLOW CONDITIONS: $M_j = 0.299$ $T_t/T_o = 0.99$

$U_j = 102.4$ m . s^{-1} $T_t = 296.0$ K

$Re_j = 342,670$

Figure 6.1   Low Mach number unheated jet.
Smooth nozzle.

EXCITATION STROUHAL NUMBER EFFECTS ON RELATIVE MACH
NUMBER ON JET AXIS AT $X/D_j = 9$

FLOW CONDITIONS: M_j = 0.799 T_t/T_o = 0.99
                   U_j = 258.2 m . s^{-1} T_t = 292.3 K
                   Re_j = 1,062,804

Figure 6.2   High Mach number unheated jet.
             Smooth nozzle, Test Point 1.

the nozzle equipped with the tripping devices. Figures 6.3 and 6.4 show the excitation Strouhal number effects for tripping device A, and Figure 6.5 shows the similar effects for tripping device B. The effect of the increased nozzle exit boundary layer thickness is quite evident in these figures. The jet is less prone to excitation, especially for the high jet Mach number. The effects of excitation are higher for tripping device B than those for tripping device A, because of the thinner nozzle exit boundary layer in the case of tripping device B. In all cases, however, the most effective Strouhal number still remains in the range of $St_j = 0.4 - 0.5$.


6.1.2 Heated Subsonic Jets

The effects of excitation Strouhal number on heated jets were not consistent at different Mach numbers. For example, as may be seen by comparison of Figures 6.6 and 6.1, the excitability of the jet at the jet Mach number of $M_j = 0.3$, which was heated up to $T_t = 811$ K has improved significantly with respect to the unheated one. However, at high Mach number of $M_j = 0.8$ and total temperature of $T_t = 809$ K, no effects of upstream acoustic excitation on jet mixing were observed at all. This is true at least for the achievable excitation levels of $L_e \leq 148$ dB and Strouhal numbers of $St_j \leq 0.65$, as seen in Figure 6.7. This was rather a surprising result, and additional experiments were carried out to clarify this inconsistency. The conditions for these tests correspond to the line A in the chart of jet operating conditions, presented in Section 3.0. The results of these experiments are shown in Figures 6.8 through 6.10. The results for an intermediate total temperature and Mach number are shown in Figure 6.11. The sequence of Figures 6.2, 6.8, 6.9, 6.10, and 6.7 clearly shows the effect of increasing jet total temperature on the jet excitability at the jet Mach number of $M_j = 0.8$. The higher the jet total temperature, the less is the jet affected by upstream acoustic excitation.

The behavior of tripped, heated jets was consistent with the previously acquired results for unheated and heated jets as far as the separate effects of tripping and heating are concerned. The tripping device A decreased the excitability of the heated jet at low jet Mach number (Figure 6.12) with respect to the untripped one (Figure 6.6) in a similar way as it did for the unheated jets (Figures 6.1 and 6.3). At high jet Mach numbers no significant differences were observed between tripped and untripped heated jets (Figures 6.13 and 6.7). Similarly, at high jet Mach numbers no significant differences were observed when the boundary layer was tripped by device B (Figures 6.14 and 6.10).

Due to a program restriction, the effects of the nozzle exit boundary layer
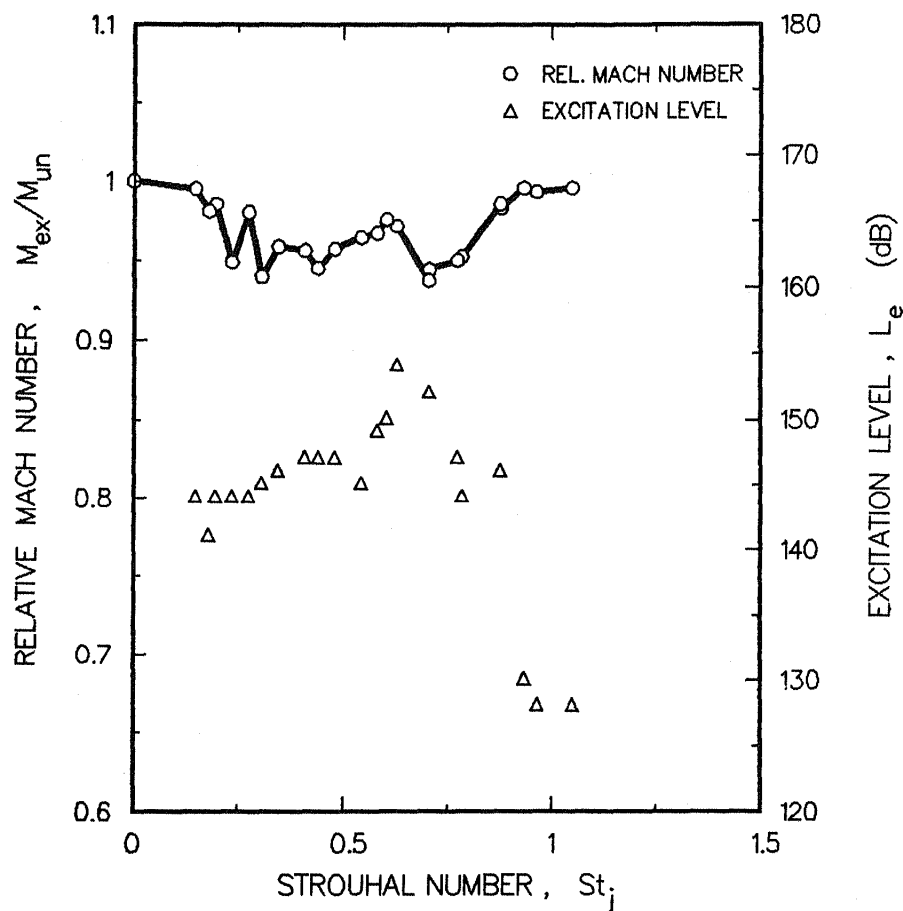
EXCITATION STROUHAL NUMBER EFFECTS ON RELATIVE MACH
NUMBER ON JET AXIS AT $X/D_j = 9$
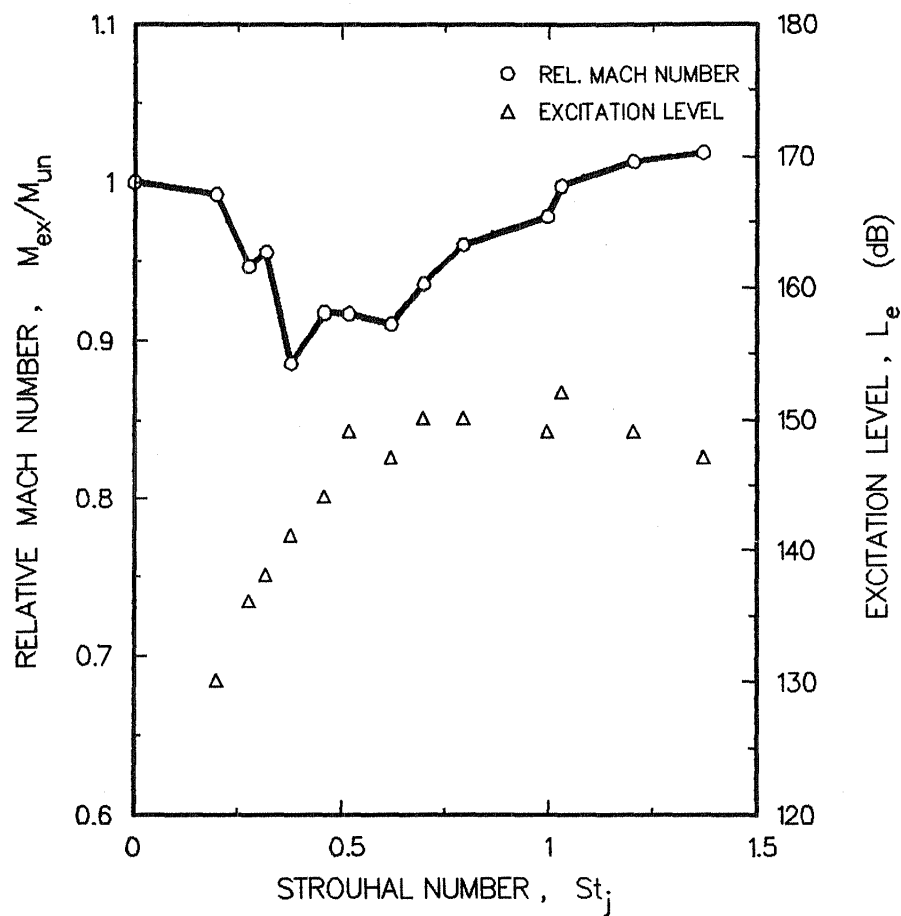
FLOW CONDITIONS: $M_j = 0.300$ $T_t/T_o = 0.98$

$U_j = 102.4 \ m.s^{-1}$ $T_t = 294.6 \ K$

$Re_j = 345,437$

Figure 6.3   Low Mach number unheated tripped jet.
Tripping device A.

EXCITATION STROUHAL NUMBER EFFECTS ON RELATIVE MACH NUMBER ON JET AXIS AT $X/D_j = 9$

FLOW CONDITIONS:

$M_j = 0.799$ $T_t/T_o = 0.97$

$U_j = 259.2 \ m \cdot s^{-1}$ $T_t = 295.0 \ K$

$Re_j = 1,051,593$

Figure 6.4 High Mach number unheated tripped jet. Tripping device A.
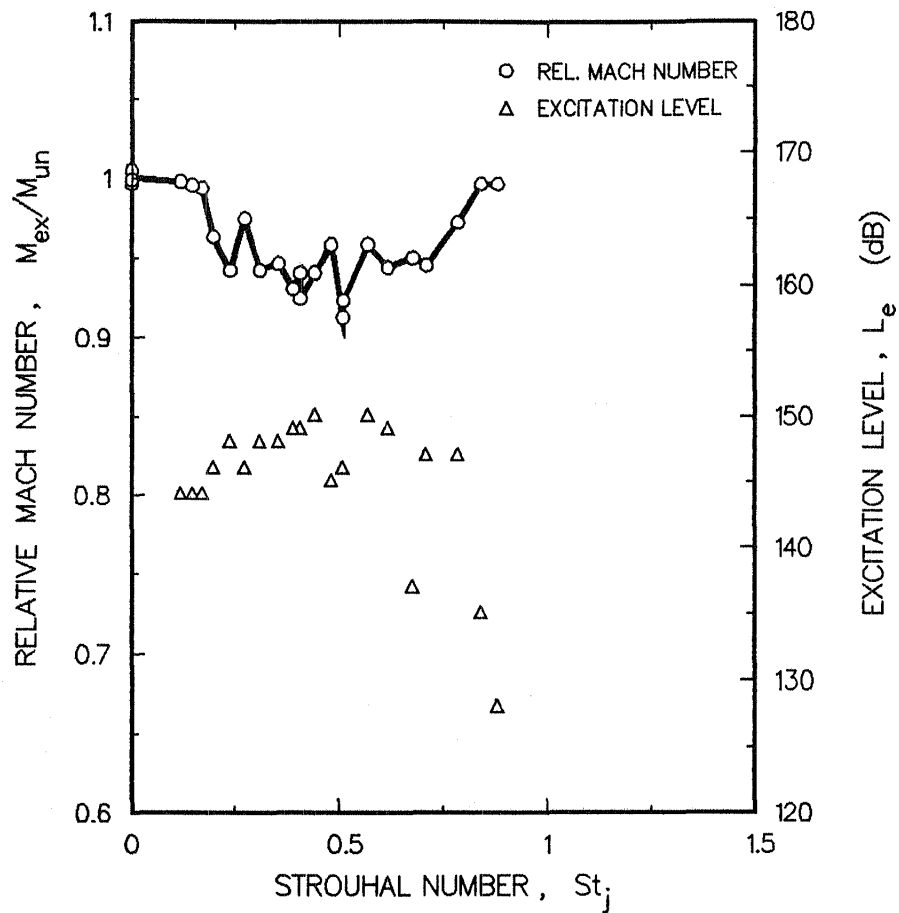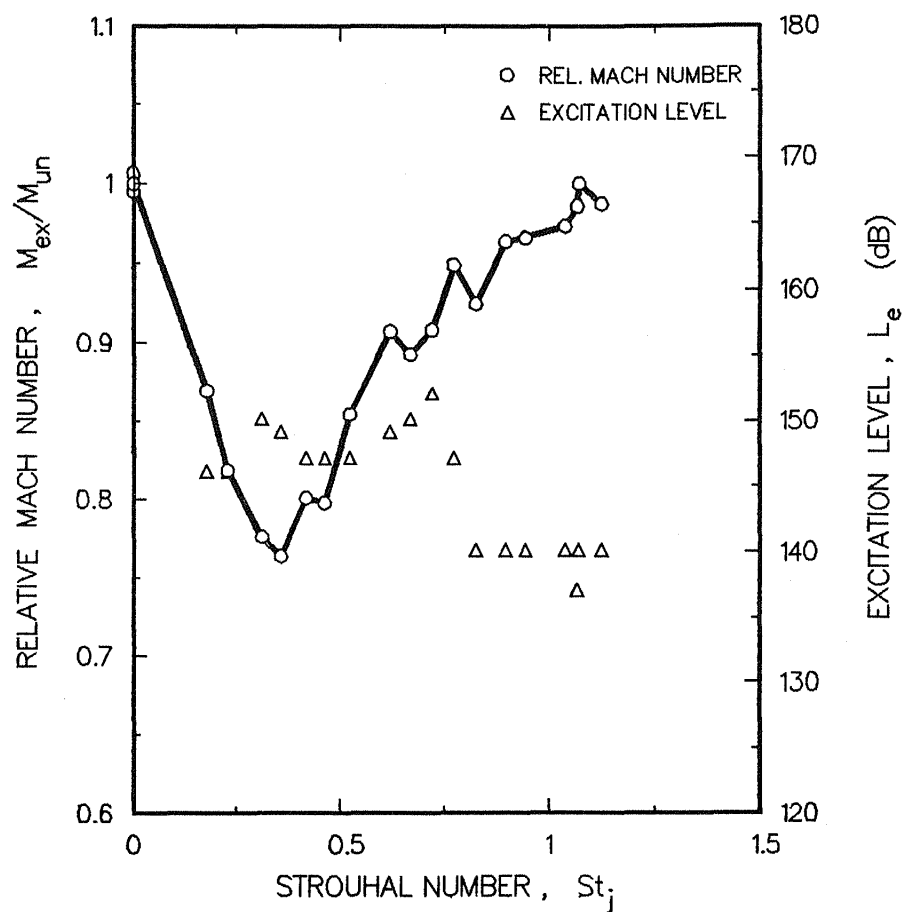
EXCITATION STROUHAL NUMBER EFFECTS ON RELATIVE MACH
NUMBER ON JET AXIS AT $X/D_j = 9$

FLOW CONDITIONS: $M_j = 0.798$ $T_t/T_o = 0.98$

$U_j = 255.4 \text{ m.s}^{-1}$ $T_t = 286.8 \text{ K}$

$Re_j = 1,092,362$

Figure 6.5   High Mach number unheated tripped jet.
Tripping device B.

EXCITATION STROUHAL NUMBER EFFECTS ON RELATIVE MACH
NUMBER ON JET AXIS AT $X/D_j = 9$

FLOW CONDITIONS: M_j = 0.305 T_t/T_o = 2.74

U_j = 170.2 m.s^{-1} T_t = 811.1 K

Re_j = 103,335

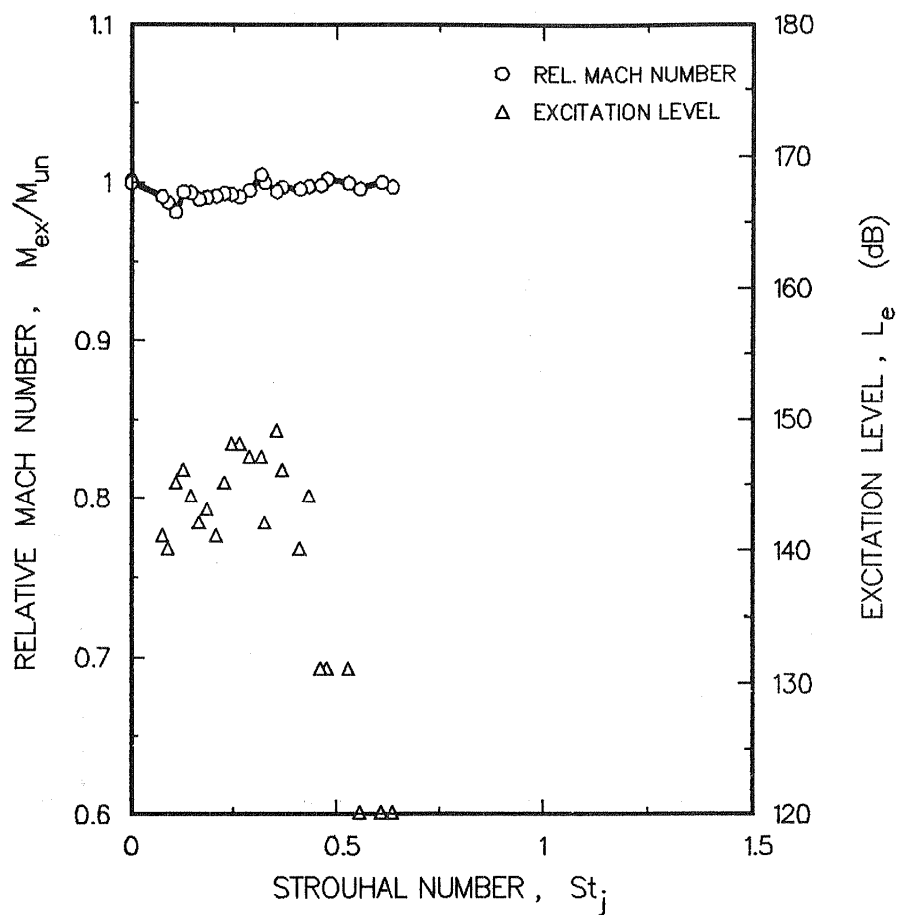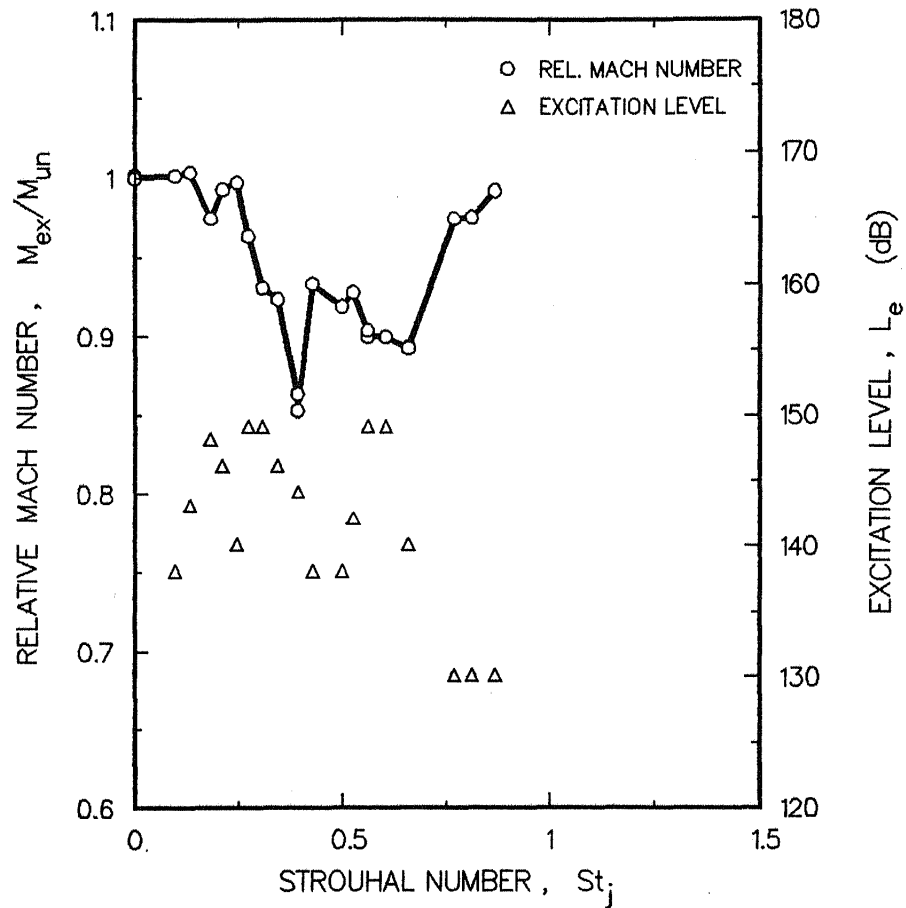Figure 6.6   Low Mach number heated jet.
Smooth nozzle.

EXCITATION STROUHAL NUMBER EFFECTS ON RELATIVE MACH

NUMBER ON JET AXIS AT $X/D_j = 9$

FLOW CONDITIONS:

$M_j = 0.809$ $T_t/T_o = 2.71$

$U_j = 430.5 \text{ m.s}^{-1}$ $T_t = 808.9 \text{ K}$

$Re_j = 306,720$

Figure 6.7 High Mach number heated jet.
Smooth nozzle, Test Point 5.

EXCITATION STROUHAL NUMBER EFFECTS ON RELATIVE MACH NUMBER ON JET AXIS AT $X/D_j = 9$

FLOW CONDITIONS:

M_j = 0.800 T_t/T_o = 1.24

U_j = 289.7 m . s^{-1} T_t = 368.1 K

Re_j = 790,035

Figure 6.8   High Mach number heated jet.
Smooth nozzle, Test Point 2.

EXCITATION STROUHAL NUMBER EFFECTS ON RELATIVE MACH
NUMBER ON JET AXIS AT $X/D_j = 9$

FLOW CONDITIONS: $M_j = 0.802$ $T_t/T_o = 1.65$
$U_j = 334.1 \, m.s^{-1}$ $T_t = 488.4 \, K$
$Re_j = 556,344$

Figure 6.9   High Mach number heated jet.
Smooth nozzle, Test Point 3.

EXCITATION STROUHAL NUMBER EFFECTS ON RELATIVE MACH
NUMBER ON JET AXIS AT $X/D_j = 9$

FLOW CONDITIONS: $M_j = 0.806$ $T_t/T_o = 2.29$

$U_j = 392.1 \ m.s^{-1}$ $T_t = 671.8 \ K$

$Re_j = 380,206$

Figure 6.10 High Mach number heated jet.
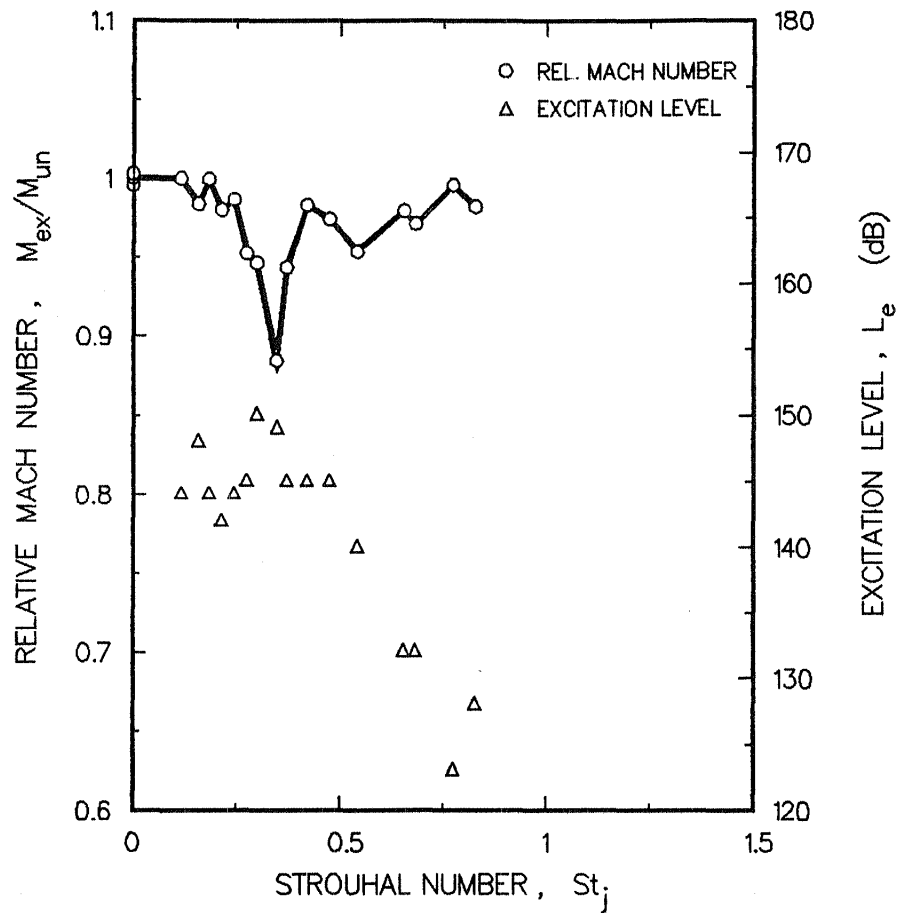Smooth nozzle, Test Point 4.

EXCITATION STROUHAL NUMBER EFFECTS ON RELATIVE MACH
NUMBER ON JET AXIS AT $X/D_j = 9$

FLOW CONDITIONS: $M_j = 0.481$ $T_t/T_o = 1.67$
                  $U_j = 207.7 \ m.s^{-1}$ $T_t = 487.9 \ K$
                  $Re_j = 305,586$

Figure 6.11   Intermediate Mach number heated jet.
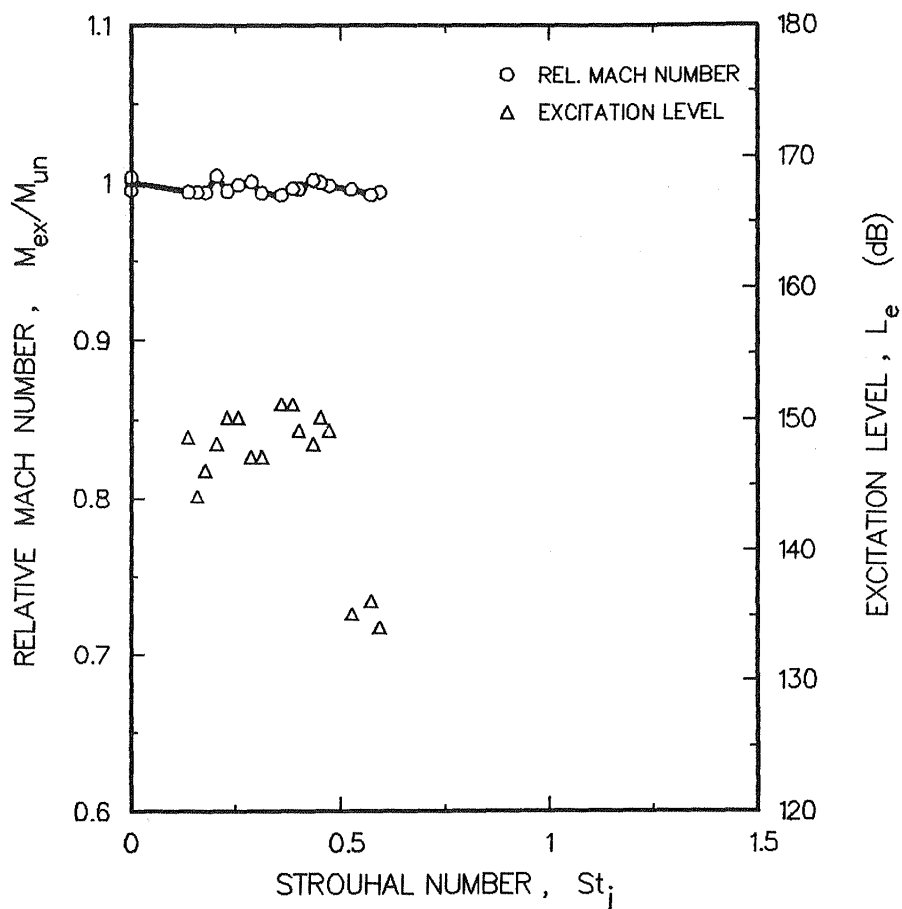   Smooth nozzle, Test Point 6.

EXCITATION STROUHAL NUMBER EFFECTS ON RELATIVE MACH

NUMBER ON JET AXIS AT $X/D_j = 9$

FLOW CONDITIONS: $M_j = 0.306$ $T_t/T_o = 2.68$

$U_j = 170.6 \ m.s^{-1}$ $T_t = 812.8 \ K$

$Re_j = 103,263$

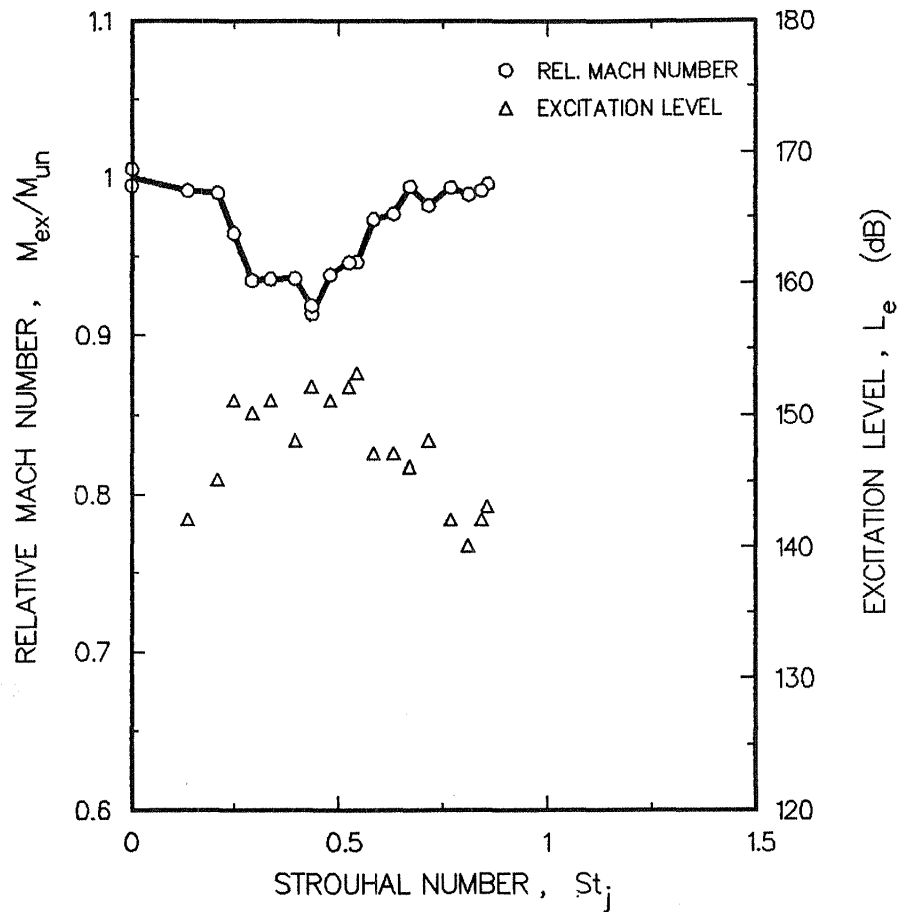Figure 6.12   Low Mach number heated tripped jet.
Tripping device A.

EXCITATION STROUHAL NUMBER EFFECTS ON RELATIVE MACH

NUMBER ON JET AXIS AT $X/D_j = 9$

FLOW CONDITIONS: $M_j = 0.810$ $T_t/T_o = 2.66$

$U_j = 431.0 \ m.s^{-1}$ $T_t = 810.6 \ K$

$Re_j = 306,878$

Figure 6.13   High Mach number heated tripped jet.
Tripping device A.
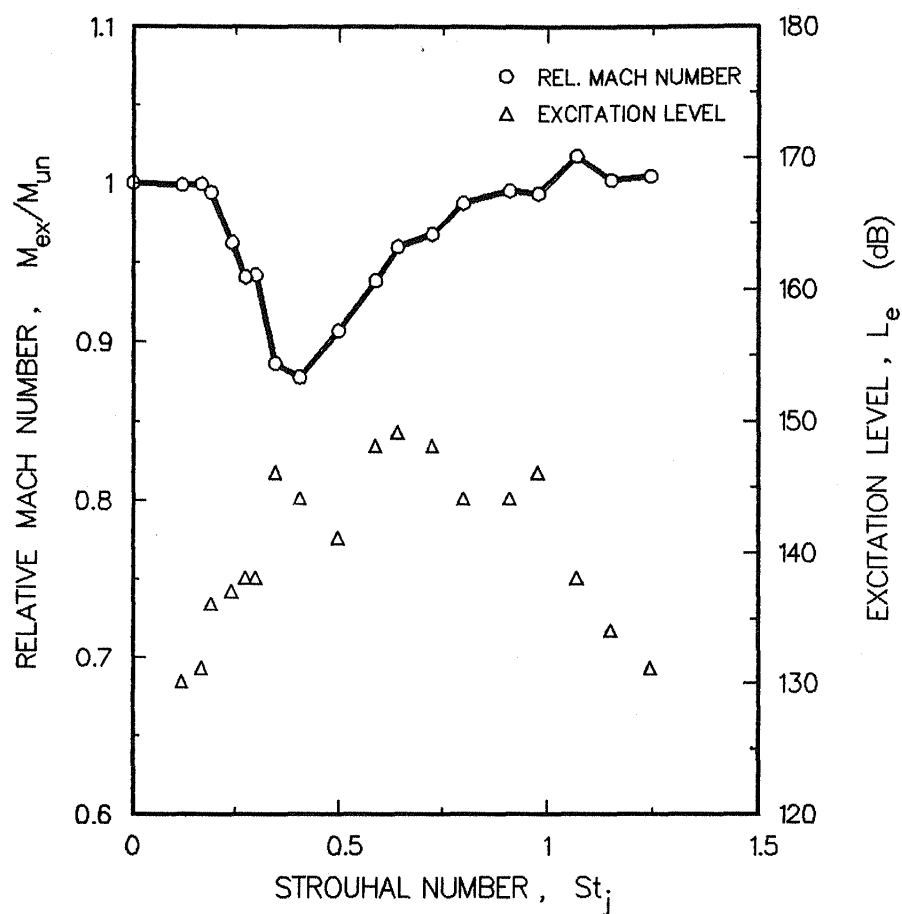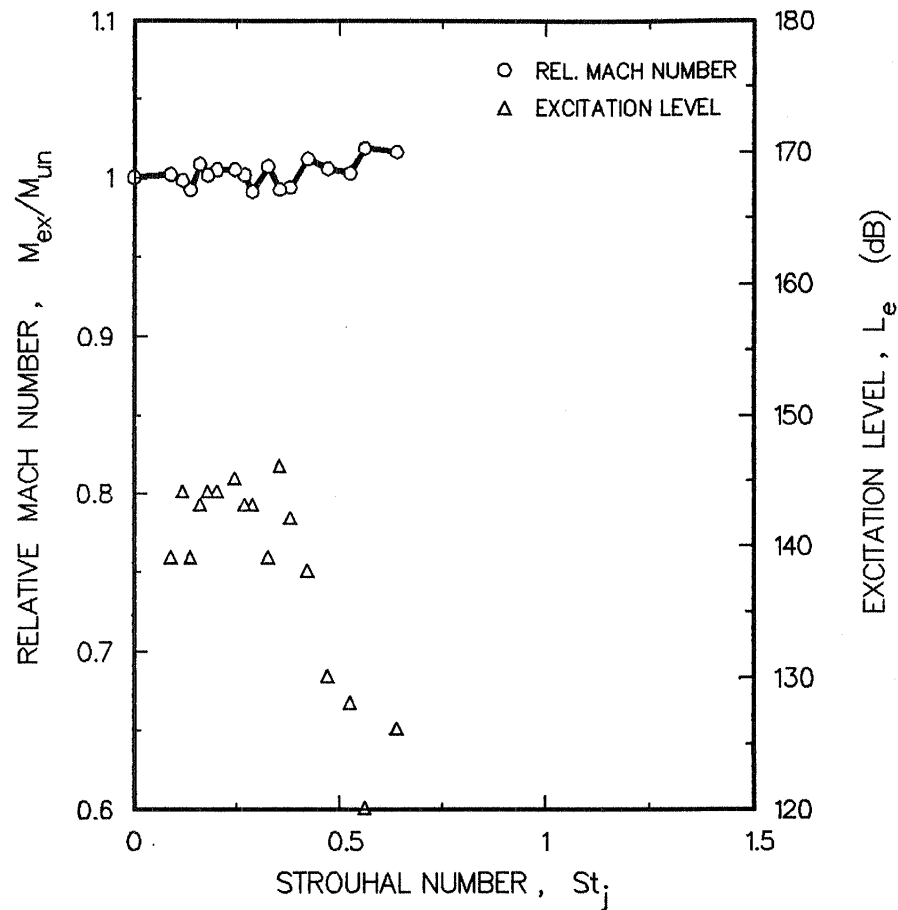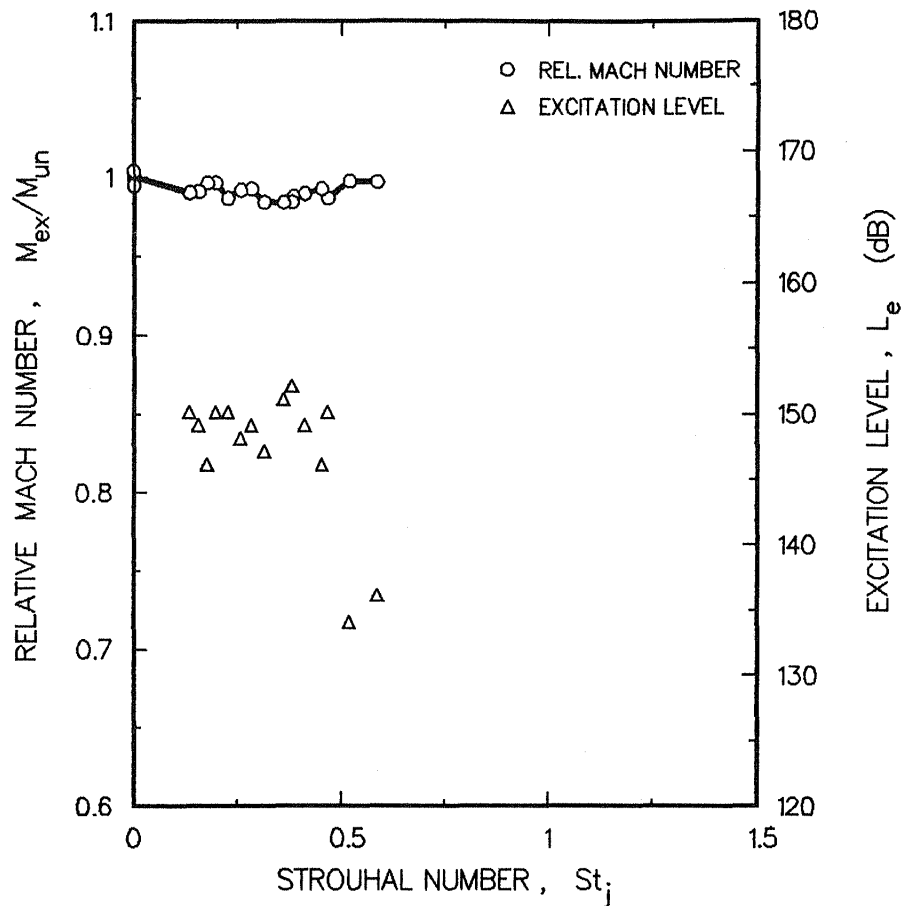
EXCITATION STROUHAL NUMBER EFFECTS ON RELATIVE MACH
NUMBER ON JET AXIS AT $X/D_j = 9$

FLOW CONDITIONS: $M_j = 0.806$ $T_t/T_o = 2.28$
                     $U_j = 391.9 \ m.s^{-1}$ $T_t = 671.2 \ K$
                     $Re_j = 381,614$

Figure 6.14 High Mach number heated tripped jet.
Tripping device B.

on the excitability of heated jets could not be investigated to provide a full understanding of this problem. Evidently, further work was needed and is covered in Part II of this report.

6.1.3 Supersonic Jets

These experiments were aimed at revealing the effects of upstream acoustic excitation on a supersonic, fully expanded, heated jet. The jet operating conditions were M_j = 1.2 and T_t = 489 K. Jet-noise spectra measurements revealed that shockless expansion, for the nozzle used, occurred actually at a jet Mach number of M_j = 1.16, which was slightly lower than the nominal Mach number 1.2 given by Test Point 7 in the Test Matrix in Section 3.0. The spectra were measured by a microphone placed at an angle α = 90 degrees, with respect to the jet axis at a distance R* = 100 mm from the nozzle axis in the nozzle exit plane. The spectra for three different Mach numbers are shown in Figures 6.15 through 6.17. Although these measurements were not carried out in an anechoic chamber, it was assumed that the spectrum at M_j = 1.16 was that for a fully expanded jet, since it contained the smallest contribution of screech-related discrete tones. The measurements for supersonic conditions were, therefore, carried out at a Mach number of M_j = 1.16.

The Strouhal number optimization experiments show that a supersonic heated jet of M_j = 1.16 and T_t = 489 K is practically unaffected by upstream acoustic excitation, as seen in Figure 6.18. Additional Strouhal number optimization experiments were carried out for supersonic unheated jets. As shown in Figure 6.19, the unheated supersonic, fully-expanded jet response to upstream acoustic excitation is similar to that of high-speed subsonic jets. In accordance with previously acquired results for high-speed subsonic jets, it appears that excitation levels achievable in our test facility may not be high enough to enhance mixing of supersonic jets heated above the total temperature of T_t ≃ 500 K in the range of excitation Strouhal numbers up to St_j = 0.6.

6.2 EXCITATION LEVEL EFFECTS

The excitation-level-effect experiments were carried out only for some of the jet operating conditions given in the Test Matrix in Section 3.0. Similar to the Strouhal number optimization experiments, the excitation-level-effect experiments were also based on the changes of the centerline local Mach number at X/D = 9 as described in Section 6.1. The excitation Strouhal number (St_j) at each test point was selected in accordance with
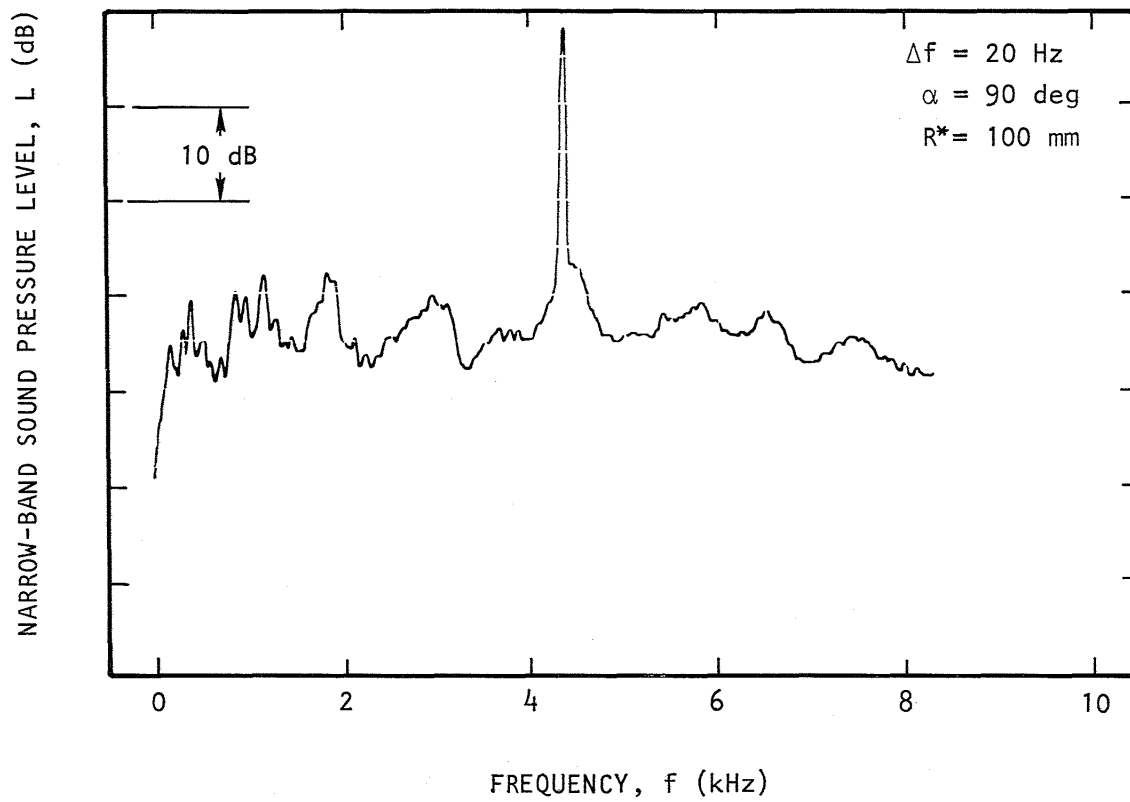
Figure 6.15   Jet-noise frequency spectrum for M_j = 1.12.
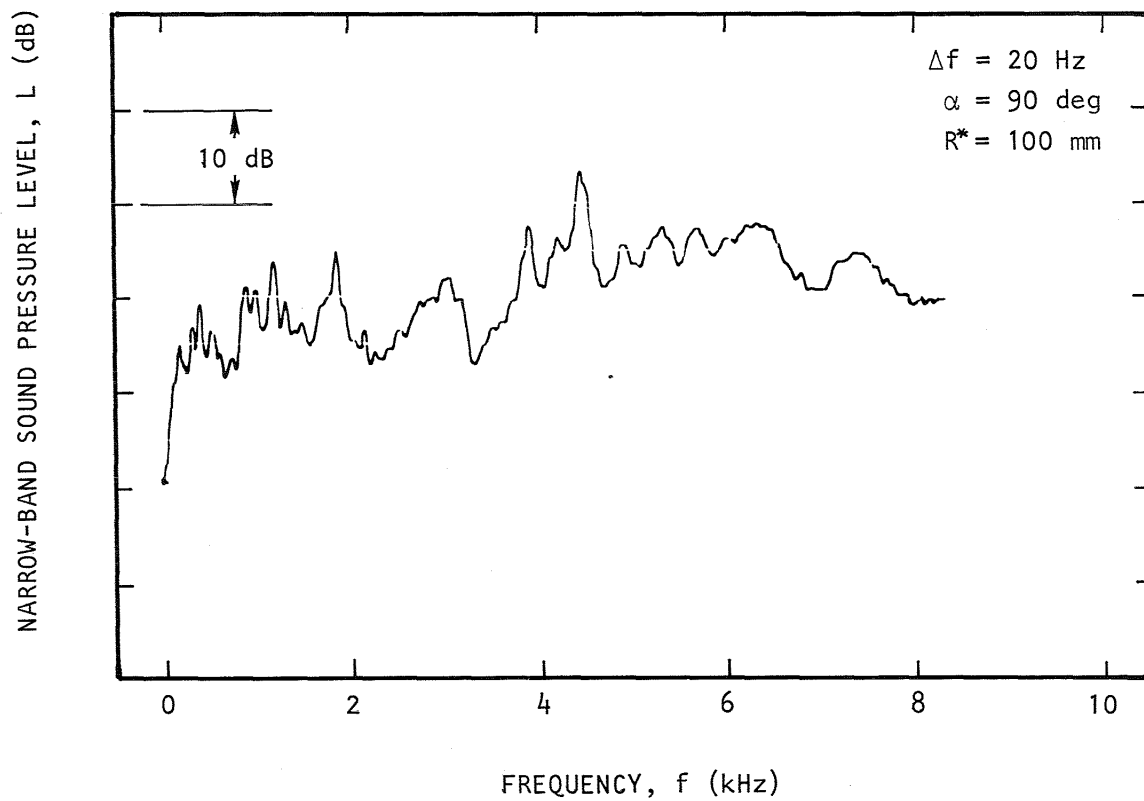
Figure 6.16   Jet-noise frequency spectrum for M_j = 1.16.
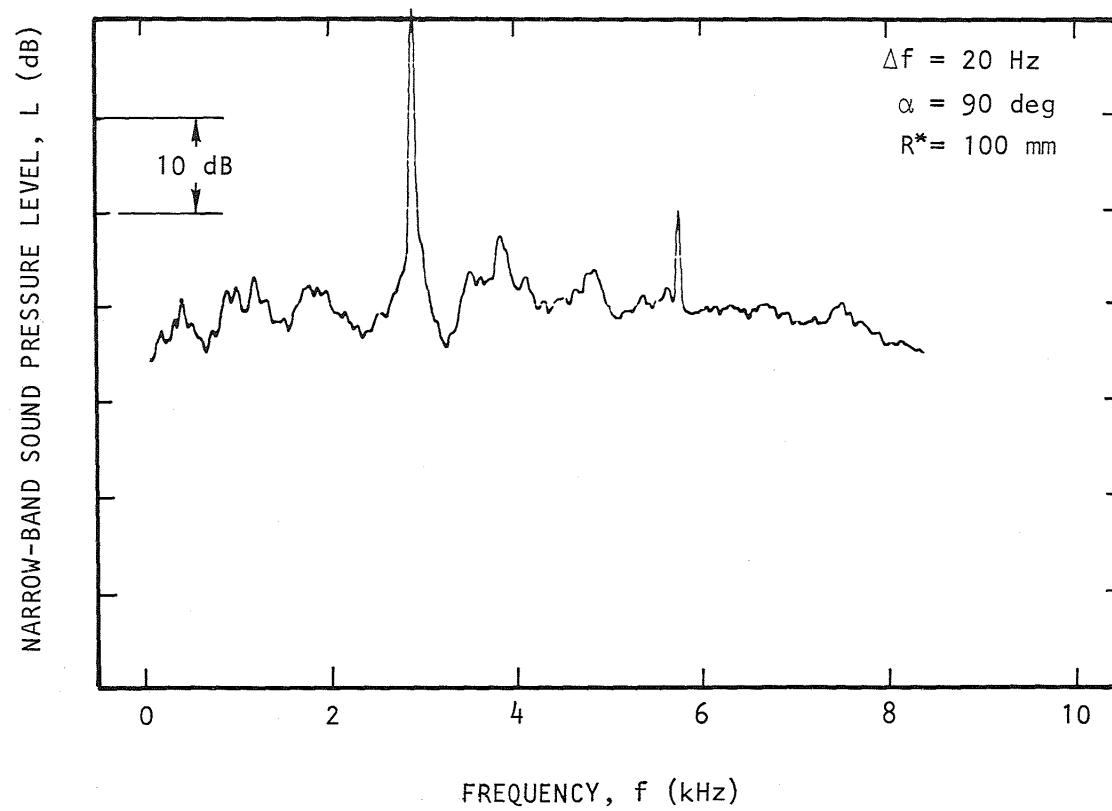
Figure 6.17   Jet-noise frequency spectrum for M_j = 1.22.

EXCITATION STROUHAL NUMBER EFFECTS ON RELATIVE MACH

NUMBER ON JET AXIS AT $X/D_j = 9$
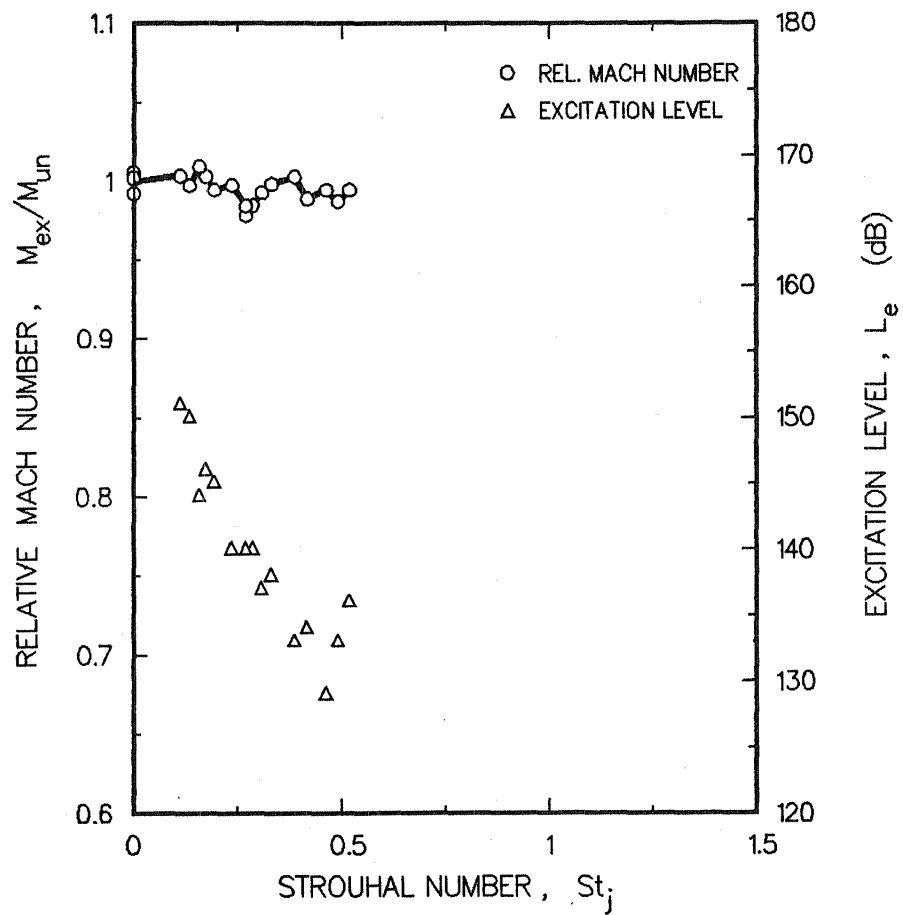
FLOW CONDITIONS: $M_j = 1.138$ $T_t/T_o = 1.70$
                  $U_j = 449.4 \ m.s^{-1}$ $T_t = 488.8 \ K$
                  $Re_j = 892,030$

Figure 6.18   Supersonic heated jet.   Test Point 7.

EXCITATION STROUHAL NUMBER EFFECTS ON RELATIVE MACH
NUMBER ON JET AXIS AT $X/D_j = 9$
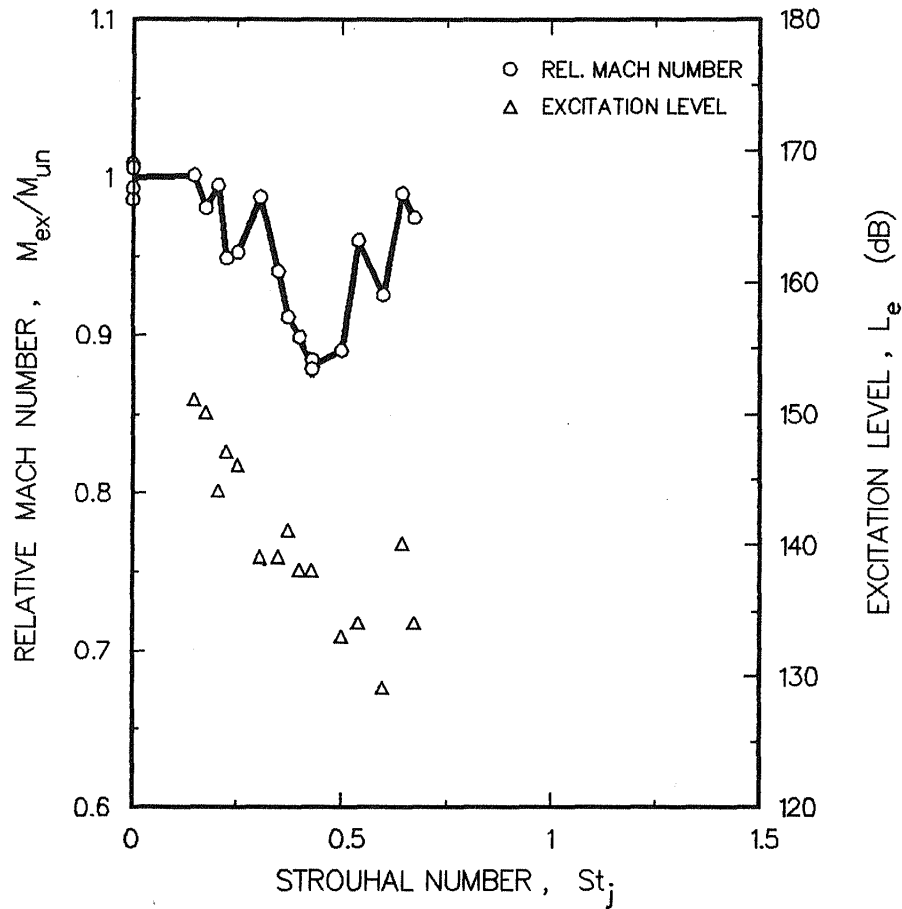
Figure 6.19   Supersonic unheated jet.

the results of the Strouhal number optimization experiments, presented above.

The excitation level effects on jets of different total temperatures are shown in Figures 6.20 through 6.23. When these figures are examined collectively, it appears that higher temperature jets require higher excitation levels for the flow to respond to this excitation. Probably due to this trend, no effects of upstream acoustic excitation were observed at jet operating conditions corresponding to Test Points 4, 5, 7, and 8 in the Test Matrix (Section 3.0). The maximum excitation level which could be generated in our test facility was 150 dB (rel. 2×10^5 Pa) or lower at high M_j and T_t, and this may not be high enough to produce measurable flow changes at the high velocity, high temperature conditions.

In summary, it has been found that the effect of upstream acoustic excitation on mixing of heated jets strongly varies with the jet operating conditions. At low Mach numbers, the heated jets were found to be highly excitable by sound. At high Mach numbers, however, little effect of sound was noticed for heated jets (above 600 K) even though the unheated jets were noticeably excitable at the same Mach number as seen in Figure 6.24. The preferential excitation Strouhal number does not change significantly with a change of the jet operating conditions. The effects of changing the nozzle exit boundary layer thickness were found to be similar, for both, heated and unheated jets at low Mach numbers in that the thicker the boundary layer, the less excitable was the jet. Finally, for heated high Mach number jets the effects of upstream acoustic excitation diminish significantly, regardless of the nozzle exit boundary layer thickness. Bear in mind, however, that the effects of nozzle exit boundary layer conditions were not investigated in full detail in this phase of the program due to a program funding limitation.

Based on the results of the optimization exercise, the proper excitation conditions were selected for each of the test points in the Test Matrix (Figure 3.1) to conduct detailed measurements of the entire flowfield. The results of these measurements are presented in the Part III of this report.
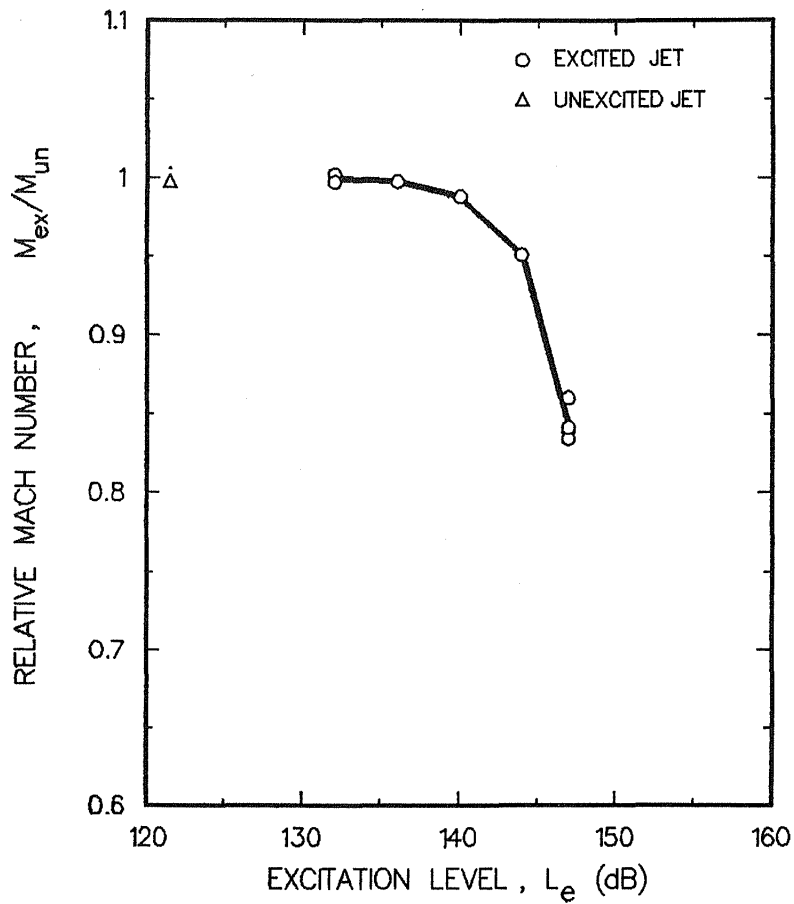
EXCITATION LEVEL EFFECTS ON RELATIVE MACH NUMBER

ON JET AXIS AT $X/D_j = 9$

FLOW CONDITIONS:
$M_j = 0.798$ $T_t/T_o = 0.99$

$U_j = 257.3 \text{ m.s}^{-1}$ $T_t = 291.1 \text{ K}$

$Re_j = 1,069,519$ $St_j = 0.41$

Figure 6.20   High Mach number unheated jet.
Test Point 1.

EXCITATION LEVEL EFFECTS ON RELATIVE MACH NUMBER
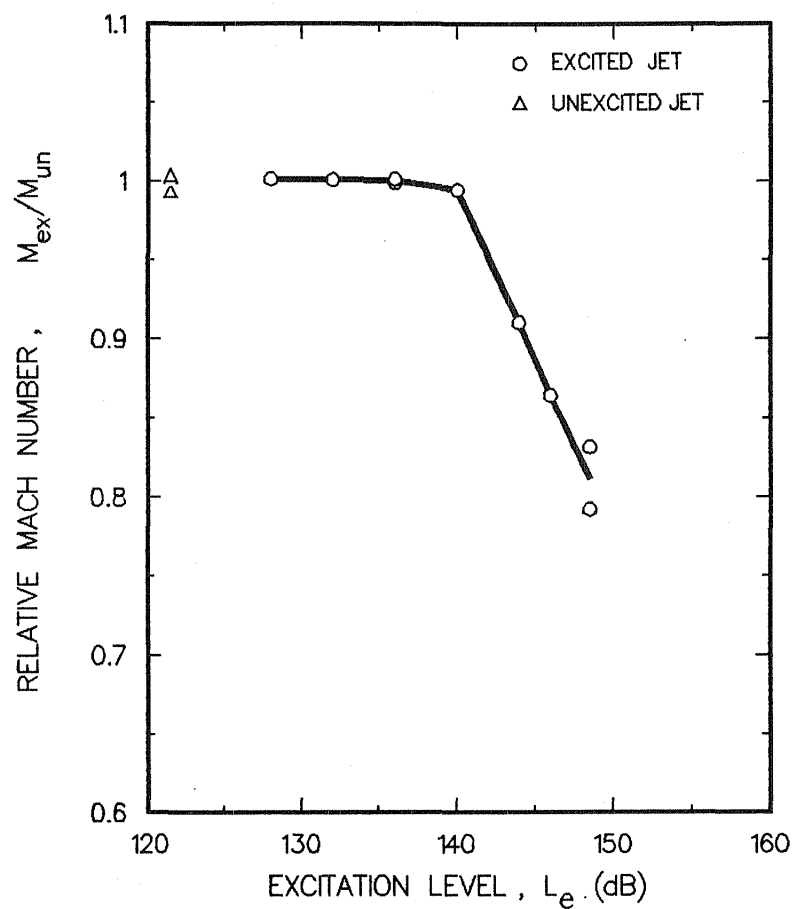
ON JET AXIS AT X/D_j = 9

FLOW CONDITIONS:
M_j = 0.800 T_t/T_o = 1.25
U_j = 289.1 m . s^{-1} T_t = 366.5 K
Re_j = 797,476 St_j = 0.39

Figure 6.21   High Mach number heated jet.
Test Point 2.

EXCITATION LEVEL EFFECTS ON RELATIVE MACH NUMBER

ON JET AXIS AT $X/D_j = 9$

FLOW CONDITIONS:

$M_j = 0.801$	$T_t/T_o = 1.66$
$U_j = 333.7\ m.s^{-1}$	$T_t = 488.2\ K$
$Re_j = 559,490$	$St_j = 0.35$

Figure 6.22   High Mach number heated jet.
Test Point 3.

EXCITATION LEVEL EFFECTS ON RELATIVE MACH NUMBER

ON JET AXIS AT X/D_j = 9

FLOW CONDITIONS: M_j = 0.807 T_t/T_o = 2.29
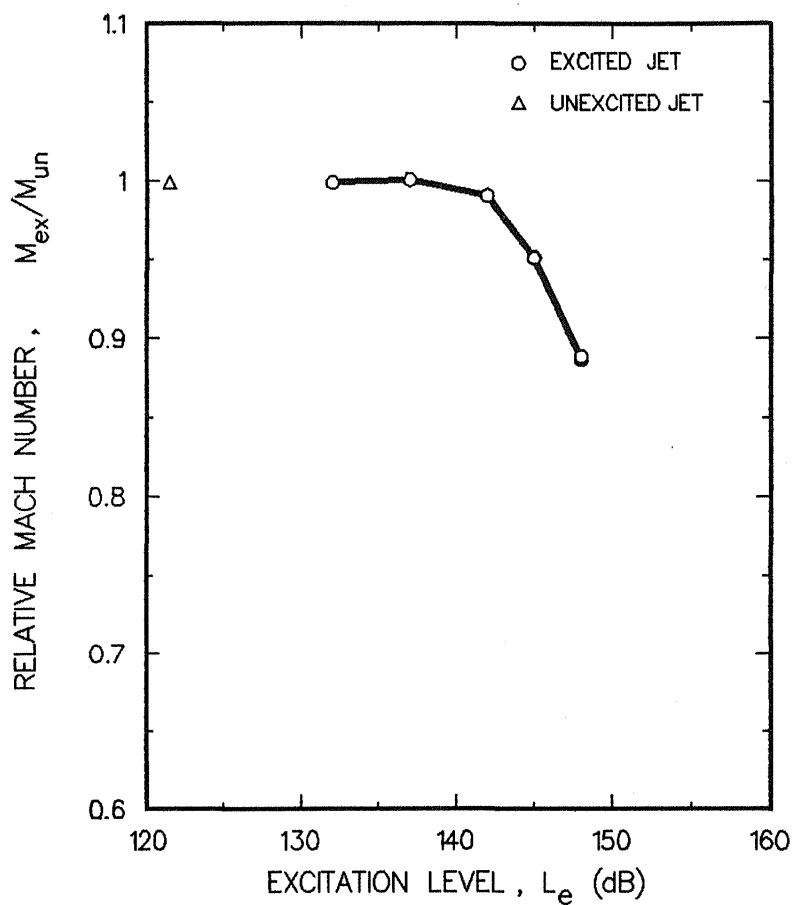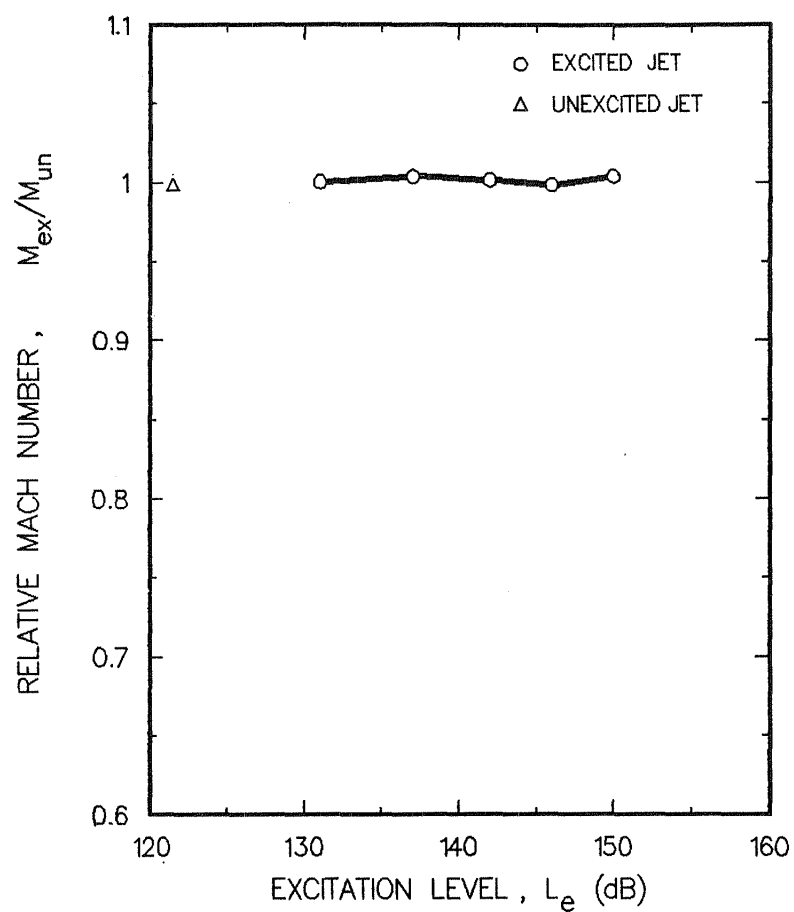
U_j = 392.5 m . s^{-1} T_t = 6716 K

Re_j = 380,934 St_j = 0.40

Figure 6.23   High Mach number heated jet.
            Test Point 4.

7.0 FLOW VISULAIZATION

Flow visualization studies of the jet nearfield started with low-speed jet
conditions. For a Mach number of 0.3, however, the sensitivity of the
schlieren system was not high enough to make good-contrast pictures.
Therefore, the Mach number was raised to increase the density gradients in
the flow and thus to improve the contrast of the schlieren pictures. In
order to visualize the development of the large-scale structure in detail,
the schlieren pictures were taken with a "corner" knife edge to utilize the
effects of both horizontal as well as vertical knife edge orientation in a
single picture. Each of the presented pictures consists of about 20
repeated 5- μs-exposures.

7.1 UNHEATED JETS

Figure 7.1 shows the response of the unheated jet to upstream acoustic
excitation at three Mach numbers 0.39, .41, and 0.43. As seen in the
figure, the vorticity shed from the nozzle lip appears to be in the form of
vortex rings. The vortex rings are obviously very stable, keeping their
form until they diffuse some 5 nozzle diameters downstream of the nozzle
exit. The essential features of the vortex movement and mutual interaction
can be observed in Figure 7.2 where a series of pictures with a constant
phase shift of 60 deg is shown. Two vortex structures are traceable in
this series. The main structure, highlighted by solid lines, tends to
maintain its formation in the flow and is convected relatively far down the
flow with a velocity of 0.67U_j. The secondary structure, highlighted by
broken lines, has a shorter lifetime, because it is convected with a lower
velocity, 0.45U_j, and its vortices are overtaken and absorbed by the
vortices of the main structure (Figure 7.2f). For the sake of
completeness, the picture of the unheated, unexcited jet of M_j = 0.48 is
shown in Figure 7.3

At high Mach number, a considerable distortion of the vortex structure in a
tone excited jet was observed. As seen in Figure 7.4, the vortex rings at
this Mach number were no longer perpendicular to the jet axis. Also, it
appears that vortices diffused faster than in the low-speed tone excited
jet. The picture of the unexcited, unheated, high-speed jet is shown in
Figure 7.5.

88
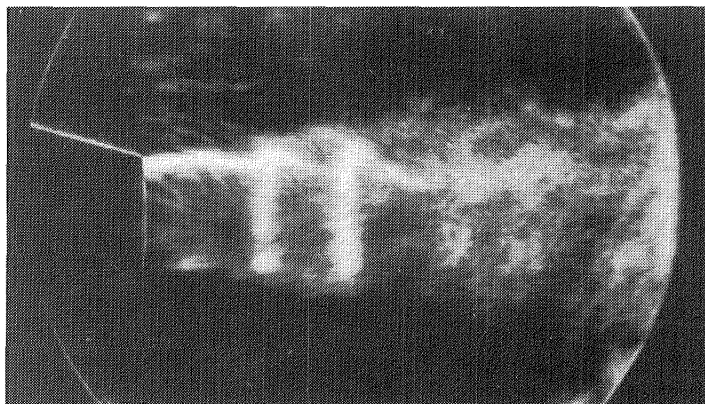
a.

$M_j = 0.39$

$T_t = 292$ K

$St_j = 0.39$

$L_e = 142$ dB
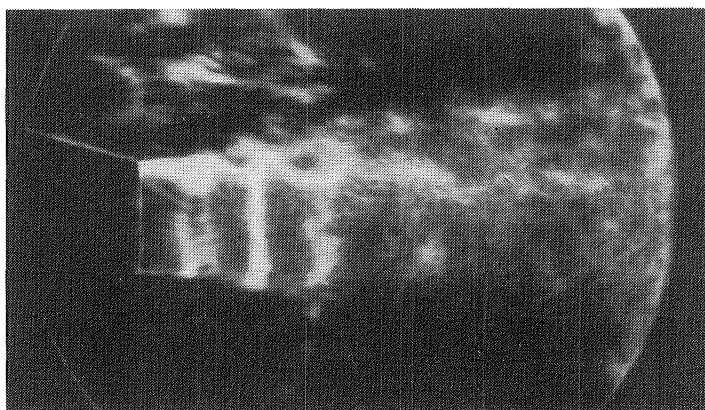
b.

$M_j = 0.41$

$T_t = 292$ K

$St_j = 0.50$

$L_e = 145$ dB
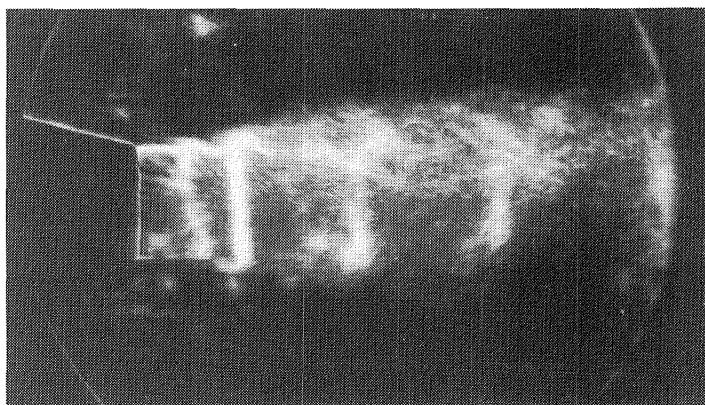
c.

$M_j = 0.43$

$T_t = 292$ K

$St_j = 0.43$

$L_e = 144$ dB

Figure 7.1 Ensemble-averaged photographs of tone-excited, unheated, low Mach number jets.

a. $\Delta\phi$ = 0 deg

b. $\Delta\phi$ = 60 deg

c. $\Delta\phi$ = 120 deg

d. $\Delta\phi$ = 180 deg

e. $\Delta\phi$ = 240 deg

f. $\Delta\phi$ = 300 deg

Figure 7.2 Phase-locked ensemble-averaged photographs of large-scale structure development in a tone-excited, unheated free jet. (M_j = 0.43, T_t = 292 K, St_j = 0.61, L_e = 145 dB)
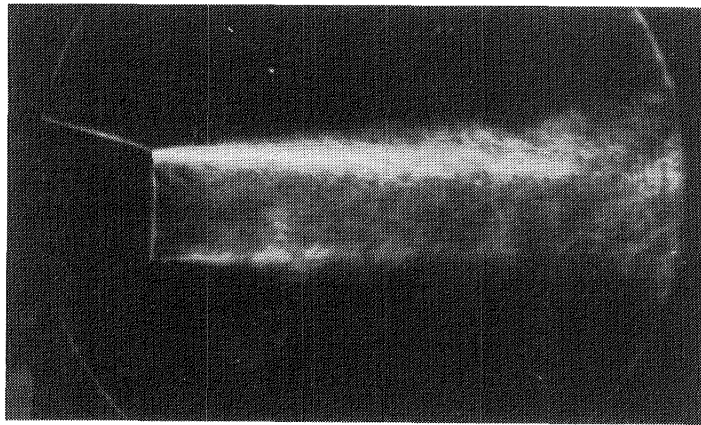
Figure 7.3   Photograph of an unexited, unheated, low Mach number jet.
(M$_j$ = 0.48, T$_t$ = 292 K)

a.

$M_j = 0.76$

$T_t = 291$ K

$St_j = 0.28$

$L_e = 143$ dB
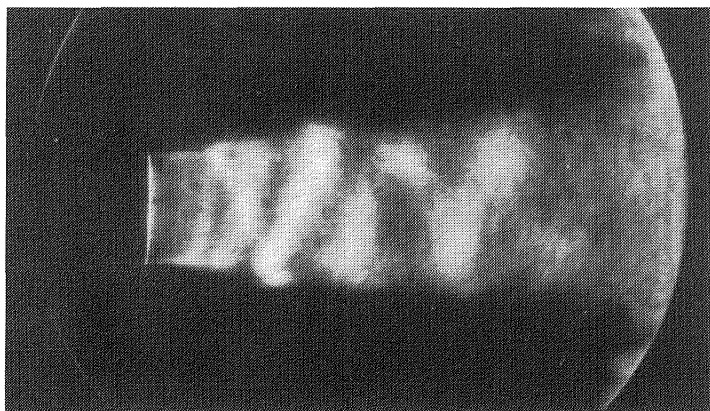
b.

$M_j = 0.80$

$T_t = 295$ K

$St_j = 0.37$

$L_e = 142$ dB
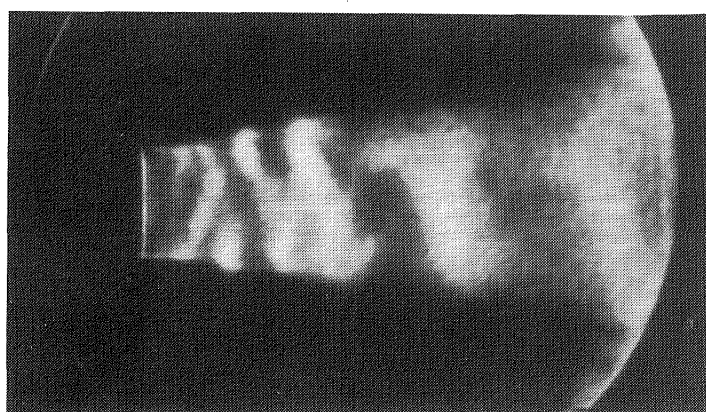
c.

$M_j = 0.80$

$T_t = 293$ K

$St_j = 0.48$

$L_e = 138$ dB

Figure 7.4   Ensemble-averaged   photographs   of   tone-excited,   unheated, high
Mach number jets.

7.2 HEATED JETS

The unexcited low Mach number jet, heated up to a total temperature of 670 K is shown in Figure 7.6.   Due to the heating of the flow, the schlieren pictures have much better contrast.   As mentioned in the previous section, heating of the low Mach number jet significantly improved its excitability. A similar conclusion may be drawn also from the flow visualization study. As seen in Figure 7.7, there is a well defined ring-vortex structure in the flowfield of a heated low Mach number jet acoustically excited in the range of Strouhal numbers from 0.25 to 0.45.

The vortex structure in the heated jet appears to diffuse faster than in the unheated, low-speed, tone-excited one.   It diffuses at approximately 4 exit diameters downstream from the nozzle exit plane. At an excitation Strouhal number of 0.25, pairing of two vortex structures was observed. As seen in Figure 7.8, two vortex structures are present in the flow. The main one (solid lines) is convected with a velocity of $0.35U_j$. The secondary structure (broken lines) is convected with a higher velocity of $0.59U_j$; its vortices thus catch up and fuse with the vortices of the main structure (Figure 7.8 a through e).   At the higher excitation Strouhal number of 0.45, no vortex pairing was observed.   As seen in Figure 7.9, vortices are convected with a velocity of $0.30U_j$ and keep a constant distance from each other.

At a high Mach number of 0.8, the jet heated to 670 K did not respond to upstream excitation at the maximum allowable level of 136 dB. As seen in Figures 7.10 and 7.11, there is no visible difference between the tone excited and unexcited jets at given jet operating and tone excitation conditions. This observation agrees with the conclusion drawn from the results of the optimization experiments.   Perhaps, much higher levels are needed to excite high Mach number, heated jets.   Further work to excite such jets using external excitation is described in Part 2 of this report.

Figure 7.5   Ensemble-averaged photograph of an unexcited, unheated, high Mach
             number jet.
             (M_j = 0.8, T_t = 291 K)
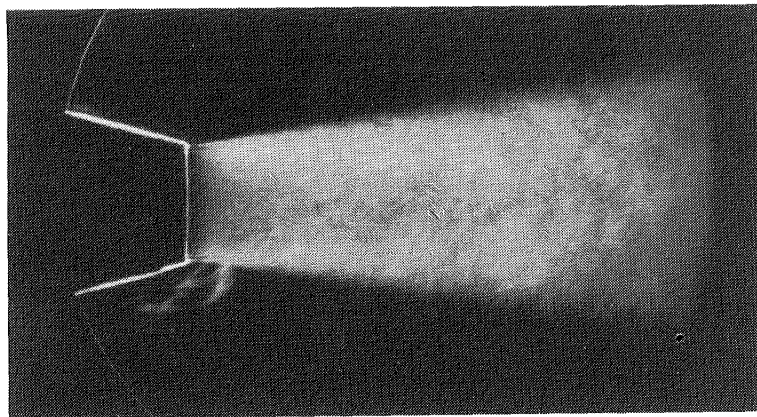
Figure 7.6 Ensemble-average photograph of an unexcited, heated, low Mach
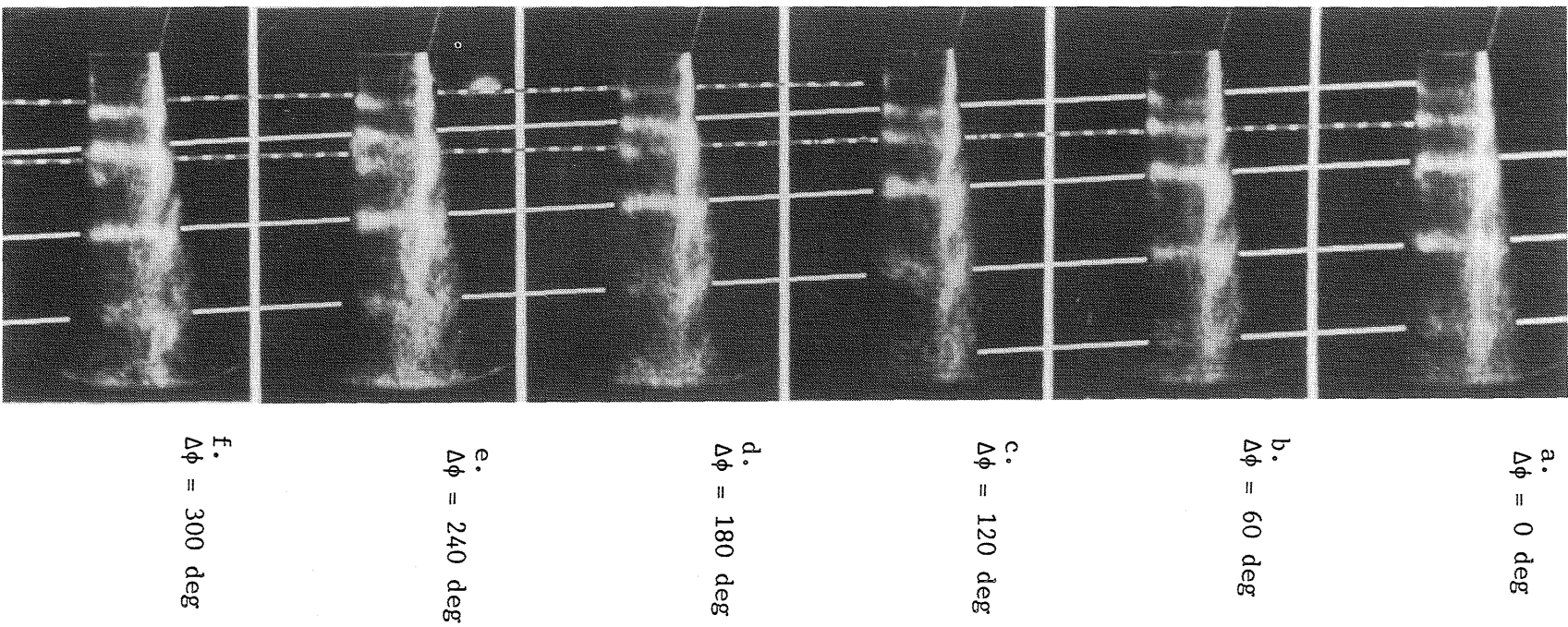   number jet.
             (M_j = 0.3, T_t = 666 K)
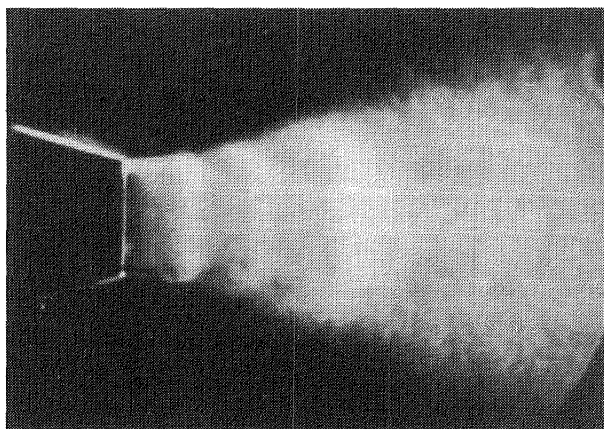
a.

M_j = 0.29

T_t = 673 K

St_j = 0.25

L_e = 144 dB

b.

M_j = 0.30

T_t = 672 K

St_j = 0.35

L_e = 142 dB
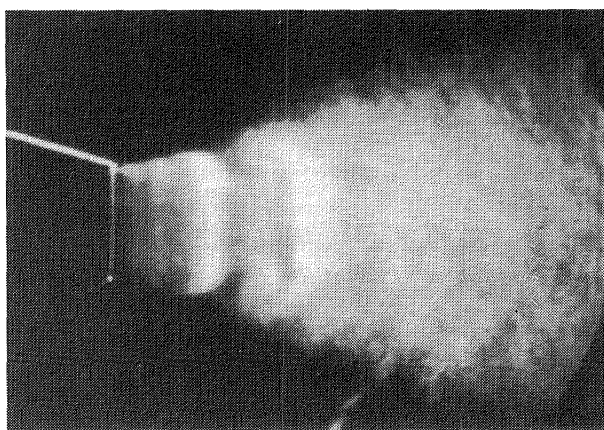
c.

M_j = 0.30

T_t = 671 K

St_j = 0.45

L_e = 145 dB

Figure 7.7   Ensemble-averaged photographs of tone-excited, heated, low Mach number jets.

a.
$\Delta\phi = 0$ deg

b.
$\Delta\phi = 60$ deg

c.
$\Delta\phi = 120$ deg

d.
$\Delta\phi = 180$ deg

e.
$\Delta\phi = 240$ deg

f.
$\Delta\phi = 300$ deg
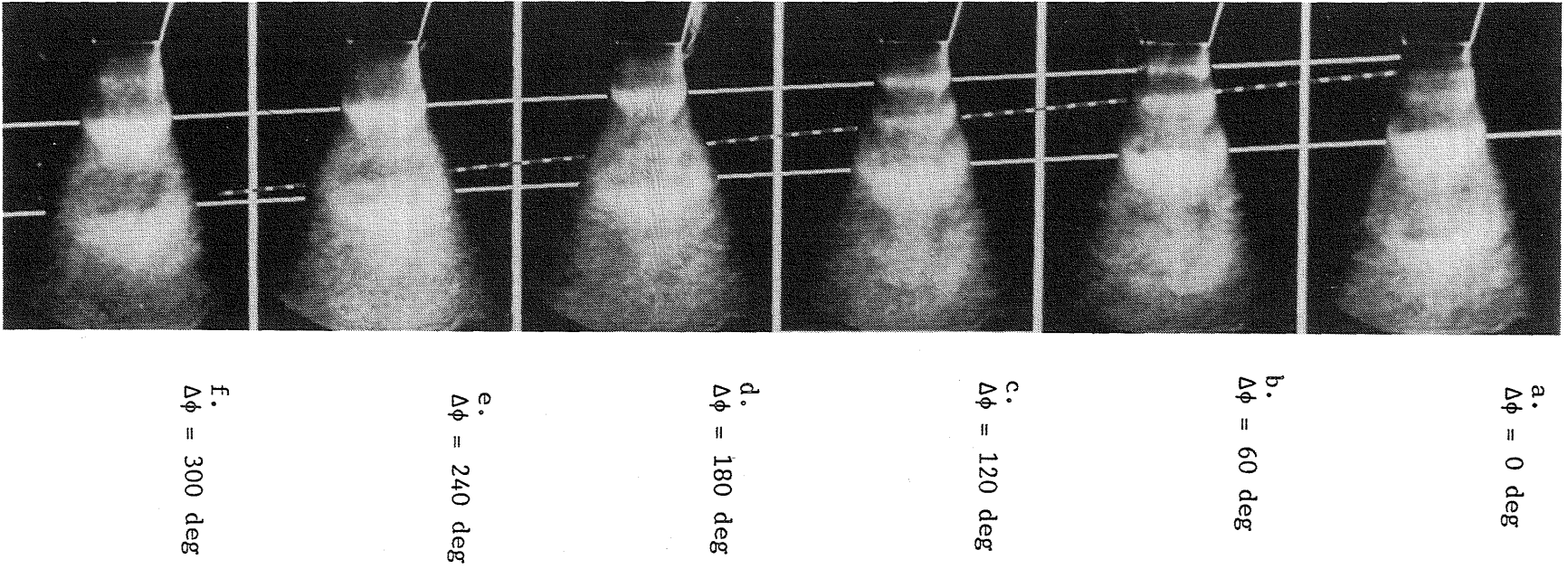
Figure 7.8   Phase-locked   ensemble-average   photographs   of   large-scale structure development in a tone-excited, heated free jet.
($M_j = 0.29$, $T_t = 673$ K, $St_j = 0.25$, $L_e = 144$ dB)
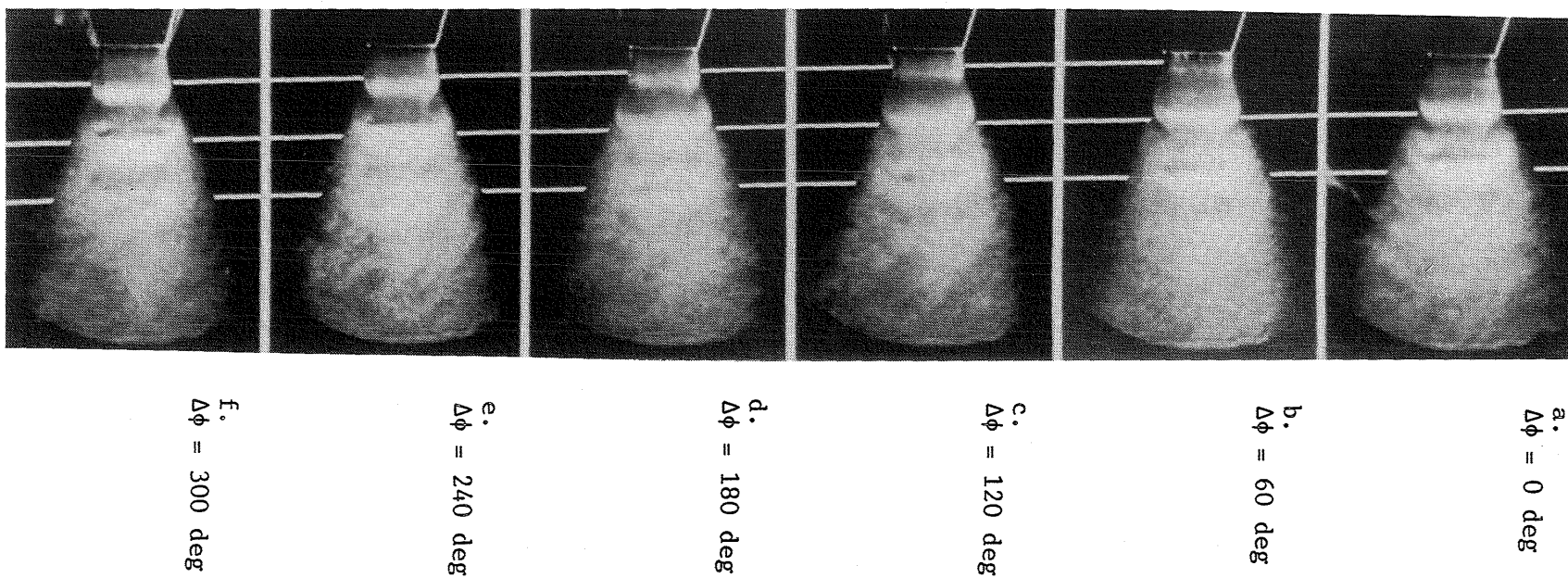
Figure 7.9 Phase-locked ensemble-averaged photographs of large-scale structure development in a tone-excited, heated free jet. (M_j = 0.30, T_t = 672 K, St_j = 0.45, L_e = 145 dB)

a. $\Delta\phi$ = 0 deg
b. $\Delta\phi$ = 60 deg
c. $\Delta\phi$ = 120 deg
d. $\Delta\phi$ = 180 deg
e. $\Delta\phi$ = 240 deg
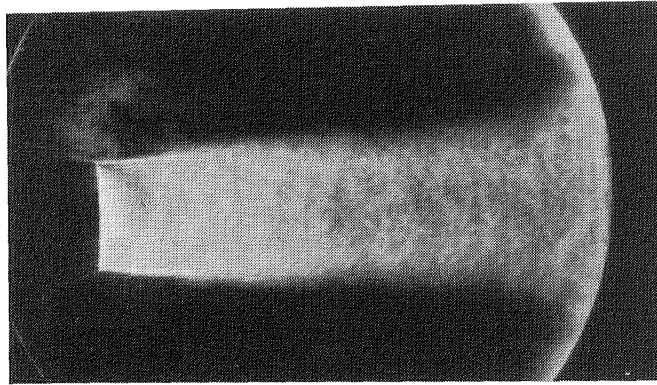f. $\Delta\phi$ = 300 deg
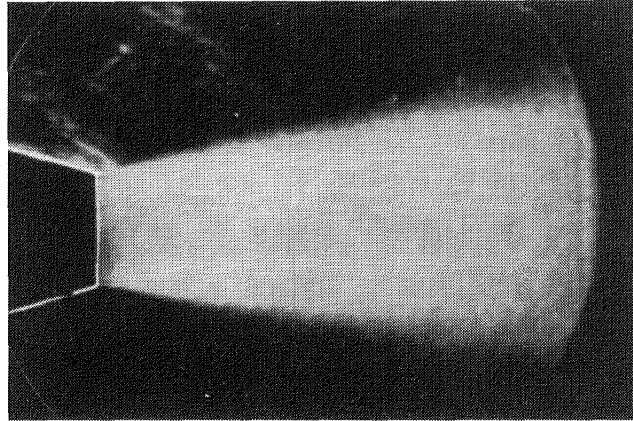
Figure 7.10 Ensemble-averaged photograph of an unexcited, heated, high Mach
number jet.
(M_j = 0.80, T_t = 663 K)
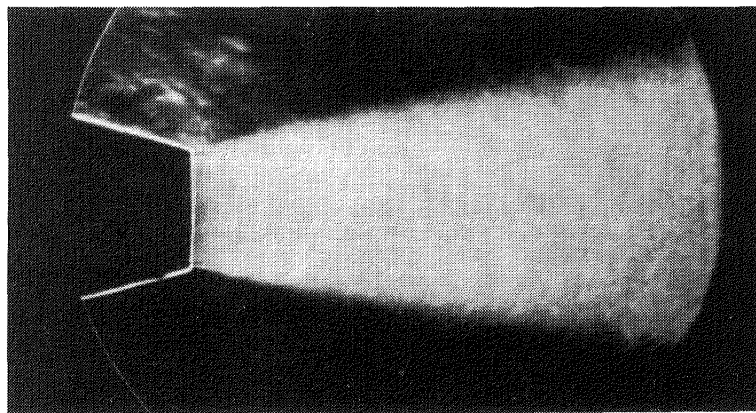
Figure 7.11 Ensemble-averaged photograph of a tone-excited, heated, high Mach
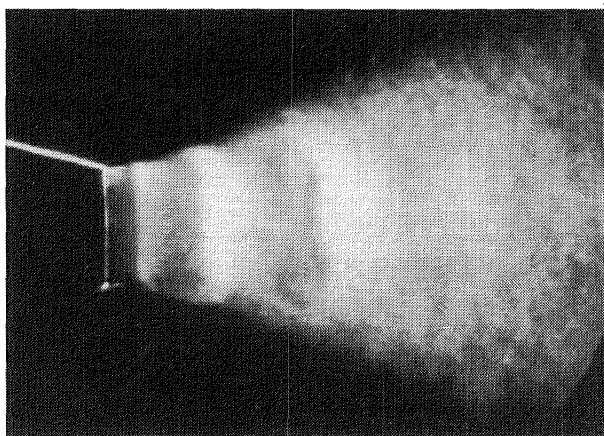number jet.
(M_j = 0.80, T_t = 674 K, St_j = 0.32, L_e = 136 dB)

8.0 THEORY AND COMPARISONS WITH EXPERIMENT

The initial formulation of the analysis is contained in Reference F.1. In this section of the report we will examine extensions to that analysis without reviewing the previous work. The new developments have enabled the predictions of the jet development to be extended beyond the end of the potential core. This means that the centerline velocity decay may be predicted. The slight decrease in the jet centerline velocity in the potential core itself, which is observed experimentally at high levels of excitation, is also now predicted by the analysis. These extensions to the analysis have involved several separate efforts. These are described in the next section.

8.1 STABILITY OF THE JET IN THE DEVELOPED JET REGION

In order to evaluate the local rate of growth or decay of the instability wave at any location in the jet, it is necessary to solve the Orr-Sommerfeld equation. The boundary conditions to be satisfied by the instability wave are relatively easy to specify, for the purposes of numerical calculation, in the potential core region of the jet. This analysis is given in Reference F.9 where it is shown that the wave depends on modified Bessel functions in the potential core and on Hankel functions outside the jet in the ambient fluid. This latter condition still applies downstream of the potential core, but close to the jet centerline, a series solution to the Orr-Sommerfeld equation must be sought. At high Reynolds numbers, in free shear flows, the stability characteristics of the waves may be obtained from the inviscid Rayleigh equation. The only difficulty with solutions to this equation is that, for decaying solutions, the solution is not valid at all real radial locations, Reference F.16. Because of this the full viscous Orr-Sommerfeld equation was solved in the potential core region, since the calculations of the coupling coefficients required the values of the eigen solutions at all real radial locations. However, downstream of the end of the potential core, as no further coupling of any significance occurs between the exciting acoustic wave and the excited instability wave then, since the calculations only require the local growth rate, the inviscid Rayleigh equation may be solved. A series solution is sought where the mean velocity and density are written

$$\bar{u} = c_o + c_2 \cdot r^2 + c_4 \cdot r^4 + \cdots \cdots$$

and

$$\bar{\rho} = b_o + b_2 \cdot r^2 + b_4 \cdot r^4 + \cdots \cdots$$

The instability wave pressure p(r) is written,

$$\hat{p} = r^m (a_o + a_2 \cdot r^2 + a_4 \cdot r^4 + \cdots \cdots)$$

These forms are substituted into the Rayleigh equation and the coefficient a_{2n} evaluated for given b_{2n} and c_{2n}. The terms were evaluated up to a_4.

The mean velocity profile is assumed to take a Gaussian form:

$$\bar{u} = \bar{u}_c \cdot \exp [-a^* \cdot r^2 / b^2],$$

where u_c is the centerline velocity, b is the jet half-width and $a^* = 0.69315$. The jet density is related to the axial mean velocity using Crocco's relationship [F.17]. The coefficients b_{2n} and c_{2n} are then readily obtained. For example,

$$c_o = \bar{u}_c, \quad c_2 = - a^* \bar{u}_c / b^2 .$$

The local growth rate of the instability wave is then obtained by integrating the Rayleigh equation subject to the series solution for small radius and matching with the Hankel function solution outside the jet flow.

As is the case in the annular mixing region of the jet, the downstream development of the jet flow beyond the end of the potential core is determined from the solution of the integral equations. These are the momentum integral equation, the mean mechanical energy equation, and the turbulent kinetic energy equation. Using the notation of Reference F.1, these equations may be written,

$$2 \int_0^\infty \rho \cdot \overline{u}^2 \cdot r \cdot dr = 1$$

$$\frac{d}{dx} \int_0^\infty \rho \cdot \frac{\overline{u}^3}{2} \cdot r \cdot dr = 2 \cdot k_i \cdot |A|^2 - \int_0^\infty \phi \cdot r \cdot dr - \int_0^\infty \overline{\rho} \cdot \varepsilon_m^* \cdot \left(\frac{\partial \overline{u}}{\partial r}\right)^2 \cdot r \cdot dr$$

and

$$\frac{d}{dx} \int_0^\infty \rho \cdot \overline{u} \cdot q \cdot r \cdot dr = \int_0^\infty \overline{\rho} \cdot \varepsilon_m^* \cdot \left(\frac{\partial \overline{u}}{\partial r}\right)^2 \cdot r \cdot dr + \int_0^\infty \phi \cdot r \cdot dr - \int_0^\infty \varepsilon^* \cdot r \cdot dr$$

Here, $\phi(r)$ represents the interaction between the instability wave and the fine-scale turbulence, ε^* denotes the viscous dissipation, and q represents the turbulent kinetic energy. Models are proposed for all the terms in the integrals on the basis of experimental observations. Thus, we write

$$\overline{u} = \overline{u}_c \cdot \exp\left[-a^* \cdot r^2 \big/ b^2\right]$$

$$q = \overline{q}(x) \exp\left[-1.7946 \left\{ r/b - \sqrt{\frac{\ln(2\overline{u}_c)}{a^*}} \right\}^2\right]$$

$$\varepsilon_m^* = c_1 \cdot q^{\frac{1}{2}} \cdot \ell \qquad ; \quad c_1 = 0.05$$

and

$$\varepsilon^* = c_2 \cdot q^{3/2} \big/ \ell \qquad ; \quad c_2 = 1.5$$

Using the same arguments as proposed in Reference F.1, the wave interaction term may be written,

$$\phi = c_3 \cdot q^{\frac{1}{2}} \cdot |A|^2 \big/ (\ell \cdot b^2)$$

The constant c_3 is an unknown empirical constant which sets the level of coupling between small scale turbulence and the instability waves. In this equation $\ell(x)$ is a local length scale defined as the radial distance between points where u is 0.9 u_c and 0.1 u_c, respectively. In this case,

for the Gaussian velocity profile,

$$\ell_c = 1.43274 \ b.$$

With these assumptions the integral equations reduce to a system of ordinary differential equations for u_c, b, and q as functions of downstream distance. The equations are solved numerically using a variable step-size fourth-order Runge-Kutta integration scheme.

The final extension to the previous analysis permits the effect of the finite amplitude instability wave on the jet centerline velocity, in the potential core region, to be determined. In the potential core region, the centerline velocity had been constrained to be equal to the jet exit velocity. However, for sufficiently high levels of excitation, the centerline velocity is observed experimentally to vary. This is due to the effect of finite amplitude instability waves growing rapidly along the jet. Their influence is felt on the jet axis. Consider the instantaneous momentum equation for axisymmetric disturbance and mean flow.

$$\rho \cdot u \cdot \frac{\partial u}{\partial x} + \rho \cdot v \cdot \frac{\partial v}{\partial r} = \frac{1}{Re} \cdot \frac{1}{r} \cdot \frac{\partial}{\partial r} \left\{ r \cdot \frac{\partial u}{\partial r} \right\}$$

Close to the jet centerline

$$u = \bar{u}_c(x) + \tilde{u}_c$$

$$v = 0$$

$$\rho = \rho_c(x) + \tilde{\rho}_c$$

Thus, on averaging, the axial momentum equation reduces to

$$\rho_c \ \bar{u}_c \ \frac{d\bar{u}_c}{dx} + \rho_c \ \overline{\tilde{u}_c \ \frac{d\tilde{u}_c}{dx}} + \overline{\tilde{\rho}_c \ \tilde{u}_c} \ \frac{d\bar{u}_c}{dx} = 0$$

For the sake of simplicity, it will be assumed that the density/velocity correlation is much smaller than the velocity/velocity correlation. Thus, the momentum equation reduces to,

$$\frac{d}{dx} (\bar{u}_c^2 + \tilde{u}_c^2) = 0$$

102

Integrating, and assuming the instability wave has zero amplitude at the jet exit gives,

$$\overline{u}_c^2 = 1 - \overline{\tilde{u}_c^2}$$

If we introduce the wave-like form of the solution for the instability wave, such that , we obtain

$$\overline{\tilde{u}_c^2} = |A|^2 \cdot |\hat{u}_c|^2 \cdot \overline{u}_c^2$$

$$\overline{u}_c^2 = 1 \Big/ (1 + |A|^2 \cdot |\hat{u}_c|^2)$$

Clearly, as the amplitude of the instability wave increases, the jet centerline velocity decreases. For example, $|A|^2 |\hat{u}_c|^2$ reaches a typical maximum amplitude of 0.025, for high excitation levels. This means that u_c falls to 98 percent of the exit velocity. This is typical of the earlier experimental observations.

The presented prediction scheme is based on the assumption that the initial boundary layer is turbulent and the only influence of the boundary layer is through its thickness at the jet exit. To include the influence of the type of the initial boundary layer in the prediction scheme would require a more detailed modeling of the initial flow development including the transition of the mean velocity profile from a laminar boundary layer to a turbulent mixing layer. Tough this would be possible, it is beyond the scope of the present prediction scheme.

All of the preceding extensions to the earlier analysis have been incorporated into a computer program, which also provides a graphical representation of the downstream jet development.

8.2 COMPARISON WITH THEORETICAL PREDICTIONS

8.2.1 Typical Predictions

The computational program, based on the upgraded theory, generates axial distributions of four basic parameters of a tone excited jet. These

characteristics are: (1) mean velocity, (2) jet half width, (3) peak turbulent kinetic energy, and (4) peak pressure level. Figures 8.1 through 8.4 show typical predicted distributions for a heated, excited jet at a Mach number of M_j = 0.48, total temperature of T_t = 488 K, excitation Strouhal number of St_j = 0.48, and excitation level L_e = 151 dB. Similar sets of plots were acquired for the other jet excitation and operating conditions also.

8.2.2 Typical Comparisons

The results of theoretical predictions were compared with experimentally acquired data. However, since the turbulence and acoustic pressure data were not obtained under this contract, only the mean velocities were compared. The comparison of mean velocities was based on the behavior of local Mach number on the jet centerline at nine nozzle exit diameters downstream of the nozzle exit plane. As described in Section 6.0, the Mach number at this location was found to strongly depend on the excitation Strouhal number. Because of the time consuming nature of the computer programs, the comparisons between prediction and measurements were made only at one jet Mach number. A moderate jet Mach number of M_j = 0.48 and jet total temperature of T_t = 488 K were selected for this comparison. As shown in Figure 8.5 at this jet operating condition, the agreement between predicted and measured behavior of the local Mach number was found to be excellent. The particular excitation levels used for the theoretical predictions were the same as the measured ones, and were presented earlier in Figure 6.11.

Because of the funding limitations, only a limited number of calculations have been made at other jet operating conditions. However, the preliminary results indicate that for the highly heated jets the predicted mean velocities somewhat differ from measured ones. It appears that for the high Mach number heated jets, the theory predicts faster velocity decay along the centerline than the measured one. On the other hand, for the low Mach number heated jets, the theory predicts more gradual velocity decay compared to the measured one.

On the whole, it may be concluded that the theory works satisfactorily, particularly for the moderate jet Mach numbers and moderate jet total temperatures. However, further calculations are necessary to verify the theory for highly heated jets at low and high jet Mach numbers.

104

$M_j = 0.481$ $St_j = 0.479$
$T_t^j/T_o = 1.67$ $L_e^j = 151$ dB
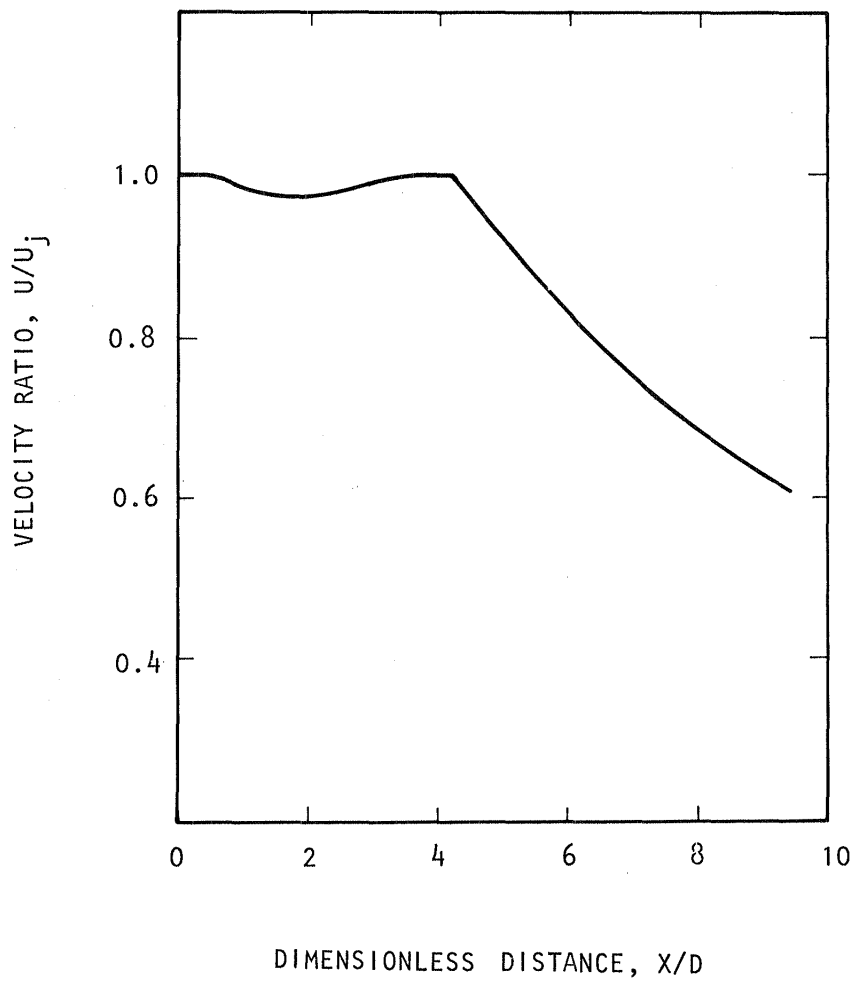
Figure 8.1 Mean velocity centerline distribution.

$M_j = 0.481$ $St_j = 0.479$
$T_t/T_o = 1.67$ $L_e = 151$ dB
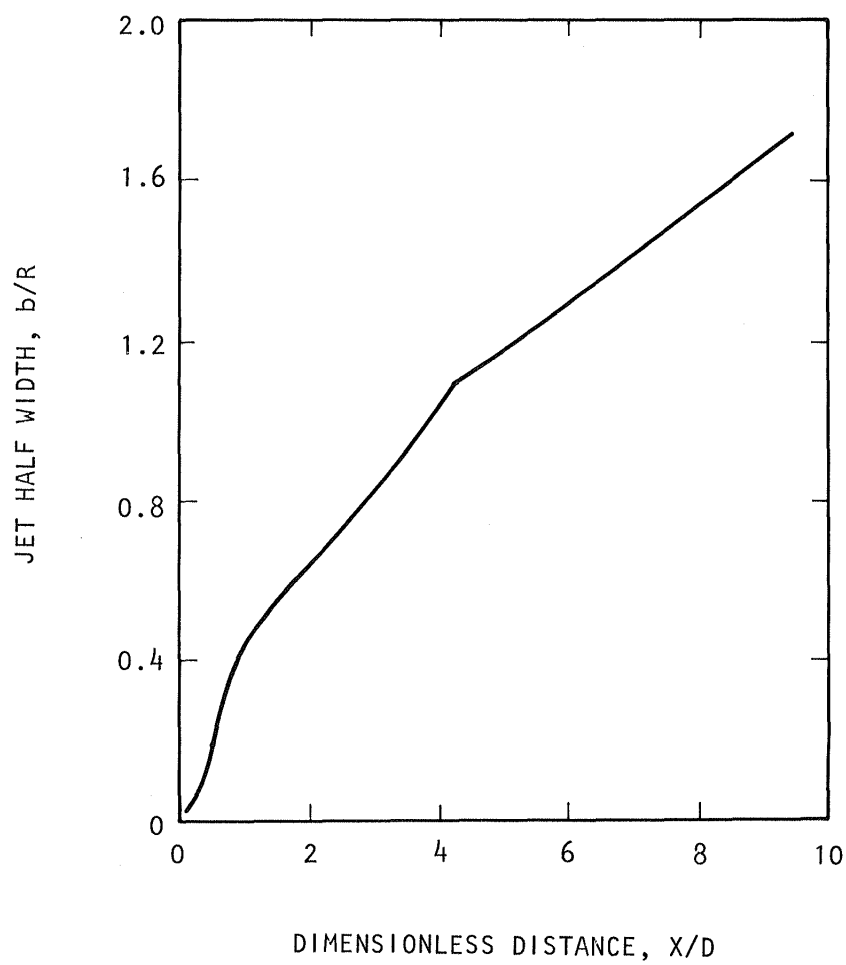
Figure 8.2 Half-jet width centerline distribution.

$M_j = 0.481$ $St_j = 0.479$
$T_t/T_o = 1.67$ $L_e = 151$ dB
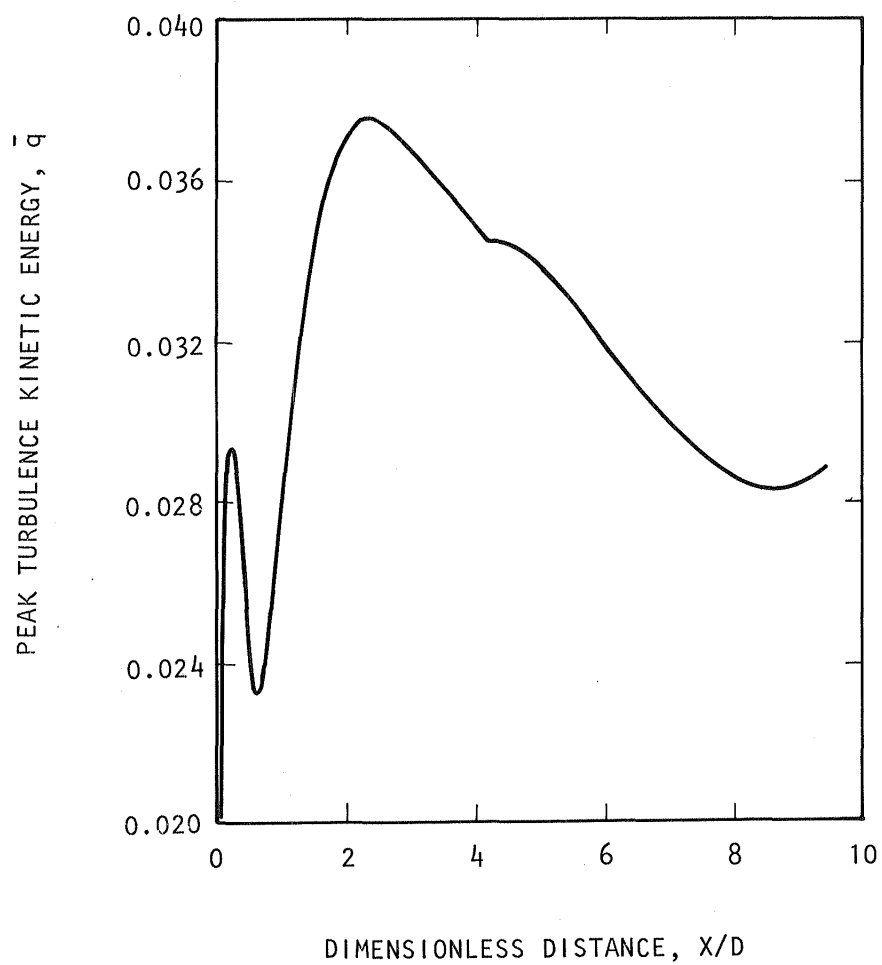
Figure 8.3 Peak turbulent kinetic energy centerline distribution.

$$M_j = 0.481 \qquad St_j = 0.479$$
$$T_t/T_o = 1.67 \qquad L_e = 151 \text{ dB}$$
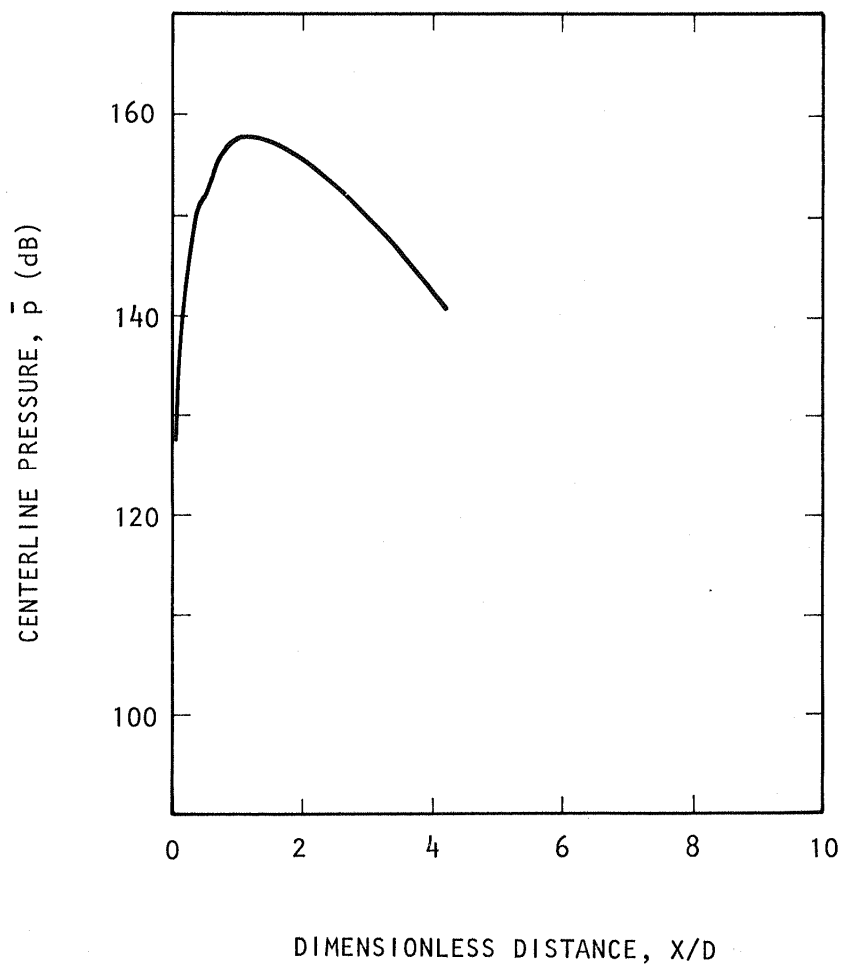
Figure 8.4   Peak pressure level centerline distribution.

EXCITATION STROUHAL NUMBER EFFECTS ON RELATIVE MACH NUMBER ON JET AXIS AT $X/D_j = 9$
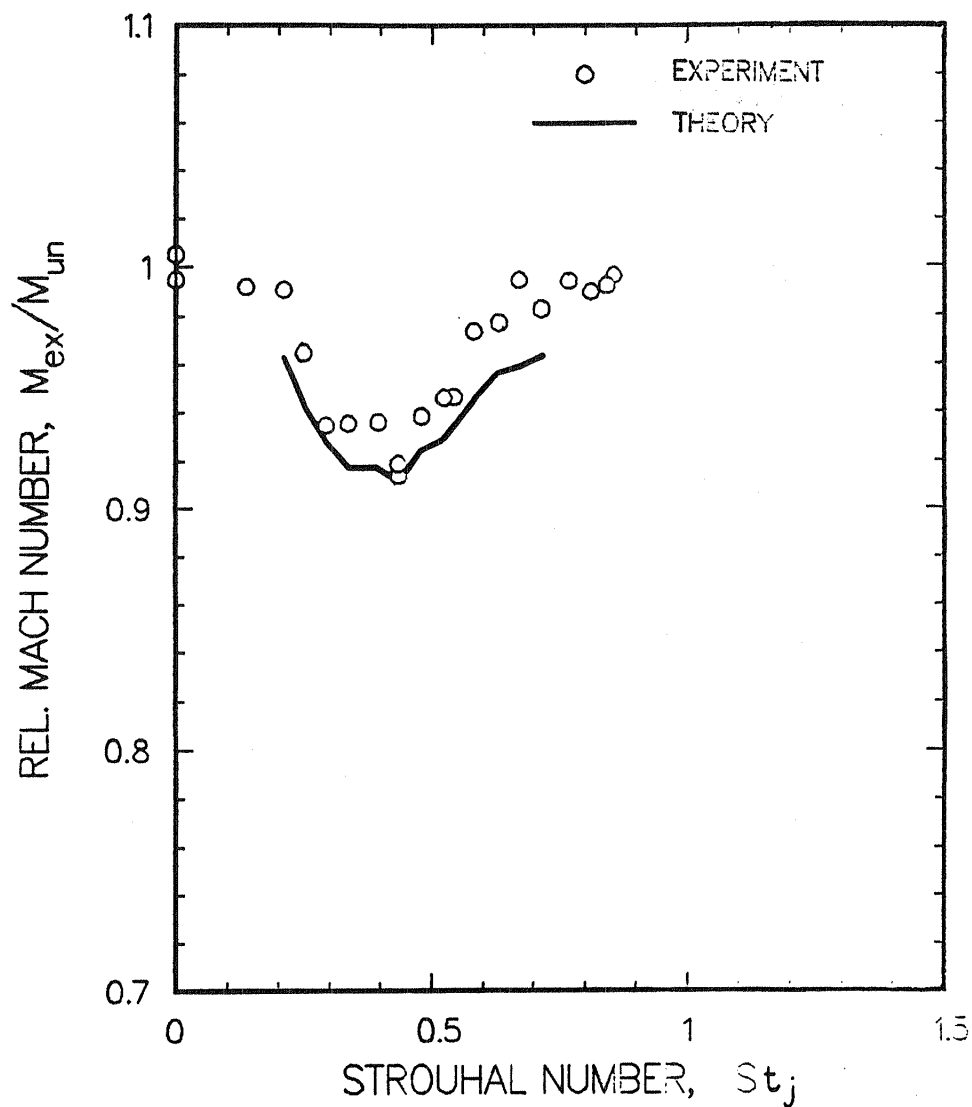
FLOW CONDITIONS:

$M_j = 0.481$ $T_t/T_o = 1.67$

$U_j = 207.7$ m/s $T_t = 487.9$ K

$Re_j = 305586$

Figure 8.5   Comparison between theory and experiment.
The particular excitation levels for each
test point are in Figure 6.11.

9.0 CONCLUSIONS FOR INTERNAL EXCITATION

To obtain a fundamental understanding of the effects of relatively strong upstream acoustic excitation on the mixing of heated jets, a fairly detailed experimental study has been carried out. A theoretical model has been extended to consider the region downstream of the jet potential core. A limited comparison between theoretical prediction and experimental results has also been made.

A summary of key observations is given below. Of course, the validity of the conclusions, presented here, is restricted to the range of investigated jet operating and flow excitation conditions.

o The sensitivity of heated jets to upstream acoustic excitation strongly varies with the jet operating conditions.

o A low Mach number jet (M_j = 0.3) shows increased sensitivity to upstream excitation as the jet temperature is raised, but the high Mach number jet (M_j = 0. 8) exhibits a decrease in the jet excitability as the jet temperature rises, as shown in Figure 9.1. This figure is based on the results presented in Section 6.0.

o Preferential excitation Strouhal number does not change significantly with a change of the jet operating conditions.

The excitation Strouhal number that produces the maximum changes in the jet flowfield practically does not depend on the jet operating conditions. As shown in Section 6.0, the most effective excitation Strouhal number remained in the range of St_j = 0.35 – 0.5 at all examined jet operating conditions.

o The effects of the nozzle exit boundary layer thickness were found to be similar for both heated and unheated jets at low Mach number.

The excitability of both heated and unheated low speed jets decreases as the nozzle exit boundary layer thickens. The artificially generated thicker nozzle exit boundary layer at low Mach numbers depressed the effects of upstream acoustic excitation regardless of the jet temperature. This outcome was demonstrated in Sections 5.0 and 6.0.

The experiments with a tripped boundary layer for the heated high speed jets did not help to clarify the effect of nozzle exit

110
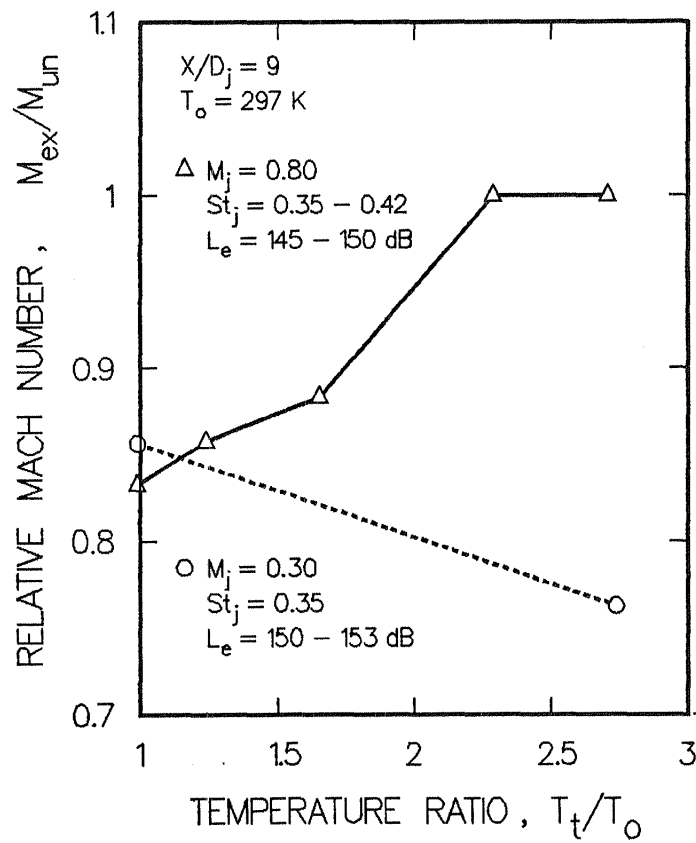
Figure 9.1 Temperature effects on acoustically excited jets.

boundary layer profile (laminar or turbulent) on heated jet
excitability. The tripping device used in our experiment
generated a boundary layer which was too thick. Jet excitability
depends also on nozzle exit boundary layer thickness, as
discussed above, thus the possible effect of the changed boundary
layer profile was hidden by the effect of increased boundary
layer thickness. No firm conclusions were drawn about effects of
nozzle exit boundary layer profile on the excitability of heated
jets at this point. Further experiments on boundary layer
effects are described in Part II.

o   This study has further confirmed the earlier Lockheed findings
     that a jet can be excited even if it is turbulent and is operated
     at high Reynolds numbers.

     Because a majority of the studies in this field have been carried
     out for low Reynolds number jets (and also mostly for laminar
     jets), there appear to prevail common misgivings amongst many
     members of the research community about the validity of the
     acoustic excitation effects for turbulent and high Reynolds
     number jets. The present studies categorically confirm earlier
     Lockheed findings (References D.2 and D.3) that a jet can be
     excited even if it is turbulent and is operated at high Reynolds
     numbers (see Figures 5.3 and 6.2).

o   The upgraded theory has been verified at moderate jet Mach number
     and moderate jet total temperatures.

     Good agreement has been found between the theory and the
     experiments in moderately heated jets. However, the theory has
     not yet been fully confirmed for highly heated jets, and a range
     of excitation conditions.

o   Further experimental and theoretical work is needed to obtain
     better understanding of heated jets under the influence of
     acoustic excitation.

     Further comparison of predicted results with the measured data
     needs to be made for a range of test conditions. The areas where
     disagreements are found need to be examined closely by way of
     measurements of the turbulence intensities in the heated, excited
     jets. Also, the sound source used for the present tests needs
     to be upgraded so as to produce much higher excitation levels at
     the jet exit. Finally, if needed, the assumptions made in the
     theory need to be reassessed in the light of measurements that
     may be generated in any future program.

The results obtained in this experimental investigation have pointed out some differences between heated and unheated jets, as far as their excitability and consequently their rates of mixing are concerned. In addition, it has provided an extensive experimental data base on heated jets under the upstream acoustic excitation, as well as without excitation.

It was these results that prompted the addition of an external excitation source, the results for which are described in Part 2 of this report. It is shown in Part 2 that heated, supersonic jets are excitable, but to understand the effects properly, further work is still needed.

LIST OF SYMBOLS

a	sound velocity
A	instability wave amplitude function
$a*, a_0, a_2, a_4$	constants
b	half jet width
b_0, b_2, b_4	constants
c_0, c_2, c_4	constants
D	nozzle exit diameter
f	frequency
H	shape factor
K	dynamic correction ratio
k	wave number
L	level
l	length scale
M	Mach number
m	exponent
m_w	circumferential mode number
n	nth term
p	pressure
q	turbulent kinetic energy
r	radius
R	nozzle exit radius
R*	distance
Re	Reynolds number
St	Strouhal number
T	temperature
U, u	axial velocity
u'	axial fluctuating velocity
V, v	radial velocity
v'	radial fluctuating velocity
X	axial coordinate
Y	radial coordinate
Z	radial coordinate
α	angle
γ	specific heat ratio
δ	displacement thickness
ε	energy thickness
$\varepsilon*$	viscous dissipation
$\varepsilon*_m$	kinematic eddy viscosity
ϕ	interaction term
ρ	density
θ	momentum thickness
ξ	pressure ratio
ζ	boundary layer thickness

Subscripts

c	centerline
e, ex	excited
j	jet, based on nozzle diameter
p	probe
s	static
t	total
un	unexcited
o	ambient
δ	based on displacement thickness
ε	based on energy thickness
θ	based on momentum thickness

Overbars

$-$	time average
$\sim$	phase average
$\wedge$	instability wave

REFERENCES

A.1   Borisov, Y. Y.; Rosenfeld, E. I.; and Smolenskii, V. G.: Effect of Acoustic Vibrations on a Gas Flame Burning in a Confined Space. Fizika Goreniya i Vzryva, Vol. 7, pp. 404-412, 1971.

A.2   Brown, G. B.: On Sensitive Flames.   Phil. Mag., Vol. 13, pp. 161-195, 1932.

A.3   Chanaud, R. C.; and Powell, A.: Experiments Concerning the Sound-Sensitive Jet. J. Acoust. Soc. Am., Vol. 34, pp. 907-915, 1962.

A.4   Cantrell, R. H.; McClure, F. T.; and Hart, R. W.: Acoustic Damping in Cavities with Mean Velocity and Thermal Boundary Layers. J. Acoust. Soc. Am., Vol. 35, pp. 500-509, 1963.

A.5   Crump, J. E.; and Price, E. W.: Effect of Acoustic Environment on the Burning Rate of Double-Base Solid Propellants. ARS Journal, Vol. 31, pp. 1026-1029, 1961.

A.6   Elias, I.: Acoustical Resonances Produced by Combustion of a Fuel-Air Mixture in a Rectangular Duct.   J. Acoust. Soc. Am., Vol. 31, pp. 296-304, 1959.

A.7   Fitaire, M.; and Sinitean, D.: Acoustic Wave Excitation in a Flame. Czechoslovak J. Physics, Vol. 22, pp. 394-397, 1972.

A.8   Hahnemann, Von H.; and Ehret, L.: Uber den Einfluss Starker Schallwellen auf eine Stationar Brennende Gasflamme. Zeit. Tech. Physik, Vol. 24, pp. 228-2 42, 1943.

A.9   Leconte, J.: On the Influence of Musical Sounds on the Flame of a Jet of Coal-Gas. Phil. Mag., Vol. 15, pp. 235-239, 1858.

A.10   Leung, C. T.; and Ko, N.W.M.:   Resonance Effect of Acoustic Excitation on Heat-Transfer. J. Sound and Vib., Vol. 79, pp. 303-305, 1981.

A.11   Loshaek, S.; Fien, R. S.; and Olsen, H. L.:   The Effect of Sound on Laminar Propane-Air Flames. J. Acoust. Soc. Am., Vol. 21, pp. 605-612, 1949.

A.12   McClure, F. T.; Hart, R. W.; and Cantrell, R. H.: Interaction between Sound and Flow: Stability of T-Burners. AIAA Journal, Vol. 1, pp. 586-590, 1963.

A.13   Morfey, C. L.: Sound Radiation Due to Unsteady Dissipation in Turbulent Flows. J. Sound and Vib., Vol. 48, pp. 95-111, 1976.

A.14   Peterka, J. A.; and Richardson, P. D.: Effect of Sound on Separated Flows. J. Fluid Mech., Vol. 37, pp. 265-287, 1969.

A.15   Rayleigh, Lord, J. W. G.: On the Instability of Jets. Scientific Papers I, pp. 361-371, Cambridge University Press, 1878.

A.16   Schneider, P. E. M.: Experimental Investigation of the Effect of Sound Waves on Diffusion Flames. Zeit. Flugwiss., Vol. 19, pp. 485-493, 1971.

A.17   Tailby, S. R.; and Berkovitch, I.: The Effect of Sonic Vibrations on Heat Transfer From Town Gas Flames. Trans. Instit. Chem. Eng., Vol. 36, pp. 13-28, 1958.

A.18   Tyndall, J.: On the Action of Sonorous Vibrations on Gaseous and Liquid Jets. Phil. Mag., Vol. 33, pp. 375-391, 1867.

A.19   Vermeulen, P. J.; Odgers, J.; and Ramesh, V.: Acoustic Control of Dilution-Air Mixing in a Gas Turbine Combustor. J. Eng. Power, Vol. 104, pp. 844-852, 1982.

A.20   Vermeulen, P. J.; Danilowich, M. S.; Heydlauff, E. P.; and Price, T. W.: The Acoustically Excited Flame. J. Eng. Power, Vol. 98, pp. 147-158, 1976.

B.1   Acton, E.: The Modelling of Large Eddies in a Two-Dimensional Shear Layer. J. Fluid Mech., Vol. 76, pp. 561-591, 1976.

B.2   Armstrong, R. R.; Fuchs, H. V.; and Michalke, A.: Coherent Structures in Jet Turbulence and Noise. AIAA Paper No. 76-490, 1976.

B.3   Bathija, P. R.: Jet Mixing Design and Applications. Chem. Eng., Vol. 89, pp. 89-94, 1982.

B.4   Beavers, G. S.; and Wilson, T. A.: Vortex Growth in Jets. J. Fluid Mech., Vol. 44, pp. 97-112, 1970.

B.5   Becker, H. A.; and Massaro, T. A.: Vortex Evolution in a Round Jet. J. Fluid Mech., Vol. 31, pp. 435-448, 1968.

B.6   Bradshaw, P.: The Effects of Initial Conditions on the Development of a Free Shear Layer. J. Fluid Mech., Vol. 26, pp. 225-236, 1966.

B.7   Bradshaw, P.; Ferriss, D. H.; and Johnson, R. F.: Turbulence in the Noise-Producing Region of a Circular Jet. J. Fluid Mech., Vol. 19, pp. 591-624, 1964.

B.8   Browand, F. K.: An Experimental Investigation of the Instability of an Incompressible, Separated Shear Layer. J. Fluid Mech., Vol. 26, pp. 281-307, 1966.

B.9   Browand, F. K.; and Weidman, P. D.: Large Scales in the Developing Mixing Layer. J. Fluid Mech., Vol. 76, pp. 127-144, 1976.

B.10   Brown, G. L.; and Roshko A.: On Density Effects and Large Structures in Turbulent Mixing Layers. J. Fluid Mech., Vol. 64, pp. 775-816, 1974.

B.11   Cantrell, R. H.; and Hart, R. W.: Interactions between Sound and Flow in Acoustic Cavities: Mass, Momentum, and Energy Considerations. J. Acoust. Soc. Am., Vol. 36, pp. 697-706, 1964.

B.12   Cantwell, B. J.: Organized Motion in Turbulent Flow. Ann. Rev. Fluid Mech., Vol. 13, pp 457-515, 1981.

B.13   Chan, Y. Y.: Spatial Waves in Turbulent Jets. Phys. Fluids, Vol. 17, pp. 46-53, 1974.

B.14   Chan, Y. Y.: Nonlinear Spatial Wave Development in an Axisymmetric Jet. Aero Report LR-585, National Research Council, Canada, National Aeronautical Establishment, 1975.

B.15   Crow, S. C.; and Champagne, F. H.: Orderly Structure in Jet Turbulence. J. Fluid Mech., Vol. 48, pp. 547-591, 1971.

B.16   Davis, M. R.: Coherence between Large-Scale Jet-Mixing Structure and its Pressure Field. J. Fluid Mech., Vol. 116, pp. 31-57, 1982.

B.17   Davis, M. R.: Control of Jet Mixing with Reference to Active Control of Jet Noise. New South Wales Univ., UNSW/Report - 1981-FMT-11, 1981.

B.18   Davies, P. O. A. L.: Structure of Turbulence. J. Sound and Vib., Vol. 28, pp. 513-526, 1973.

B.19   Davies, P. O. A. L.; and Yule, A. J.: Coherent Structures in Turbulence. J. Fluid Mech., Vol. 69, pp. 513-537, 1975.

B.20   Gaster, M.: The Role of Spatially Growing Waves in the Theory of Hydrodynamic Stability. Kuchemann, D.; and Steme, L.H.G. (eds): Progress in Aeronautical Sciences, pp. 251-270, 1965.

B.21   Grant, A. J.: A Numerical Model of Instability in Axisymmetric Jets. J. Fluid Mech., Vol. 66, pp. 707-724, 1974.

B.22   Grant, H. L.: The Large Eddies of Turbulent Motion. J. Fluid Mech., Vol. 4, pp. 149-190, 1958.

B.23   Hendricks, C. J.; and Brighton, J. A.: Prediction of Swirl and Inlet Turbulence Kinetic Energy Effects on Confined Jet Mixing. ASME Paper No. 75-FE-2, 1975.

B.24   Husain, Z. D.; and Hussain, A. K. M. F.: Axisymmetric Mixing Layer: Influence of the Initial and Boundary Conditions. AIAA Journal, Vol. 17, pp. 48-55, 1979.

B.25   Hussain, A. K. M. F.: Coherent Structures and Studies of Perturbed and Unperturbed Jets. Invited Lecture at the Int. Conf. on the Role of Coherent Structures in Modelling Turbulence and Mixing, Madrid, Spain, 1980.

B.26   Hussain, A. K. M. F.; and Clark, A. R.: On the Coherent Structure of the Axisymmetric Mixing Layer: a Flow-Visualization Study. J. Fluid Mech., Vol. 10 4, pp. 263-294, 1981.

B.27   Hussain, A. K. M. F.; and Husain, Z. D.: Turbulence Structure in the Axisymmetric Free Mixing Layer. AIAA Journal, Vol. 18, pp. 1462-1469, 1980.

B.28   Hussain, A. K. M. F.; Kleis, S. J.; and Sokolov, M.: A Turbulent Spot in an Axisymmetric Free Shear Layer. Part 2. J. Fluid Mech, Vol. 98, pp. 97-135, 1 980.

B.29   Jenkins, P. E.: A Study of the Intermittent Region of a Heated Two-Dimensional Plane Jet. Ph. D. Thesis, Purdue University, 1974.

B.30   Jenkins, P. E.: Some Measured Temperature Characteristics in a Two-Dimensional Heated Jet of Air. J. Eng. Power, Vol. 98, pp. 501-505, 1976.

B.31   Jenkins, P. E.; and Goldschmidt, V. W.: Mean Temperature and Velocity in a Plane Turbulent Jet. J. Fluids Eng., Vol. 95, pp. 581-584, 1973.

B.32   Kelly, R. E.: On the Stability of an Inviscid Shear Layer which is Periodic in Space and Time. _J. Fluid Mech._, Vol. 27, pp. 657-689, 1967.

B.33   Ko, N. W. M.; and Davies, P. O. A. L.: The Near Field within the Potential Cone of Subsonic Cold Jets. _J. Fluid Mech._, Vol. 50, pp. 49-78, 1971.

B.34   Krothapalli, A.; Baganoff, D.; and Karamcheti, K.: Partially Confined Multiple Jet Mixing. _AIAA Journal_, Vol. 19, pp. 324-328, 1981.

B.35   Lane, A. G. C.; and Rice, P.: An Investigation of Liquid Jet Mixing Employing an Inclined Side Entry Jet. _Trans. Instit. Chem. Eng._, Vol. 60, pp. 171-17 6, 1982.

B.36   Lau, J. C.; and Fisher, M. J.: The Vortex-Street Structure of 'Turbulent' Jets. Part 1. _J. Fluid Mech._, Vol. 67, pp. 299-337, 1975.

B.37   Lau, J. C.; Fisher, M. J.; and Fuchs, H. V.: The Intrinsic Structure of Turbulent Jets. _J. Sound and Vib._, Vol. 22, pp. 379-406, 1972.

B.38   Laufer, J.: New Trends in Experimental Turbulence Research. _Ann. Rev. Fluid Mech._, Vol. 7, pp. 307-326, 1975.

B.39   Long, M. B.; and Chu, B. T.: Mixing Mechanism and Structure of an Axisymmetric Turbulent Mixing Layer. _AIAA Journal_, Vol. 19, pp. 1158-1163, 1980.

B.40   Mattingly, G. E.; and Criminale, W. O., Jr.: Disturbance Characteristics in a Plane Jet. _Phys. Fluids_, Vol. 14, pp. 2258-2264, 1971.

B.41   Michalke, A.: On Spatially Growing Disturbances in an Inviscid Shear Layer. _J. Fluid Mech._, Vol. 23, pp. 521-544, 1965.

B.42   Moore, C. J.: The Role of Shear-Layer Instability Waves in Jet Exhaust Noise. _J. Fluid Mech._, Vol. 80, pp. 321-367, 1977.

B.43   Morrison, G. L.; and McLaughlin, D. K.: Instability Process in Low Reynolds Number Supersonic Jets. _AIAA Journal_, Vol. 18, pp. 793-800, 1980.

B.44   Morrison, G. L.; and Whitaker, K.: Mach Number Dependence of the Coherent Structure in High Speed Subsonic Jets. AIAA Paper 82-0049, 1982.

B.45   Pierrehumbert, R. T.; and Widnall, S. E.: The Structure of Organized Vortices in a Free Shear Layer. J. Fluid Mech., Vol. 102, pp. 301-313, 1981.

B.46   Plaschko, P.: Stochastic Model Theory for Coherent Turbulent Structures in Circular Jets. Phys. Fluid, Vol. 24, pp. 187-193, 1981.

B.47   Rajagopalan, S.; and Antonia, R. A.: Properties of the Large Structure in a Slightly Heated Turbulent Mixing Layer of a Plane Jet. J. Fluid Mech., Vol. 105, pp. 261-281, 1981.

B.48   Roshko, A.: Structure of Turbulent Shear Flows: A New Look. AIAA Journal, Vol. 14, pp. 1349-1357, 1976.

B.49   Sato, H.; and Sakao, F.: An Experimental Investigation of the Instability of a Two-Dimensional Jet at Low Reynolds Numbers. J. Fluid Mech., Vol. 20, pp . 337-352, 1964.

B.50   Sokolov, M.; Hussain, A.K.M.F.; Kleis, S. J.; and Husain, Z. D.: A 'turbulent spot' in an axisymmetric free shear layer. Part 1. J. Fluid Mech., Vol. 98, pp. 65-95, 1980.

B.51   Tabakoff, W.; and Blasenak, J. H.: Non-Isoenergetic Turbulent Jet Mixing in a Constant-Area Duct. AIAA Journal, Vol. 20, pp. 488-495, 1982.

B.52   Tso, J.; Kovasznay, L.S.G.; and Hussain, A.K.M.F.: Search for Large-Scale Coherent Structures in the Nearly Self-Preserving Region of an Axisymmetric Turbulent Jet. AIAA Paper 80-1355, 1980.

B.53   Uram, E. M.; and Goldschmidt, V. W. (eds): Proc. ASME Symp. Fluid Mech. of Mixing. Atlanta, Georgia., 1973.

B.54   Wooldridge, C. E.; and Wooten, D. C.: A Study of the Large-Scale Eddies of Jet Turbulence Producing Jet Noise. AIAA Paper No. 71-154, 1971.

B.55   Wooldridge, C. E.; Wooten, D. C.; and Amaro, A. J.: The Structure of Jet Turbulence Producing Jet Noise. AIAA Paper No. 72-158, 1972.

B.56   Wygnanski, I.; and Fiedler, H. E.: The Two-Dimensional Mixing
       Region. J. Fluid Mech., Vol. 41, pp. 327-361, 1970.

B.57   Wygnanski, I.; Oster, D.; Fiedler, H.; and Dziomba, B.: On the
       Perseverence of a Quasi-Two-Dimensional Eddy-Structure in a
       Turbulent Mixing Layer. J. Fluid Mech., Vol. 93, pp. 325-335, 1979.

B.58   Yule, A. J.: Large-Scale Structure in the Mixing Layer of a Round
       Jet. J. Fluid Mech., Vol. 89, pp. 413-432, 1978.

C.1   Binder, G.; and Favre-Marinet, M.: Mixing Improvement in Pulsating
       Turbulent Jets. Proc. ASME Symp. Fluid Mech. of Mixing, Atlanta,
       Georgia, pp. 167-172, 1973.

C.2   Collins, D. J.; Platzer, M. F.; Lai, J. C.; and Simmons, J.:
       Experimental Investigation of Oscillating Subsonic Jets. Paper
       presented at Ejector Workshop for Aerospace Applications,
       Sponsored by AFWAL and AFOSR, Dayton, Ohio, 1981.

C.3   Curtet, R. M.; and Girard, J. P.: Visualization of a Pulsating Jet.
       Proc. ASME Symp. Fluid Mech. of Mixing, Atlanta, Georgia, pp. 173-
       180, 1973.

C.4   Foa, J. V.: Considerations on Steady- and Nonsteady-Flow Ejectors.
       Paper presented at Ejector Workshop for Aerospace Applications,
       Sponsored by AFWAL and AFOSR, Dayton, Ohio, 1981.

C.5   Hohenmser, K. H.: Flow Induction by Rotary Jets. J. Aircraft, Vol.
       3, pp. 18-24, 1966.

C.6   Hohenmser, K. H.; and Porter, J. L.: Contribution to the Theory of
       Rotary Jet Flow Induction. J. Aircraft, Vol. 3, pp. 339-346, 1966.

C.7   Khare, J. M.; and Kentfield, J. A. C.: A Simple Apparatus for the
       Experimental Study of Non-Steady Flow Thrust-Augmenter Ejector
       Configurations. NASA Conference Publication 2093, pp. 325-349,
       1978.

C.8   Lopez, A. E.; Koenig, D. G.; Green, D. S.; and Nagaraja, K. S.
       (eds): Proceedings of the NASA-Air Force-Navy Workshop on Thrust
       Augmenting Ejectors. NASA CP-2093, Moffett Field, California,
       1978.

C.9   McNair, C. H., Jr.: An Analytical and Experimental Investigation of
       the Performance of a Direct Acting Thrust Augmenter Utilizing a
       Rotating Disk to Induce Unsteady Flow. Thesis, Georgia Institute of
       Tech., 1963.

C.10   Petrie, H. L.; and Addy, A. L.: An Investigation of Planar, Two Dimensional Ejectors with Periodic or Steady Supersonic Driver Flow. Paper presented at Ejector Workshop for Aerospace Applications, Sponsored by AFWAL and AFOSR, Dayton, Ohio, 1981.

C.11   Rockwell, D. O.: External Excitation of Planar Jets. J. Applied Mech., Vol. 39, pp. 883-890, 1972.

C.12   Rockwell, D. O.; and Niccolls, W. O.: Natural Breakdown of Planar Jets. J. Basic Eng., Vol. 94, pp. 720-730, 1972.

C.13   Sarohia, V.; Bernal, L.; and Bui, T.: Entrainment and Thrust Augmentation in Pulsatile Ejector Flows. Jet Propulsion Laboratory Report 81-35, 1981.

C.14   Simmons, J. M.; Lai, J. C. S.; and Platzer, M. F.: Jet Excitation by an Oscillating Vane. AIAA Journal, Vol. 19, pp. 673-676, 1981.

C.15   Simmons, J. M.; Platzer, M. F.; and Smith, T. C.: Velocity Measurements in an Oscillating Plane Jet Issuing into a Moving Airstream. J. Fluid Mech., Vol. 84, pp. 33-53, 1978.

C.16   Viets, H.: Flip-Flop Jet Nozzle. AIAA Journal, Vol. 13, pp. 1375-1379, 1975.

C.17   Viets, H.; Piatt, M.; Ball, M.; Bethke, R.; and Bougine, R.: Unsteady Flows Applicable to Ejector Mechanics. Paper presented at Ejector Workshop for Aerospace Applications, Sponsored by AFWAL and AFOSR, Dayton, Ohio, 1981.

C.18   Viets, H.; Piatt, M.; Ball, M.; Bethke, R. J.; and Bougine, D.: Problems in Forced, Unsteady Fluid Mechanics. AFWAL Report TM-81-148-FIMM, 1981.

C.19   Zukoski, E. E.; and Auerbach, J. M.: Experiments Concerning the Response of Supersonic Nozzles to Fluctuating Inlet Conditions. J. Eng. Power, Vol. 98, pp. 60-64, 1976.

D.1   Ahuja, K. K.: Basic Experimental Study of the Coupling Between Flow Instabilities and Incident Sound. NASA CR-3789, March 1984.

D.2   Ahuja, K. K.; Lepicovsky, J.; and Burrin, R. H.: Noise and Flow Structure of a Tone-Excited Jet. AIAA Journal, Vol. 20, pp. 1700-1706, 1982.

D.3   Ahuja, K. K.; Lepicovsky, J.; Tam, C.K.W.; Morris, P. J.; and Burrin, R. H.: Tone Excited Jet -- Theory and Experiments. NASA CR-3538, 1982.

D.4   Ajagu, C. O.: Foldover, Intermittency, and Crossing Frequency of a Plane Jet Interface with and without an Acoustic Disturbance. MSME Thesis, Purdue University, 1976.

D.5   Bechert, D.; and Pfizenmaier, E.: On the Amplification of Broadband Jet Noise by a Pure Tone Excitation. J. Sound and Vib., Vol. 43, pp. 321-367, 1975.

D.6   Bell, W. A.; and Lepicovsky, J.: Conditional Sampling with a Laser Velocimeter. AIAA Paper No. 83-0756, 1983.

D.7   Berman, C. H.: Turbulence and Noise Characteristics of Acoustically Excited Bypass Jet Flows. AIAA Paper No. 81-2009, 1981.

D.8   Borisov, Y. Y.; and Rosenfeld, E. I.: Action of Acoutic Oscillations on Flow Stability and Structure. Soviet Physics-Acoustics, Vol. 17, pp. 154-168, 1971.

D.9   Brown, G. B.: On Vortex Motion in Gaseous Jets and the Origin of their Sensitivity to Sound. Phys. Soc. of London Proc., Vol. 47, pp. 703-732, 1935.

D.10   Chambers, F. W.; and Goldschmidt, V. W.: Acoustic Interaction with a Turbulent Plane Jet. Naval Research Report No. 7, HL77-31, 1977.

D.11   Chambers, F. W.; and Goldschmidt, V. W.: Acoustic Interaction with a Turbulent Plane Jet: Effects on Mean Flow. AIAA Journal, Vol. 20, pp. 797-804, 1982.

D.12   Chanaud, R. C.; and Powell, A.: Experiments Concerning the Sound Sensitive Jet. J. Acoust. Soc. Am., Vol. 34, pp. 907-915, 1962.

D.13   Crow, S. C.; and Champagne, F. H.: Orderly Structure in Jet Turbulence. J. Fluid Mech., Vol. 48, pp. 547-591, 1971.

D.14   Deneuville, P.; and Jacques, J.: Jet Noise Amplification: A Practically Important Problem. AIAA Paper No. 77-1368, 1977.

D.15   Glass, D. R.: Effects of Acoustic Feedback on the Spread and Decay of Supersonic Jets. AIAA Journal, Vol. 6, pp. 1890-1897, 1968.

D.16   Goldschmidt, V. W.; and Kaiser, K. F.: Interaction of an Acoustic Field and a Turbulent Plane Jet: Mean Flow Measurements. AICHE Chem. Eng. Prog. Symp. Series, Vol. 67, pp. 91-98, 1971.

D.17   Heavens, S. N.: Visualization of the Acoustic Excitation of a Subsonic Jet. J. Fluid Mech., Vol. 100, pp. 185-192, 1980.

D.18   Hill, W. G; and Greene, P. R.: Increased Turbulent Jet Mixing Rates Obtained by Self-Excited Acoustic Oscillations. ASME Paper No. 77-FE-18, 1977.

D.19   Hribar, A. E.: On the Interaction of Intense Acoustic Fields and Viscous Fluid Flows. J. Basic Eng., Vol. 91, pp. 74-80, 1969.

D.20   Hussain, A.K.M.F.; and Zaman, K.B.M.Q.: Effect of Acoustic Excitation on the Turbulent Structure of a Circular Jet. Third Interagency Symposium on University Research in Transportation Noise, University of Utah, Salt Lake City, Utah, pp. 314-326, 1975.

D.21   Hussain, A.K.M.F.; and Zaman, K.B.M.Q.: Vortex Pairing in a Circular Jet Under Controlled Excitation. Part 2. Coherent Structure Dynamics. J. Fluid Mech., Vol. 101, pp. 493-544, 1980.

D.22   Hussain, A.K.M.F.; and Thompson, C. A.: Controlled Symmetric Perturbation of the Plane Jet: an Experimental Study in the Initial Region. J. Fluid Mech., Vol. 100, pp. 397-431, 1980.

D.23   Kaiser, K. F.: An Experimental Investigation of the Interaction of an Acoustic Field and a Plane Turbulent Jet. M. S. Thesis, Purdue University, 1971.

D.24   Kibens, V.: Discrete Noise Spectrum Generated by an Acoustically Excited Jet. AIAA Paper No. 79-0592, 1979.

D.25   Lebedev, N. G.; and Telenin, G. F.: Interaction between a Supersonic Jet and an Acoustic Field. Izv. AN SSSR, Mekhanika Zhidkosti i Gaza, Vol. 4, pp. 82 -94, 1970.

D.26   Lepicovsky, J.; Bell, W. A.; and Ahuja, K. K.: Conditional Sampling with a Laser Velocimeter and its Application for Large-Scale Turbulent Structure Measurement. Lockheed-Georgia Co., Report LG83ER0007, 1983.

D.27   Lu, H. Y.: Effect of Excitation on Coaxial Jet Noise as Observed by an Elliptical Mirror. AIAA Paper No. 81-2044, 1981.

D.28   Mollo-Christensen, E.: Jet Noise and Shear Flow Instability Seen From an Experimenter's Viewpoint. J. Applied Mech., Vol. 89, pp. 1-7, 1967.

D.29   Moore, C. J.: The Role of Shear-Layer Instability Waves in Jet Exhaust Noise. J. Fluid Mech., Vol. 80, pp. 321-367, 1977.

D.30   Morkovin, M. V.; and Paranjape, S. V.: On Acoustic Excitation of Shear Layers. Zeit.Flugwiss., Vol. 19, pp. 328-335, 1971.

D.31   Quinn, B.: Effect of Aeroacoustic Interactions on Ejector Performance. J. Aircraft, Vol. 12, pp. 914-916, 1975.

D.32   Quinn, B.: Interactions between Screech Tones and Ejector Performance. J. Aircraft, Vol. 14, pp. 467-473, 1977.

D.33   Rockwell, D. O.: The Macroscopic Nature of Jet Flows Subjected to Small Amplitude Periodic Disturbances. AICHE Chem. Eng. Prog. Sym. Series, Vol. 67, pp . 99-107, 1971.

D.34   Rockwell, D. O.; and Toda, K.: Effects of Applied Acoustic Fields on Attached Jet Flows. J. Basic Eng., Vol. 93, pp. 63-73, 1971.

D.35   Roffman, G. L.; and Toda, K.: A Discussion of the Effects of Sound on Jets and Flueric Devices. J. Eng. Ind., Vol. 91, pp. 1161-1167, 1969.

D.36   Ronneberger, D.; and Ackermann, U.: Experiments on Sound Radiation due to Non-Linear Interaction of Instability Waves in a Turbulent Jet. J. Sound and Vib., Vol. 62, pp. 121-129, 1979.

D.37   Sarohia, V.; and Massier, P. F.: Experimental Results of Large Scale Structures in Jet Flows and Their Relation to Jet Noise Production. AIAA Paper No. 77-1350, 1977.

D.38   Sato, H.: The Stability and Transition of a Two-Dimensional Jet. J. Fluid Mech., Vol. 7, pp. 53-80, 1960.

D.39   Schmidt, C.: Aerodynamic Characterization of Excited Jet. J. Sound and Vib., Vol. 61, pp. 148-152, 1978.

D.40   Simcox, C. D.: A Theoretical Investigation of Acoustic-Turbulence Interactions with Application to Free-Jet Spreading. Ph.D. Thesis, Purdue University, 1969.

126

D.41   Simcox, C. D.; and Hoglund, R. F.: Acoustic Interactions with Turbulent Jets. J. Basic Eng., Vol. 93, pp. 42-46, 1971.

D.42   Thompson, C. A.: Organized Motions in a Plane Turbulent Jet under Controlled Excitation. Ph.D. Thesis, University of Houston, 1975.

D.43   Viets, H.: Acoustic Interactions in Ejectors. AIAA Paper No. 81-2045, 1981.

D.44   Vlasov, E. V.; and Ginevskii, A. S.: Acoustic Modification of the Aerodynamic Characteristics of a Turbulent Jet. Izv. AN SSSR, Mekhanika Zhidkosti i Gaza, Vol. 2, pp. 133-138, 1967.

D.45   Vlasov, E. V.; and Ginevskii, A. S.: The Aeroacoustic Interaction Problem (review). Sov. Phys. Acoust., Vol. 26, pp. 1-7, 1980.

D.46   Vulis, L.A.: Turbulent Mixing of Free Gas Jets. Fluid Mech.-Soviet Research, Vol. 1, pp. 130-135, 1972.

D.47   Whiffen, M. C.; and Ahuja, K. K.: An Improved Schlieren System and Some New Results on Acoustically Excited Jets. J. Sound and Vib., Vol. 86, pp. 99-105 , 1983.

D.48   Zaman, K.B.M.Q.; and Hussain, A.K.M.F.: Vortex Pairing in a Circular Jet Under Controlled Excitation. Part 1. General Jet Response. J. Fluid Mech., Vol. 101, pp. 449-491, 1980.

D.49   Zaman, K.B.M.Q.; and Hussain, A.K.M.F.: Turbulence Suppression in Free Shear Flows by Controlled Excitation. J. Fluid Mech., Vol. 103, pp. 133-159, 1981.

D.50   Zhangwei, H.: Jet Response to Pure Tone Excitation. UTIAS Technical Note No. 232, CN ISSN 0082-5263, University of Toronto, 1982.

E.1   Ahuja, K. K.; Lepicovsky, J.; Tam, C.K.W.; Morris, P. J.; and Burrin, R. H.: Tone Excited Jet-Theory and Experiments. NASA CR-3538, 1982.

E.2   Ivanov, N. N.: Acoustic Effect on the Root Part of a Turbulent Jet. Izv. AN SSSR, Mekhanika Zhidkosti i Gaza, Vol. 4, pp. 182-186, 1970.

E.3   Jubelin, B.: New Experimental Studies on Jet Noise Amplification. AIAA Paper No. 80-0961, 1980.

E.4   Lu, H. Y.: Effect of Excitation on Coaxial Jet Noise as Observed by an Elliptic Mirror. AIAA Paper No. 81-2044, 1981.

E.5   Mickelsen, W. R.; and Baldwin, L. V., Aerodynamic Mixing Downstream from Line Source of Heat in High-Intensity Sound Field. NACA TN 3760, 1956.

E.6   Vermeulen, P. J.; Odgers, J.; and Ramesh, V.: Acoustic Control of Dilution-Air Mixing in a Gas Turbine Combustor. J. Eng. Power, Vol. 104, pp. 844-852, 1 982.

F.1   Ahuja, K. K.; Lepicovsky, J.; Tam, C.K.W.; Morris, P. J.; and Burrin, R. H.: Tone Excited Jet -- Theory and Experiments. NASA CR-3538, 1982.

F.2   Maestrello, L.; and Bayliss, A.: Flowfield and Far Field Acoustic Amplification Properties of Heated and Unheated Jets. AIAA Journal, Vol. 20, pp. 1539- 1546, 1982.

F.3   McCormack, P. D.; and Cochran, D.: Periodic Vorticity and its Effect on Jet Mixing. Phys. Fluids, Vol. 9, pp. 1555-1560, 1966.

F.4   Mickelsen, W. R.; and Baldwin, L. V.: Aerodynamic Mixing Downstream from Line Source of Heat in High-Intensity Sound Field. NACA TN 3760, 1956.

F.5   Morris, P. J.: Flow Characteristics of the Large-Scale Wave-Like Structure of Supersonic Round Jet. J. Sound and Vib., Vol. 53, pp. 223-244, 1977.

F.6   Morris, P. J.: A Model for Broadband Jet Noise Amplification. AIAA Paper 80-1004, 1980.

F.7   Morris, P. J.; and Baltas, C.: Turbulence in Sound Excited Jets: Measurements and Theory. AIAA Paper No. 81-0058, 1981.

F.8   Morris, P. J.; and Tam, C.K.W.: Near- and Far-Field Noise from Large-Scale Instabilities of Axisymmetric Jets. AIAA Paper No. 77-1351, 1977.

F.9   Morris, P.J.: Viscous Stability of Compressible Axisymmetric Jets. AIAA Journal, Vol. 21, pp. 481-482, 1982.

F.10   Rayleigh, Lord, J.W.S.: On the Instability of Jets. Scientific Papers I, pp. 361-371, Cambridge University Press, 1878.

F.11   Savic, P.: Acoustically Effective Vortex Motion in Jets. <u>Phil. Mag.</u>, Vol. 32, pp. 245-251, 1941.

F.12   Tam, C.K.W.: Excitation of Instability Waves in Two-Dimensional Shear Layer by Sound. <u>J. Fluid Mech.</u>, Vol. 89, pp. 357-367, 1978.

F.13   Tam, C.K.W.: The Effects of Upstream Tones on the Large-Scale Instability Waves and Noise in Jets. Mechanics of Sound Generation in Flows, IUTAM/ICA/AIA A-Symposium, Gottingen, Germany, pp. 41-47, 1979.

F.14   Tam, C.K.W.: The Excitation of Tollmien-Schlichting Waves in Low Subsonic Boundary Layers by Free-Stream Sound Waves. <u>J. Fluid Mech.</u>, Vol. 109, pp. 483- 501, 1981.

F.15   Tam, C.K.W.; and Chen, K. C.: A Statistical Model of Turbulence in Two-Dimensional Mixing Layers. <u>J. Fluid Mech.</u>, Vol. 92, pp. 303-326, 1979.

F.16   Tam, C.K.W.; and Morris, P. J.: The Radiation of Sound by the Instability Waves of a Compressible Plane Turbulent Shear Layer. <u>J. Fluid Mech.</u>, Vol. 98, pp. 349-381, 1980.

F.17   Tam, C. K. W; and Morris, P. J.: Tone Excited Jets, Part V: A Theoretical Model and Comparison with Experiment. <u>J. Sound and Vib.</u>, Vol. 102, pp. 119-151, 1985.

NASA
National Aeronautics and
Space Administration

Report Documentation Page

1. Report No.	2. Government Accession No.	3. Recipient's Catalog No.
NASA CR-4129, Part I		

4. Title and Subtitle	5. Report Date
Acoustically Excited Heated Jets	June 1988
I - Internal Excitation	6. Performing Organization Code

7. Author(s)	8. Performing Organization Report No.
J. Lepicovsky, K.K. Ahuja, W.H. Brown, M. Salikuddin, and P.J. Morris	LG86ER0022 (E-4001)

10. Work Unit No.
505-62-91

9. Performing Organization Name and Address	11. Contract or Grant No.
Lockheed Aeronautical Systems Company - Georgia Dept. 72-74, Zone 403 Marietta, Georgia 30063	NAS3-23708

13. Type of Report and Period Covered
Contractor Report
Final

12. Sponsoring Agency Name and Address	
National Aeronautics and Space Administration Lewis Research Center Cleveland, OH 44135-3191	14. Sponsoring Agency Code

15. Supplementary Notes

Project Manager, Edward J. Rice, Internal Fluid Mechanics Division, NASA Lewis Research Center. J. Lepicovsky, K.K. Ahuja, W.H. Brown, and M. Salikuddin, Lockheed Aeronautical Systems - Georgia. P.J. Morris, Pennsylvania State University, University Park, Pennsylvania.

16. Abstract

A detailed, mostly experimental, study to understand the effects of relatively strong upstream acoustic excitation on the mixing of heated jets with the surrounding air was carried out. To determine the extent of the available information on experiments and theories dealing with acoustically excited heated jets, an extensive literature survey was carried out at the outset of this program. The experimental program consisted of flow visualization and flowfield velocity and temperature measurements for a broad range of jet operating and flow excitation conditions. A 50.8-mm-diam nozzle was used for this purpose. Parallel to the experimental study, an existing theoretical model of excited jets was refined to include the region downstream of the jet potential core. Excellent agreement was found between the theory and the experiments in moderately heated jets. However, the theory has not yet been confirmed for highly heated jets. It was found that the sensitivity of heated jets to upstream acoustic excitation varies strongly with the jet operation conditions and that the threshold excitation level increases with increasing jet temperature. Furthermore, the preferential Strouhal number is found not to change significantly with a change of the jet operating conditions. Finally, the effects of the nozzle exit boundary layer thickness appear to be similar for both heated and unheated jets at low Mach numbers.

17. Key Words (Suggested by Author(s))	18. Distribution Statement
Sound-flow interaction; Jet mixing; Flow visualization; Velocity and temperature measurement; Large-scale structures	Unclassified - Unlimited Subject Category 02

19. Security Classif. (of this report)	20. Security Classif. (of this page)	21. No of pages	22. Price*
Unclassified	Unclassified	134	A07

End of Document